

Decay of ^{86m}Y and ^{83}Y

ABSTRACT
DECAY OF $^{86m}\gamma$ AND $^{83}\gamma$

by

Margaret Simpson

Foster Radiation Laboratory
Physics Department
McGill University

MSc Thesis
July 1972

The decay of the 8^+ isomeric level of $^{86}\gamma$ has been investigated. A weak β^+ branch of $0.69 \pm 0.04\%$ with a $\log ft$ of 6.51 to an 8^+ level at 2955.5 keV in ^{86}Sr is observed. γ - γ coincidence measurements indicate four successive cascade transitions from the 8^+ state to the ground state of ^{86}Sr with γ -rays at 98.6 ± 0.1 , 627.2 ± 0.2 , 1076.6 ± 0.3 , 1153.1 ± 0.3 keV. A new decay scheme is proposed.

The decay of $^{83m}\gamma$ (2.85 min) and $^{83g}\gamma$ (7.06 min) has been investigated. Two transitions are observed associated with the decay of $^{83m}\gamma$ and seventeen with the decay of the ground state. On the basis of γ - γ coincidence, internal conversion, and lifetime measurements a decay scheme is proposed. The level structure of ^{83}Sr is discussed in the context of the shell model.

Attempts to observe γ -rays from the decay of $^{82}\gamma$ were unsuccessful. An upper limit of 30 sec. on its half-life is estimated.

DECAY OF ^{86}mY AND ^{83}Y

by

Margaret Simpson B.Sc.

A thesis submitted to the Faculty of Graduate Studies
and Research in partial fulfilment of the requirements
for the degree of Master of Science.

Foster Radiation Laboratory
Physics Department
McGill University
Montreal, Quebec

July 1972

© Margaret Simpson 1973

ABSTRACT

The decay of the 8^+ isomeric level of ^{86}Y has been investigated. A weak β^+ branch of $0.69 \pm 0.04\%$ with a $\log ft$ of 6.51 to an 8^+ level at 2955.5 keV in ^{86}Sr is observed. γ - γ coincidence measurements indicate four successive cascade transitions from the 8^+ state to the ground state of ^{86}Sr with γ -rays at 98.6 ± 0.1 , 627.2 ± 0.2 , 1076.6 ± 0.3 , 1153.1 ± 0.3 keV. A new decay scheme is proposed.

The decay of $^{83\text{m}}\text{Y}$ (2.85 min) and $^{83\text{g}}\text{Y}$ (7.06 min) has been investigated. Two transitions are observed associated with the decay of $^{83\text{m}}\text{Y}$ and seventeen with the decay of the ground state. On the basis of γ - γ coincidence, internal conversion, and lifetime measurements a decay scheme is proposed. The level structure of ^{83}Sr is discussed in the context of the shell model.

Attempts to observe γ -rays from the decay of ^{82}Y were unsuccessful. An upper limit of 30 sec. on its half-life is estimated.

ACKNOWLEDGMENTS

To Dr. J.E. Kitching for cheerful aid and many hours spent in planning, executing, and analyzing experiments, I would like to express my sincere gratitude.

I would like to thank Dr. S.K. 'Tommy' Mark for the time spared from his busy schedule as Director of the Foster Radiation Laboratory to discuss difficulties and to render able assistance with recalcitrant electronics.

Other members of the Foster Laboratory (and a radiochemist, JJHMCP) provided illuminating discussion on many topics. Some have assisted in experimental work, notably Messrs. R. Turcotte and R. lafigliola who made available the rapid extractor facility for some experiments, and Mr. Alain Houdayer who set up the apparatus for electrodeposition of thin radiation sources for electron counting.

Thanks are also due those who helped in the production of this manuscript: Miss Helen Levesque, who typed it; Mr. Gee Shan, who performed the photographic work; and Mr. Geoffrey Lyman, who proofread the final version.

To Marc Spencer go special thanks for help with the drawings and for his encouragement and affection at difficult moments.

Finally, I acknowledge with gratitude the financial support provided by the laboratory on behalf of the Atomic Energy Control Board of Canada.

TABLE OF CONTENTS

	<u>Page</u>
Abstract	i
Acknowledgments	ii
Table of Contents	iii
List of Figures	v
List of Tables	viii
Chapter I	1
Introduction	1
Models of Spherical Nuclei	1
Decay Modes of Nuclear States	4
Electromagnetic Transitions	4
Beta Decay	8
Nuclear Isomerism	12
Chapter II	13
A Review of Previous Work	13
^{86}Sr	13
^{83}Rb	13
^{82}Pb	14
Chapter III	23
Experimental Techniques	23
Source Preparation	23
The Production of ^{86}Sr	23
The Production of ^{83}Rb and ^{82}Pb	26
Gamma Ray Spectroscopy Sources	26
Electron Spectroscopy Sources	27
Gamma Ray Detectors	28
The Electron Detector	30
Experimental Configurations and Procedures	30
Energy and Half-life Measurements	30
Gamma Ray Coincidence Measurements	33
The Coincidence Circuit Electronics	34
Internal Conversion Coefficient Measurements	37
The Counting Chamber	39
The Electronics	39

	<u>Page</u>
Chapter IV	47
The Decay of ^{86}mY	47
The Background	47
Experimental Results	48
Discussion and Conclusions	50
Chapter V	58
The Decay of ^{83}Y and $^{83\text{m}}\text{Y}$	58
Background	58
Experimental Results	59
Energy and Half-life Measurements	59
Gamma-Gamma Coincidence Measurements	62
Internal Conversion Coefficient Measure- ments	63
Discussion	63
The Decay of $^{83\text{m}}\text{Y}$	64
The Decay of ^{83}Y	65
Conclusions	69
Chapter VI	82
The Search for ^{82}Y Decay	82
Background	82
Experimental Results	82
Speculations on Reasons for the Failure to Observe ^{82}Y Activity	83
Conclusions	86
References	87
Appendix 1	
Gamma Ray Energy Standards	
Appendix 2	
Systematics	
Appendix 3	
Reprint of Publication 'The Decay of ^{86}mY '.	

LIST OF FIGURES

		<u>Page</u>
Figure 1	A Partial Decay Scheme of $^{86}\text{g}_{\gamma 21}$ Showing Levels up to 3 MeV	15
Figure 2	The Decay Scheme of $^{86}\text{m}_{\gamma}$ Proposed by Kim et al. (23).	16
Figure 3	The $(1g_{9/2})_{\gamma}^{-2}$ Multiplet of States in $^{86}\text{Sr}_{24}$.	17
Figure 4	The Decay Scheme of $^{83,83}\text{m}_{\gamma}$ Proposed by Kitching.	18
Figure 5	The Decay Scheme of $^{83,83}\text{m}_{\gamma}$ Proposed by Abdyrazakov et al. (28).	19
Figure 6	The Level Structure of ^{83}Sr .	20
Figure 7	The Level Structure of ^{82}Sr from $^{74}\text{Ge}(\text{C}^{12}, 4n)^{82}\text{Sr}$ Reaction Studies (35).	21
Figure 8	The Level Structure of ^{82}Sr from the Effective Interaction Shell Model Calculations of Kitching et al. (10).	22
Figure 9	Apparatus for Electrodeposition of Thin Electron Sources	40
Figure 10	Counting System for Energy and Half-life Measurements.	41
Figure 11	Fast-slow Coincidence Circuit.	42
Figure 12	Detector Configuration for Coincidence Experiments.	43
Figure 13	Circuit Diagram of Routing Box Used in Coincidence Experiments.	44
Figure 14	Vacuum Chamber for Internal Conversion Measurements.	45
Figure 15	Counting System for Internal Conversion Measurements.	46

		<u>Page</u>
Figure 16	A Partial Gamma Ray Spectrum of ^{86m}Y Obtained with the X-ray Detector.	54
Figure 17	Half-life Curves of Gamma Rays from the 4.6 hr ^{86}Y Decay Showing Traces of a Shorter Half-life.	55
Figure 18	Comparison of the Relevant Portion of the Gamma Ray Spectra from the Decay of ^{86m}Y and ^{86}Y (ground state).	56
Figure 19	Proposed Decay Scheme for the 48 min. ^{86m}Y .	57
Figure 20	A Gamma Ray Spectrum of $^{83,83m}\text{Y}$ Activity from a Target of Enriched ^{84}Sr Bombarded at 31 MeV.	71
Figure 21	A Gamma Ray Spectrum of $^{83,83m}\text{Y}$ from the Yttrium Fraction Separated from an Enriched ^{84}Sr Target Bombarded at 40 MeV.	72
Figure 22	A Gamma Ray Spectrum From the Contaminant Fraction of an Enriched ^{84}Sr Target Bombarded at 40 MeV, Recorded Eighty Minutes After Separation.	73
Figure 23	Half-life Plots of Some Prominent Gamma Rays in the Decay of $^{83,83m}\text{Y}$.	74
Figure 24	Coincidence Spectrum Gated by all Gamma Rays Above 511 keV and Below 1.5 MeV.	75
Figure 25	Coincidence Spectrum Gated by the 489.9 keV Transition.	76
Figure 26	Coincidence Spectrum Gated by the 454.3 keV Transition.	77
Figure 27	Coincidence Spectrum Gated by the 882.1 keV Transition.	78

		<u>Page</u>
Figure 28	Coincidence Spectrum Gated by the 421(d) Transitions.	79
Figure 29	The K-electron Internal Conversion Line from the 259.3 keV Transition.	80
Figure 30	Proposed Decay Scheme of $^{83,83m}\text{Y}$.	81

LIST OF TABLES

	<u>Page</u>
Table 1.....	6
Table 2.....	11
Table 3.....	11
Table 4.....	24
Table 5.....	25
Table 6.....	29
Table 7.....	53
Table 8.....	61
Table 9.....	68
Table 10.....	84

CHAPTER I
INTRODUCTION

Models of Spherical Nuclei

The structure of nuclei in the mass region $A \approx 90$ is often described in the shell model context. The most striking evidence of shell structure is the enhanced stability of nuclei with certain 'magic' numbers of protons or neutrons: e.g. ${}^4\text{He}$ with two neutrons and two protons or tin ($Z = 50$) which has ten stable isotopes, more than any other element. In the shell model^{1,2,3,4)} the characteristics of (even-odd) nuclei are attributed to a single unpaired nucleon moving in a central potential arising from the inert spherical core made up of the remaining nucleons coupled to form pairs of zero spin. Calculations based on simple central potentials, such as the square well or harmonic oscillator, do not correctly reproduce the 'magic' numbers. This discrepancy can be remedied by the introduction of a spin-orbit potential proportional to $\bar{L} \cdot \bar{s}$ which energetically splits states of the same value ℓ of orbital angular momentum into two groups with total spin $j = \ell \pm 1/2$. This potential accounts in a natural way for the observed 'magic' numbers by predicting large energy gaps between certain adjacent shells. It also predicts accurately the zero ground state spins of even-even nuclei, and the ground state spins of even-odd nuclei except in the regions where nuclear deformation occurs. This extreme single particle model has been extended⁵⁾ so that calculations of nuclear excited

states can be performed taking into account not just one unpaired nucleon, but several nucleons outside a closed shell and the interactions between these nucleons.

Interest in the mass region $A \approx 90$ is largely due to the fact that these nuclei, being associated with the filling of the $2p_{1/2}$ and $1g_{9/2}$ nucleon shells, provide a natural testing ground for shell model predictions. A wide energy gap between the $1g_{9/2}$ orbital and the first unoccupied shell above it, the $2d_{5/2}$ shell, is responsible for a strong shell closure at N or $Z = 50$; therefore, the structure of nuclei with N or Z near fifty can often be understood quite well in terms of the shell model. Further interest in this region is generated by the high incidence of nuclear isomerism associated with the large spin difference but small energy difference between the neighbouring $2p_{1/2}$ and $1g_{9/2}$ states.

The shell model assumption of an inert spherical core of nucleons which does not contribute to dynamic nuclear properties is an oversimplification. The model can be improved by considering the vibrational modes of the nuclear core. The properties of low-lying nuclear excited states may be derived by coupling the motions of the particles outside the core to vibrational states of the core which possess zero, one, or two phonons of energy. When the nuclear core is not grossly deformed from sphericity the coupling can be treated by perturbation methods and is called the weak coupling model⁶⁾. In more extreme cases of deformity, perturbation methods must be abandoned and the strong coupling or the Nilsson⁷⁾ model employed.

The weak coupling model has been applied to nuclei in the mass region $A \approx 90$, as well as the shell model.

Talmi and Unna⁸⁾ carried out the first effective interaction shell model calculation in this region, assuming equality of equivalent matrix elements for protons and neutrons. When experimental data became more abundant a second calculation⁹⁾ was carried out which verified the conservation of seniority among $1g_{9/2}$ protons. Seniority is a quantum number labelling the number of unpaired nucleons of a particular kind in a given configuration. Conservation of seniority requires that only configurations with the same number of unpaired protons or neutrons mix to form an excited state. More recently Kitching et al.¹⁰⁾ have done an effective interaction shell model calculation for the strontium isotopes to check on seniority conservation among the $1g_{9/2}$ neutrons. The assumption of equality of equivalent matrix elements for neutrons and protons was shown to be invalid; however, seniority among $1g_{9/2}$ neutrons is approximately conserved.

Subsequently, a weak coupling calculation for several isotopes, including some strontium isotopes, has been performed¹¹⁾. In general, the results are an improvement over the shell model calculations in that they predict a richer structure in better agreement with available data. The weak coupling model is, however, unable to account for certain low-lying $7/2^+$ states which are assumed to be seniority three, 'shell model' states.

The present study of several yttrium isotope decays

namely, ^{86m}Y to ^{86}Sr , ^{83m}Y to ^{83}Sr , and ^{82m}Y to ^{82}Sr , was undertaken in search of more detailed information concerning the excited states of strontium isotopes for comparison with shell model and weak coupling model predictions.

Decay Modes of Nuclear States

Electromagnetic Transitions

i. Gamma Radiation

Since the theory of the electromagnetic interaction is well understood, selection rules governing the electromagnetic transitions by which excited states of nuclei decay can be determined and consequently much can be deduced about nuclear structure from the observation of gamma radiation.

When the wavelength of the emitted gamma ray is large compared to the nuclear radius an approximate expression for the transition rate between an initial state $|i\rangle$, labelled by total angular momentum J_i and its third component M_i , and a final state $|f\rangle$, similarly labelled by J_f and M_f , is given by¹²⁾

$$T_{if}(\sigma, \lambda, \mu) = \frac{8(\lambda+1)}{\lambda(2\lambda+1!!)^2} \frac{k^{2\lambda+1}}{\pi} |\langle f | O_{\lambda\mu}^{\sigma} | i \rangle|^2$$

where $O_{\lambda\mu}^{\sigma}$ represents a multipole operator of order λ with third component μ , and $\sigma = E, M$ denotes electric or magnetic multipole. Since the orientation of the nucleus is not of concern, this expression must be summed over all final orien-

tations M_f and averaged over initial orientations M_i of the nucleus. It is convenient to define the reduced matrix element

$$B(\sigma, \lambda) = \frac{1}{2J_i + 1} \sum_{M_i, M_f} |\langle f | O_{\lambda\mu}^\sigma | i \rangle|^2$$

Then

$$T_{if}(\sigma, \lambda) = \frac{2(\lambda+1)}{\lambda(2\lambda+1!!)^2} \frac{k^{2\lambda+1}}{4\pi} B(\sigma, \lambda)$$

From this expression for $T(\sigma, \lambda)$ selection rules governing changes in angular momentum and parity can be deduced for each type of multipole transition. These rules are shown in Table 1. Conservation of angular momentum forbids single gamma ray transitions connecting two zero spin states because a photon carries an intrinsic spin of one unit.

When a transition may proceed by emitting gamma rays of different multiplicities a question arises concerning which will predominate. A rough estimate of relative strengths of competing multipole radiations calculated with simple approximations for the matrix elements¹²⁾

$$\langle f | O_{\lambda\mu}^E | i \rangle \approx ZeR^\lambda$$

$$\langle f | O_{\lambda\mu}^M | i \rangle \approx \frac{Ae\hbar}{2Mc} R^{\lambda-1}$$

indicates that in general only the lowest possible order of multipole radiation contributes significantly. The most common

TABLE 1

	E1	E2	E3	E4
	Yes	No	Yes	No
$ \Delta J \leq$	1	2	3	4
	M1	M2	M3	M4
	No	Yes	No	Yes
$ \Delta J \leq$	1	2	3	4

exception to this rule is the mixing of M1 and E2 multiplicarities in some transitions.

Since the stability of a state against electromagnetic decay depends strongly on the multipolarity of the transitions which de-excite it, measurement of the half-life of an excited state gives an indication of the multipolarity of transitions from it. Tabulations of approximate lifetimes as a function of multipolarity and transition energy, based on single particle estimates, are available¹³⁾.

ii. Internal Conversion

Internal conversion, a process of nuclear de-excitation in which energy is transferred to an orbiting electron which subsequently escapes from the atom, competes with the emission of gamma rays of all multiplicarities. In the particular case of $0 \rightarrow 0$ transitions, for which gamma decay is entirely forbidden, internal conversion of atomic electrons is the dominant decay mode. (At energies greater than two electron masses (1.022MeV) internal pair creation becomes an important competing mechanism.)

The ratio of the rate of emission of conversion electrons, N_e , to the rate of emission of gamma rays, N_γ , is called the internal conversion coefficient, $\alpha = N_e/N_\gamma$, of the transition. Partial conversion coefficients may be defined according to the electron shell from which the converted electron was ejected and α comprises the sum of these partial coefficients.

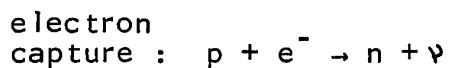
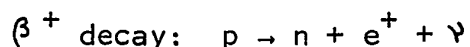
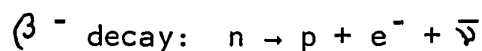
$$\alpha = \alpha_K + \alpha_L + \alpha_M + \dots$$

where K, L, M, etc. refer to the usual atomic electron shells.

The theory of the internal conversion process is well known¹⁴⁾ and predictions of coefficients as a function of Z, energy, and multipolarity are available.¹⁵⁾ A comparison of measured values to theoretical predictions may indicate the multipolarity of a transition, thus providing information helpful in determining level spins and parities.

Beta decay

Three types of fundamental nuclear beta decay processes have been observed:



In 1934 Fermi¹⁶⁾ put forward a theory of beta decay based on the statistical sharing of phase space between the two emitted leptons (electron and neutrino). His result for the number of electrons, $N(W)$, emitted in an energy interval, dW , is:

$$N(W)dW = KF(Z, W)pW(W-W_0)^2dW$$

where W is the electron energy; p is the electron momentum; W_0 is the total energy available in the decay; and K is the

factor containing the nuclear matrix elements. For allowed transitions K contains two types of matrix elements¹⁷⁾:

$$K = \frac{g^2}{2\pi^3} \cdot [C_V^2 |M_F|^2 + C_A^2 |M_{GT}|^2]$$

where g is a universal constant characteristic of beta decay, C_V and C_A are vector and axial vector interaction coupling constants, and M_F and M_{GT} are Fermi and Gamow-Teller matrix elements respectively. These matrix elements are due to the two nuclear beta moments which remain significant in the non-relativistic treatment of the interaction.

$$M_F = \langle f | T | i \rangle$$

$$M_{GT} = \langle f | \vec{\sigma} | i \rangle$$

$\vec{\sigma}$ is an axial vector operator whose components are the Pauli spin matrices. The conditions for these matrix elements to be non-zero are:

$$\begin{array}{lll} \text{for } M_F : & \Delta J = 0 & \Delta \pi = \text{no} \\ \text{for } M_{GT} : & \Delta J = 0, \pm 1 & \Delta \pi = \text{no} \quad \text{no } 0 \rightarrow 0 \text{ transitions} \end{array}$$

These rules can be interpreted in terms of the spin states of the emitted leptons. In a Fermi decay the leptons are emitted

in a singlet state, whereas in a Gamow-Teller decay the leptons are emitted in a triplet state.

For allowed transitions K does not depend on the energy, W , of the electron. Integrating $N(W)dW$ over all possible energy values one obtains the decay rate

$$\begin{aligned}\lambda &= \int_1^{W_0} K F(Z, W) p W (W - W_0)^2 dW \\ &= K f(Z, W_0)\end{aligned}$$

where $f(Z, W_0) = \int_1^{W_0} F(Z, W) p W (W - W_0)^2 dW$ and has been tabulated¹⁸⁾.

For a transition of half-life t , it is convenient to define the comparative half-life, ft , (usually quoted as $\log_{10} ft$ because it is a large number) which is inversely proportional to K . Thus, this number contains information concerning the nuclear structure effects in a decay and is useful in classifying beta decays into categories (Table 2). For other than allowed transitions $\log_{10} ft$ values are ambiguous.

Even when allowed transitions are not possible between two states, beta decay may proceed via higher order interactions which are weak compared to the allowed case, but still non-zero¹⁷⁾. These are called forbidden decays. The angular momentum and parity selection rules for allowed and forbidden decays are listed in Table 3.

TABLE 2

$\log_{10} ft$	Possible Transition Types
≤ 4.0	Superaallowed
≤ 5.8	Allowed
$5.8 \leq \log ft \leq 10.6$	Allowed or First Forbidden
$10.6 \leq \log ft \leq 15$	Allowed, First or Second Forbidden
$\log ft \geq 7.6$	First Forbidden Unique

TABLE 3

Transition Type	J	$\Delta\pi$
Allowed:		
Fermi	0	no
G.T.	0, 1	no
First Forbidden:		
non-unique	0, 1	yes
unique	2	yes
Second Forbidden	2, 3	no
Third Forbidden	3, 4	yes

Nuclear Isomerism

When the decay of an excited state may proceed only by a transition involving a large angular momentum transfer, a long-lived metastable or isomeric state may result¹⁹⁾.

Isomeric transitions have $\Delta J \geq 3$, hence are of multiplicities E3, M3, M4 and higher orders. Some isomeric transitions are so highly retarded that beta decay competes significantly with electromagnetic decay.

Isomers tend to occur in nuclei with N or Z just below the 'magic numbers'. It is in just these regions, according to the shell model, that nucleon shells with very different spins are filling. For example, as N or Z approaches fifty the $2p_{1/2}$ and $1g_{9/2}$ shells are partially filled and nuclei with isomeric states of $J^\pi = 1/2^-$ and $J^\pi = 9/2^+$ are abundant²⁰⁾. Other 'islands of isomerism' are observed near closed shells at N or Z = 82 and N = 126. Isomers with more complex structures involving several particles (or holes), so-called spin gap isomers, also occur.

CHAPTER II
A REVIEW OF PREVIOUS WORK

86, 86m_γ

Decay schemes have been published previously for the two activities associated with the decay of ^{86, 86m_γ}: a 14.6 hour ground state decay to levels in ⁸⁶Sr^{21,22} (Figure 1) and a 48 minute isomeric decay to levels in ⁸⁶Y²³ (Figure 2). The level structure of ⁸⁶Sr has also been probed via the ⁸⁷Sr(p,d) ⁸⁶Sr reaction²⁴. Among the states of ⁸⁶Sr observed in the last experiment was a sequence of even spin, even parity levels (Figure 3), identified as members of a $(1g_{9/2})_{\nu}^{-2}$ multiplet of states with seniority two.

83, 83m_γ

Some preliminary work concerning the decay of ^{83, 83m_γ} has been done by Kitching²⁵ who observed several gamma rays from this activity and proposed a tentative decay scheme (Figure 4) and by Turcotte²⁶ who measured the half-lives of ⁸³Y (7.06 ± 0.08 minutes) and ^{83m_γ} (2.85 ± 0.02 minutes) and found an isomeric state in ⁸³Sr (4.95 ± 0.12 seconds) at 258.8 keV energy. Doron and Blann²⁷ observed a 259.1 keV activity with a half-life of 2.6 ± .2 minutes which they assigned to ^{83m_γ} and several other unidentified gamma rays possibly associated with the decay of ^{83, 83m_γ}. During the course of the present work an additional tentative decay

scheme for ^{83}Sr , $^{83\text{m}}\text{Sr}$ (Figure 5) was published²⁸⁾ based on gamma ray singles spectra and the $^{84}\text{Sr}(d,t)^{83}\text{Sr}$ reaction results of Bercaw et al.²⁹⁾ Figure 6 compares level schemes for ^{83}Sr from weak coupling calculations¹¹⁾, shell model calculations¹⁰⁾ and experimental data²⁹⁾.

^{82}Y

Much confusion surrounds the decay and half-life of ^{82}Y . Several conflicting half-life measurements have been reported by experimenters using radiochemical techniques based on the growth of ^{82}Sr ^{30,31,32)}. Others report being unable to observe any ^{82}Y activity^{33,34)} and place an upper limit of 1.5 minutes on the half-life of ^{82}Y ³³⁾.

Inamura et al.³⁵⁾ have reported the observation of gamma rays in ^{82}Sr via the $^{74}\text{Ge}(C^{12},4n)^{82}\text{Sr}$ reaction and proposed a level scheme (Figure 7) for ^{82}Sr . Turcotte²⁶⁾ has observed gamma rays of energy 143.4, 147.2, 155.0, and 160.8 keV and half-life 22.80 ± 0.34 minutes, tentatively assigning them to the decay of ^{82}Y .

In Figure 8 is shown the ^{82}Sr level scheme from the effective interaction shell model calculation of Kitching et al.¹⁰⁾

FIGURE 1
A Partial Decay Scheme of $^{86}\text{gY} 21)$
Showing Levels up to 3 MeV

^{86}Sr
38 48

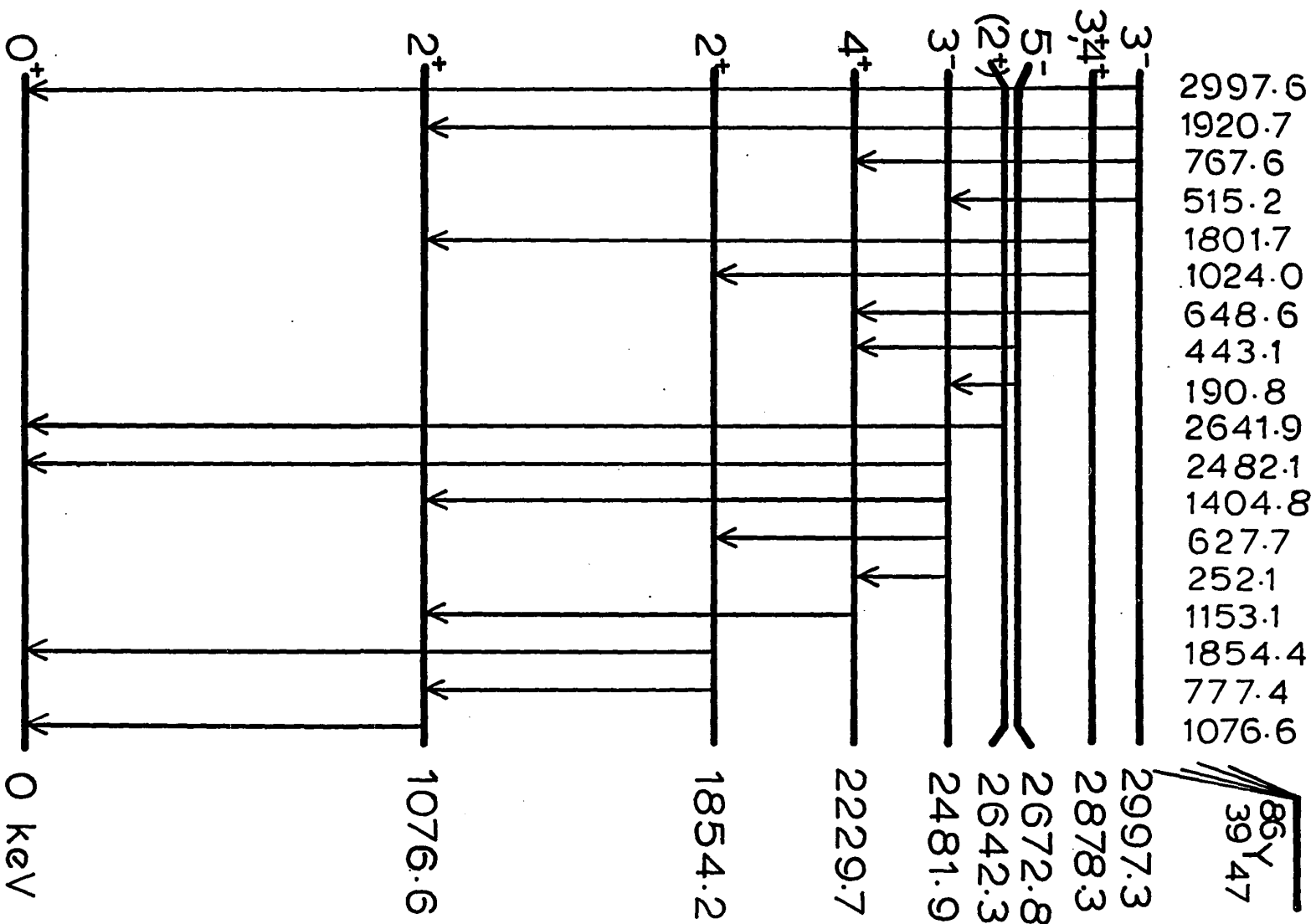
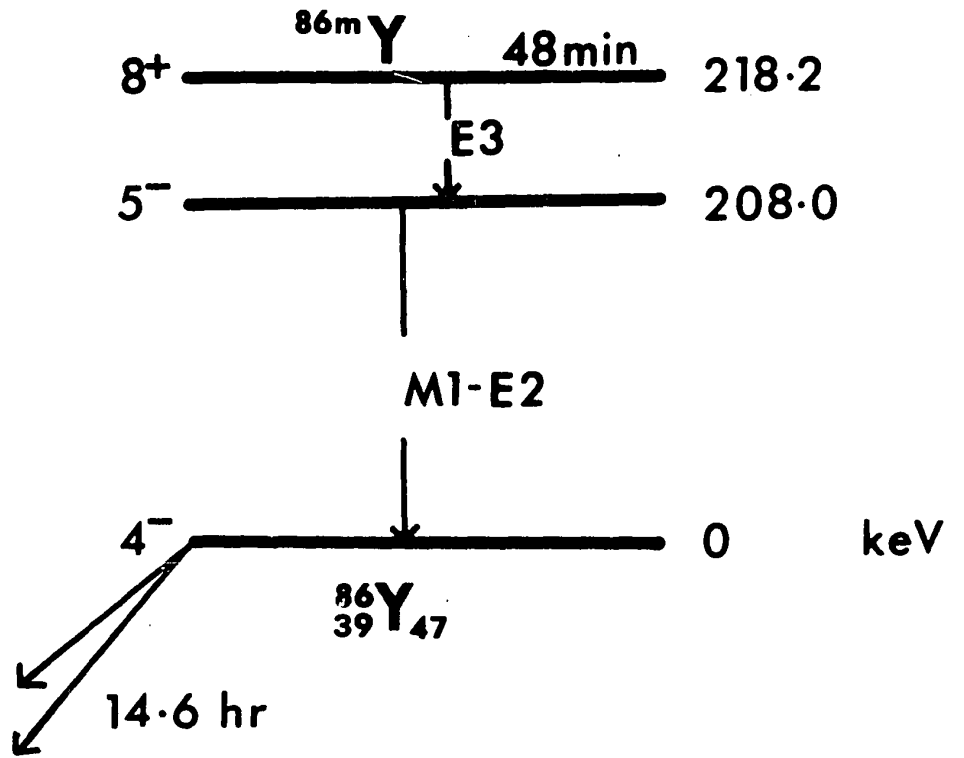


FIGURE 2

The Decay Scheme of ^{86m}Y Proposed by Kim et al. 23)



$^{86}_{38}\text{Sr}_{48}$

FIGURE 3
The $(1g_{9/2})_{\nu}^{-2}$ Multiplet of States
in ^{86}Sr (24)

J^π	E (MeV)	$\sigma/2J+1$
8^+	2.955	100
6^+	2.855	108
4^+	2.232	82
2^+	1.854	27
2^+	1.077	76
0^+	0	98

$^{86}_{38}\text{Sr}_{48}$

FIGURE 4
The Decay Scheme of $^{83}_{83m}\text{Y}$ Proposed by Kitching ¹¹⁾

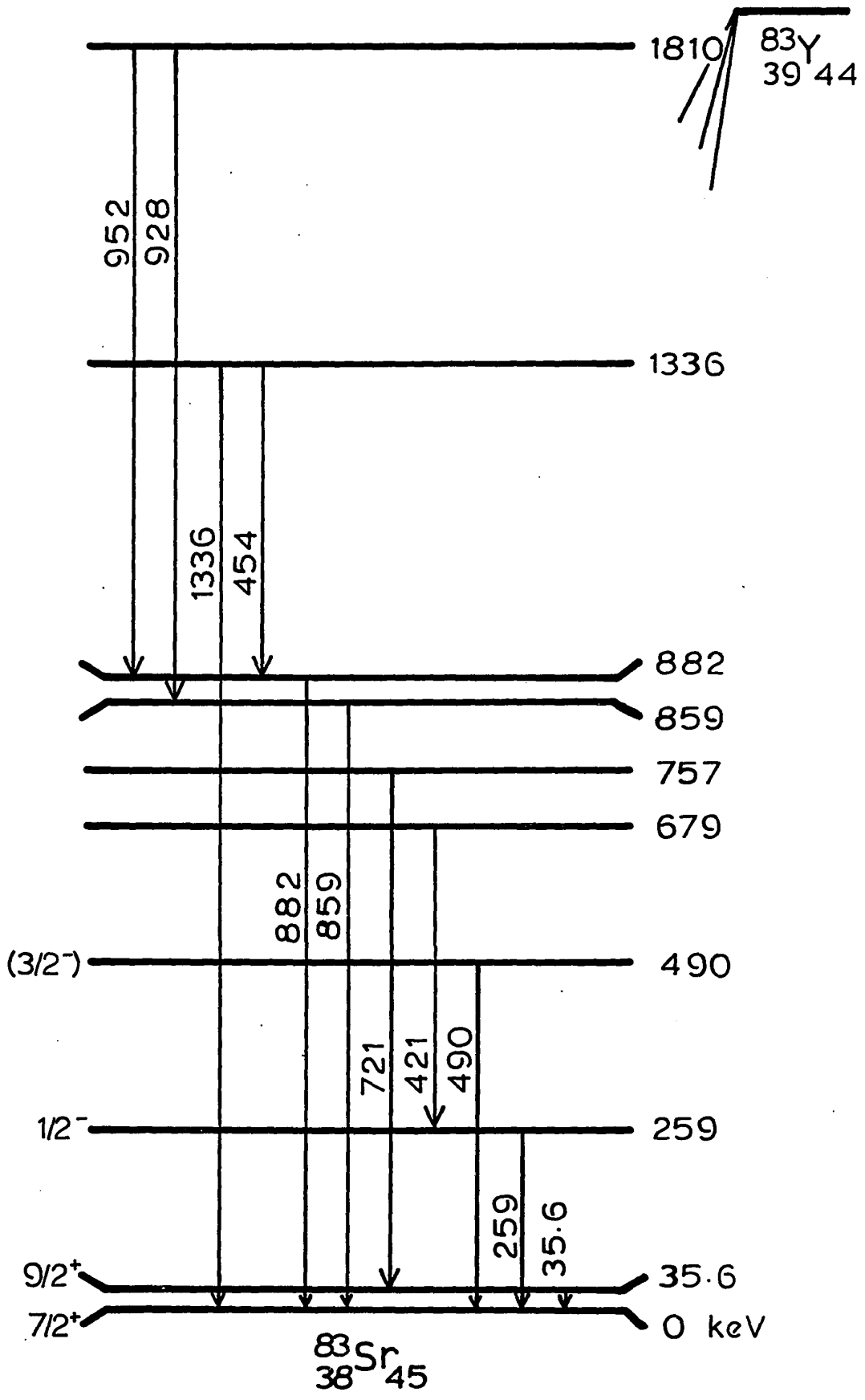


FIGURE 5
The Decay Scheme of ^{83}Rb , $83\text{m}\gamma$ Proposed
by Abdyrazakov et al. (28)

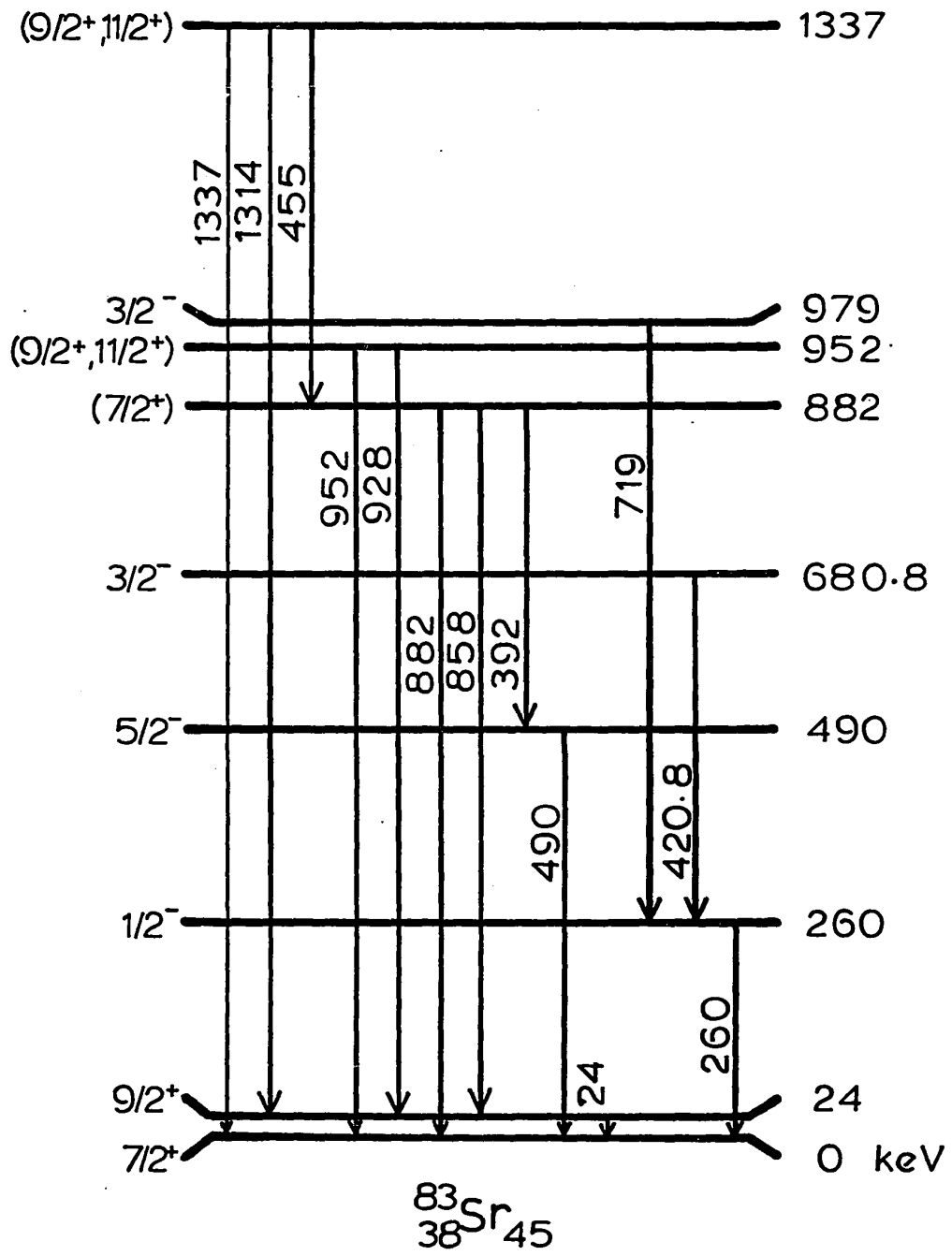
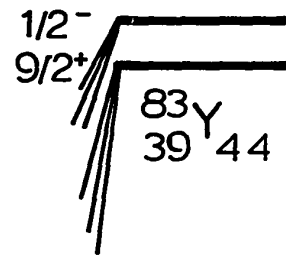


FIGURE 6

The Level Structure of ^{83}Sr 11)
(a) weak coupling model prediction 11)
(b) effective interaction shell model prediction 10)
Experimental results shown are those
of Bercaw et al. 29)

E (MeV)

^{83}Sr

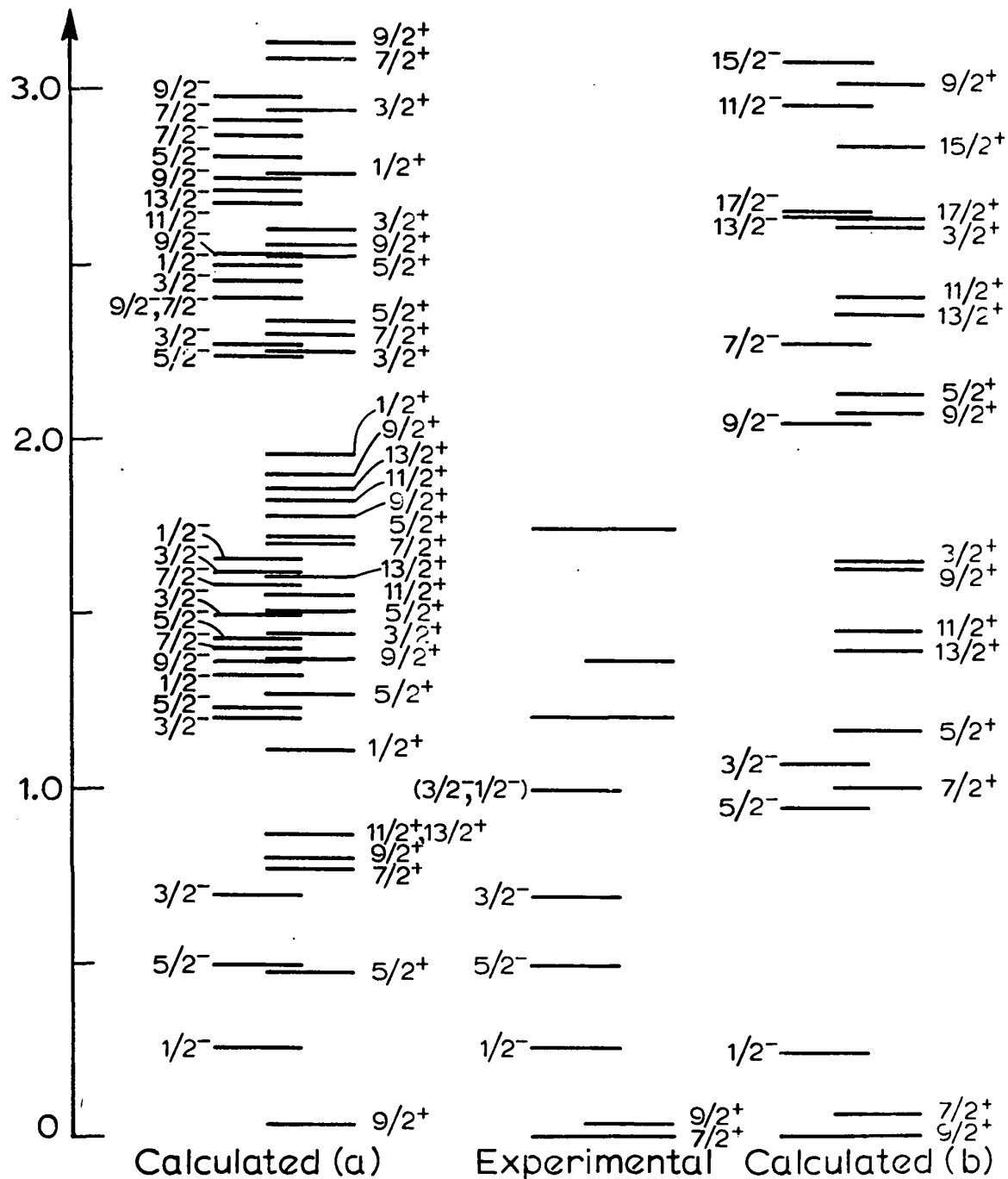


FIGURE 7
The Level Structure of ^{82}Sr from
 $^{74}\text{Ge}(\text{C}^{12}, 4\text{n})^{82}\text{Sr}$ Reaction Studies ³⁵⁾

6⁺----- 2.154

4⁺————— 1.332

2⁺————— 0.576

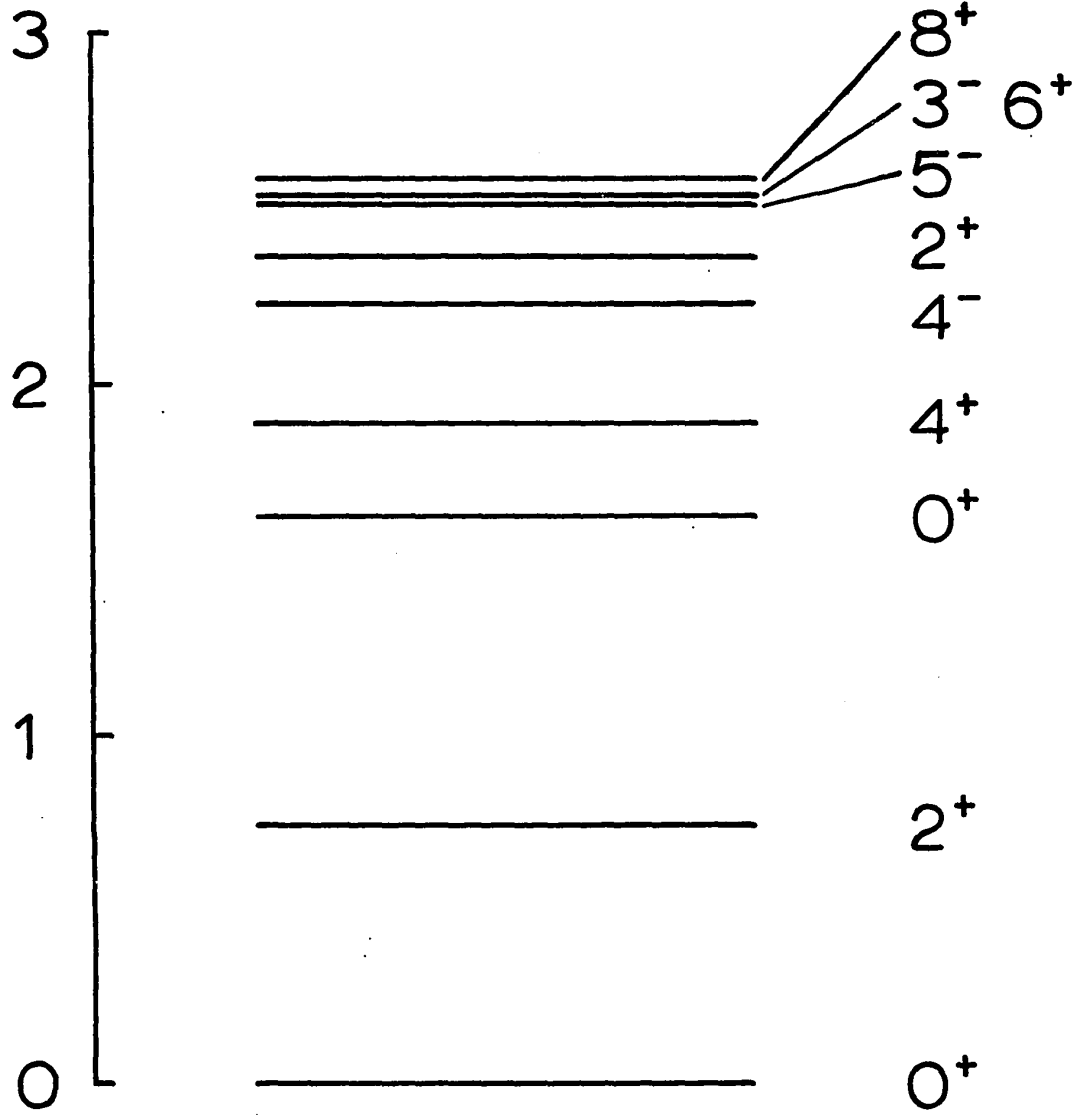
0⁺————— 0 Mev

$^{82}_{38}\text{Sr}_{44}$

FIGURE 8
The Level Structure of ^{82}Sr from the
Effective Interaction Shell Model Calculations
of Kitching et al. (10)

E (MeV)

J^π



$^{82}_{38}\text{Sr}_{44}$

CHAPTER III
EXPERIMENTAL TECHNIQUES

Source Preparation

Targets of enriched strontium isotopes (Table 4) were prepared by enclosing a few milligrams of powder in thin-walled aluminum tubing and firmly crimping the ends. The target was then clamped in an aluminum holder, attached to a water-cooled probe, and inserted into the McGill Synchrocyclotron for proton bombardment at appropriate energies to produce the reactions $^{87}\text{Sr}(p,2n)^{86,86m}\gamma$, $^{84}\text{Sr}(p,2n)^{83,83m}\gamma$, and $^{84}\text{Sr}(p,3n)^{82}\gamma$. Q-values for these reactions are shown in Table 5 and were extracted from published Q-value tables³⁶⁾ and mass tables³⁷⁾.

The Production of $^{86m}\gamma$

The reaction $^{87}\text{Sr}(p,2n)^{86,86m}\gamma$ was induced to populate the 8^+ isomeric level of $^{86}\gamma$ so that the possibility of a direct β^+ decay from this level to levels in ^{86}Sr could be investigated.

At low energies the (p,2n) reaction proceeds via the mechanism of the compound nucleus which generally favours the population of the low-lying, low spin member of an isomer pair³⁸⁾; but this effect can be somewhat mitigated by using high bombarding energies and high spin targets to shift the spin distribution of the compound nucleus toward higher values. In

TABLE 4

Analysis Enriched Isotope	% ^{88}Sr	% ^{87}Sr	% ^{86}Sr	% ^{84}Sr
$^{87}\text{Sr}(\text{NO}_3)_2$	5.99	93.29	0.72	0.05
$^{84}\text{Sr}(\text{NO}_3)_2$	12.49	1.56	3.71	82.24

TABLE 5
Beta Decay
and (p,xn) Reaction Q values³⁷⁾

Beta Decay	Q Value
$^{82}\text{Y} \rightarrow ^{82}\text{Sr}$	-8.4 MeV
$^{83}\text{Y} \rightarrow ^{83}\text{Sr}$	-5.1 MeV
$^{86}\text{Y} \rightarrow ^{86}\text{Sr}$	-5.2 MeV
Reaction	Q Value
$^{84}\text{Sr}(p, 2n) ^{83}\text{Y}$	17.3 MeV
$^{84}\text{Sr}(p, 3n) ^{82}\text{Y}$	30.7 MeV
$^{84}\text{Sr}(p, 4n) ^{81}\text{Y}$	41.5 MeV
$^{84}\text{Sr}(p, 5n) ^{80}\text{Y}$	55.2 MeV
$^{84}\text{Sr}(p, 6n) ^{79}\text{Y}$	67.8 MeV
$^{84}\text{Sr}(p, p5n) ^{79}\text{Sr}$	57.2 MeV
$^{84}\text{Sr}(p, \alpha 2n) ^{79}\text{Rb}$	21.5 MeV
$^{87}\text{Sr}(p, 2n) ^{86}\text{Y}$	14.5 MeV
$^{87}\text{Sr}(p, 3n) ^{85}\text{Y}$	24.0 MeV

the present work targets of ^{87}Sr (ground state spin $9/2^+$), bombarded at 25 MeV well above the (p,2n) reaction threshold, were employed with satisfactory results.

The possibility of using ^{86}Sr and the $^{86}\text{Sr}(p,n)^{86,86\text{m}}\text{Y}$ reaction to produce $^{86\text{m}}\text{Y}$ was discarded because of the low ground state spin (0^+) of ^{86}Sr .

The Production of 83 , $^{83\text{m}}\text{Y}$ and ^{82}Y

The isotope 83 , $^{83\text{m}}\text{Y}$ was produced via the $^{84}\text{Sr}(p,2n)^{83}$, $^{83\text{m}}\text{Y}$ reaction at 31 MeV proton bombarding energy. Bombardments of ^{84}Sr targets at 40 and 45 MeV were performed to produce $^{84}\text{Sr}(p,3n)^{82}\text{Y}$ reactions. In both instances ^{84}Sr was chosen as the target because it is the stable strontium isotope of lowest mass and in general cross sections for (p,xn) reactions are higher for lower x.

Gamma Ray Spectroscopy Sources

Gamma ray counting was usually performed without removing the samples from their aluminum casings. No troublesome activities were observed arising from proton reactions on the aluminum tubing or on the oxygen and nitrogen in the strontium nitrate [$\text{Sr}(\text{NO}_3)_2$] targets²⁰⁾.

In some experiments it was necessary to separate the yttrium which was the object of study from interfering strontium and rubidium activities. This was accomplished by standard chemical techniques³⁹⁾.

After bombardment the target material was dissolved in water containing a small amount of Y^{+++} carrier. Addition of concentrated ammonium hydroxide (NH_4OH) precipitated the yttrium as yttrium hydroxide ($Y(OH)_3$) but left the strontium and rubidium in solution. The solution containing the gelatinous $Y(OH)_3$ precipitate was passed through a glass fibre filter paper and the residue washed several times with dilute NH_4OH to remove trapped strontium and rubidium. No known strontium or rubidium activities were observed in the initial spectra of sources treated in this way, indicating a clean separation.

Electron Spectroscopy Sources

Because electrons lose energy rapidly in passing through any material, samples for electron counting were removed from the aluminum cases in which they were bombarded and deposited in a thin layer on a foil holder. The manufacture of thin sources was accomplished by two different methods: electrodeposition and evaporation of an aqueous solution.

Figure 9 is a sketch of the system used for electrodeposition of thin sources. It is a much simplified version of the system designed by Carter⁽⁴⁰⁾ to make thin sources of krypton. After bombardment the finely divided radioactive powder was placed on an aluminum foil on the cathode in the central area defined by a teflon insulating cap and the electrode was inserted into the system. After evacuation of the chamber a voltage of approximately 1500 volts was applied across

the terminals. The pressure in the chamber was controlled by means of a stopcock to maintain a glow discharge in the tube. The duration of electron bombardment was chosen in keeping with the half-life of the activity under study. At the end of the deposition process excess powder was shaken off the foil and the source was introduced into the the spectrometer system. This technique made possible the fabrication of samples of activity that were very thin but relatively weak due to inefficient deposition.

The second method of sample preparation resulted in stronger sources of activity since no material was lost. The radioactive target material was dissolved in a drop of water on a holder and the water evaporated in a hot oven. The holder was designed to fit a plexiglass mount in the detector chamber. This method of electron source production resulted in the saving of time and target material at the price of slight deterioration of energy resolution because of increased source thickness.

Gamma_Ray_Detectors

The gamma ray detectors employed in this study were of the high resolution, cooled, lithium drifted germanium type, generally referred to as Ge(Li) detectors. Table 6 lists the various counters used and some of their significant parameters.

TABLE 6

Gamma Ray Detectors Used in This Work

Model & Serial No.	Eff. rel. to 3" x 3" NaI(Tl) at 25 cm.	Resolution FWHM on 1.33 MeV Co ⁶⁰ line	Peak /Compton ratio for 1.33 MeV Co ⁶⁰ line
LGTC - L622	4.85%	2.5 keV	25/1
L364 - LGC	4.0%	3.45 keV	-
LGTC - L831	10.9%	2.0 keV	36/1
LGTC - L813	8.0%	2.0 keV	35/1

In addition an Ortec X-ray spectrometer (GX-R17-8113-10500) was used with resolution:

- 400 ev at 6.4 keV
- 550 ev at 59.5 keV
- 850 ev at 208 keV

The Electron Detector

A Simtec diffuse junction detector 500 μ thick with 100 mm² area was used to detect conversion electrons. The efficiency of a charged particle detector is 100% – that is, every particle falling on the detector will deposit some energy. If, however, the device is to be used as an energy spectrometer, a detector thick enough to stop the electrons in the energy range of interest, causing them to lose all of their energy in the detector and thus contribute to a 'full energy' peak, is required. In this study the most energetic electrons measured were the conversion electrons from the 388 keV transition in ^{87m}Sr. From range-energy graphs for electrons in silicon⁴¹⁾ it can be seen that a 500 μ thick detector can stop electrons of energies up to approximately 425 keV. To reduce noise levels the detector was cooled to liquid nitrogen temperature during operation and leads to the preamplifier were made as short as was feasible. To prevent deterioration of energy resolution due to electrons' losing energy in intervening atmosphere and condensation on the face of the detector both the source of activity and the detector were mounted in an evacuated chamber for counting. Source-detector geometry is illustrated in the schematic drawing of the counting chamber (Figure 14).

Experimental Configurations and Procedures

Energy and Half-life Measurements

The initial step in the investigation of the decay scheme of an isotope is the identification by energy and half-

life of the gamma rays belonging to that decay. These measurements were performed with the experimental set-up represented schematically in Figure 10.

Targets were bombarded for appropriate times depending on the reaction cross-sections for production and the half-life of the desired activity. Successive spectra were collected for equal time intervals to trace the growth and decay of gamma rays from the target. To obtain accurate half-life values deadtime corrections were necessary.

The major source of deadtime in this system was the multichannel analyzer (ADC). From the time this unit was triggered by a pulse at the input to the time that pulse had been digitized and recorded in the memory the ADC input was disabled. This processing time consisted of two parts — a fixed period of approximately 15 μ sec due to the time required for the incoming pulse to reach its full height and the time required to store the datum in the memory, and a variable digitization time depending on the pulse height and on the digitizing rate of the analyzer. For example, the time necessary for a 100 Mhz ADC to analyze a pulse and record it in channel 4000 would be the fixed 15 μ sec period plus 40 μ sec for digitization. The higher the countrate, the larger was the percentage of the events counted by the detector which was lost due to system deadtime. To monitor these losses the output from a standard pulser was fed into the preamplifier and analyzing system and scaled as well. The ratio of pulser pulses counted by the

scaler to pulser pulses recorded by the analyzer was the deadtime correction factor. Care was taken in choosing counting intervals to ensure that the count rate did not change by more than a factor of two in any interval, and the error in the deadtime correction factor due to varying count rate was therefore negligible. Some half-life measurements were performed with the rapid extractor and automated counting system described by Turcotte²⁶⁾. A different deadtime correction method was required for this system since a pile-up rejection unit, not the ADC, was the principal source of deadtime.

Calibration of the energy scale in each experiment was based on a comparison with gamma ray peaks of well-known energies from the spectra of standard sources (Appendix 1) which were recorded just prior to or immediately after a counting experiment under similar conditions or recorded simultaneously with the spectra to be analyzed. Simultaneous counting of standard and unknown ensured that no discrepancies were introduced by gain shifts due to counting rate differences, but it also presented the problem of standard peaks masking portions of the spectrum. A least squares fit to a quadratic polynomial, calculated by means of the PDP-8 computer, was used to fit the calibration peaks in some experiments. In other experiments a calibration was made using a linear fit to several close-lying states to determine the energy of an unknown peak. These techniques produced consistent energy measurements.

For each Ge(Li) detector in the laboratory a relative efficiency versus gamma ray energy curve has been established based on standard sources. These efficiency curves were utilized in making the relative intensity corrections necessitated by the variation of detector efficiency with energy. The efficiency curves of some detectors were redetermined after a period of time to check for deterioration of efficiency. No changes were found.

Gamma Ray Coincidence Measurements

Gamma ray coincidence experiments are a useful tool in the investigation of nuclear decay schemes since they may identify members of gamma ray cascades. The relative intensities of cascade members, corrected for internal conversion, when this process is significant, can suggest the ordering of the levels. The probable decay schemes constructed from this information can be compared with evidence from measurements of gamma ray multipolarities, beta decay measurements, and direct reaction experiments concerning level spins and parities.

A difficulty encountered in investigating nuclei possessing metastable levels is that any gamma rays from states whose lifetimes are long compared to the resolving time of the coincidence unit will not appear as members of a cascade; therefore, coincidence experiments alone cannot determine whether a cascade feeds the ground state of a nucleus or a long-lived excited state.

In an experiment measuring coincidence between two cascading gamma rays with a disintegration rate of N per second the singles and true coincidence count rates are:

$$N_1 = N\epsilon_1 w_1 \quad N_2 = N\epsilon_2 w_2 \quad N_T = N(\epsilon_1 w_1)(\epsilon_2 w_2)$$

where ϵ , w are efficiency and solid angle factors for the two detectors. Since the counters also detect radiations other than the two coincident gamma rays, chance coincidence events are also registered. The chance coincidence rate is given by

$$N_C = 2tN_1'N_2'$$

where t is the resolving time of the coincidence unit and N_1' , N_2' are the total singles count rates at the coincidence unit inputs. It is essential to design coincidence experiments with reasonable true-to-chance coincidence ratios.

The Coincidence Circuit Electronics

The fast-slow coincidence circuit illustrated in a block diagram (Figure 11) allowed the simultaneous collection of up to four coincidence spectra. The two Ge(Li) counters were positioned at right angles to each other as shown in Figure 12 to eliminate annihilation radiation (511keV) coincidence events and shielded with a lead slab to prevent gamma rays scattered in one counter from entering the other.

Energy pulses from Ge(Li) #1 were processed by a cooled, charge sensitive preamplifier and fed into a Tennelec (TC203BLR) linear amplifier for shaping and amplification. Output from this amplifier was directed to an Ortec 455 timing single channel analyzer (TSCA) to generate a timing pulse for the coincidence circuitry and through a delay amplifier to the input of one analogue to digital converter (ADC), hereafter referred to as the X ADC.

The TSCA generated a logic pulse, or time marker, for each input pulse in an energy range defined by adjustable bias levels. In this case the discriminator levels were set to accept all pulses above the noise level. Of the time mark generation modes offered by the Ortec 455 unit, constant fraction of pulse height timing (CFPHT) with small fractions proved to be the best choice in most instances. For all methods of timing used the timing 'walk' could be reduced to 10 to 15 nsec over a dynamic range of ten by use of the built-in walk adjustment facility. There was a delay, continuously variable from 0.9μ sec to 11μ sec between the input and output pulses. The output of the TSCA was fed into an Ortec 414a fast coincidence unit.

Energy pulses from Ge(Li) #2 were used to drive the gating circuitry in the coincidence system. Output from this detector was processed by a preamplifier and linear amplifier similar to those connected with Ge(Li) #1. Pulses from the amplifier were fed to an Ortec 455 TSCA and to the energy signal inputs of four Ortec 413 strobed single channel analyzers.

The TSCA discriminators could be set to include only the portion of the spectrum on which 'energy windows' were to be set, thus eliminating many unwanted coincidences. The output of this TSCA was fed to an input of the fast coincidence unit with its resolving time set so that if pulses arrived at both inputs within 120 nsec of each other a standard logic pulse was generated at its input. Pulser pulses fed into the test inputs of both Ge(Li)s' preamplifiers were used to set TSCA adjustable delays to ensure that real coincidence events would be registered as such by the coincidence unit, and to measure its resolving time. Tests for good coincidence adjustment were made using known gamma ray cascades, e.g. the ^{60}Co lines at 1.13 Mev and 1.17 Mev²⁰⁾. The coincidence output signals were sent to an Ortec 416 gate and delay generator to be suitably lengthened for use as gating signals at the X and Y ADC's.

Pulses from the TSCA were also employed to trigger the four SSCA's. The energy pulses from the amplifier were fed into the signal inputs of these SSCA's and the discriminator levels of each unit set to accept a narrow band of pulse heights, thus defining four energy windows. An SSCA would produce an output pulse only when simultaneously it was strobed by the TSCA output and received an energy pulse in the designated range.

Signals from the SSCA's were fed into a routing box (circuit diagram in Figure 13). This module generated a square output pulse whose amplitude depended on which input

was stimulated. This set of pulses, their origin identifiable by their height, was stretched and sent to the Y ADC. The amplitude of the routing pulses could be adjusted so that when a coincidence event occurred and the output of the fast coincidence unit opened the ADC gates, the event was recorded in a two-dimensional array labelled by energy according to the pulse height of the input to the X ADC and by coincidence group according to the routing pulse height — that is, events coincident with each of the four windows were sorted into four spectra stored in different quadrants of the system memory.

Data was stored in a Nuclear Data 2200 System Analyzer with a 4096 channel memory and later transferred to magnetic tape for processing on the PDP8 computer.

Internal Conversion Coefficient Measurements

To determine the K-electron internal conversion coefficient, α_K , of a transition it was necessary to measure the ratio of I_{e_K} , the K-conversion electron intensity, to I_γ , the corresponding gamma ray intensity. This entailed consideration of the effects of detector efficiencies and solid angle factors on the areas of the peaks from both counters.

Consider a source of activity with at least one transition for which α_K is known and one or more transitions for which α_K is to be measured. For the known transition

$$\alpha_K = \frac{I_{e_K}}{I_\gamma} = \frac{N_e / \omega_e \epsilon_e}{N_\gamma / \omega_\gamma \epsilon_\gamma} = \frac{N_e}{N_\gamma} \cdot \frac{\epsilon_\gamma}{\epsilon_e} \cdot \frac{\omega_\gamma}{\omega_e}$$

where N is the number of counts in the peak recorded by the detector; ϵ the efficiency of the detector; ω the solid angle correction; and subscripts e and γ denote the electron and gamma ray data respectively. Similarly for the transition of which the coefficient α_K^i is to be determined

$$\alpha_K^i = \frac{I_{eK}^i}{I_{\gamma}^i} = \frac{N_e^i}{N_{\gamma}^i} \cdot \frac{\epsilon_{\gamma}^i}{\epsilon_e^i} \cdot \frac{\omega_{\gamma}}{\omega_e}$$

If the electron detector is thick enough to stop the electrons from both transitions then $\epsilon_e = \epsilon_e^i$ for full energy peaks. Since the two transitions were observed simultaneously from the same source the solid angle factor ω_{γ}/ω_e is the same for both. Then

$$\alpha_K^i = \alpha_K \cdot \frac{N_e^i \epsilon_{\gamma}^i}{N_{\gamma}^i} \cdot \frac{N_{\gamma}}{N_e \epsilon_{\gamma}}$$

- The ratio of efficiencies ϵ_{γ}^i to ϵ_{γ} can be found from the relative efficiency curve for the gamma ray detector. Then α_K^i can be calculated from knowledge of α_K and experimental data.

With reliably reproducible source geometry it was possible to use standard sources counted separately from the unknown to calibrate the system.

The Counting Chamber

The vacuum chamber sketched in Figure 14 was used in the measurement of internal conversion coefficients. A diffuse junction electron detector was mounted on a movable sleeve which contained a reservoir of liquid nitrogen to cool the detector. When it was necessary to open the main chamber to change samples the detector could be retracted, isolated by a vacuum gate, and maintained under vacuum to prevent condensation on the detector face. It was prudent to shield the detector from light when it was biased to prevent damage to the field effect transistor (FET) in the preamplifier.

Samples of radioactivity were mounted in a plexiglass holder which was rigidly attached to the transparent inner lid of the counting chamber. This arrangement facilitated the alignment of the sample with both detectors and made the position of the sample reproducible for consecutive samples. A light-tight aluminum cap was placed over the plexiglass mount.

Opposite the electron detector sleeve was a concave sleeve into which could be inserted a Ge(Li) detector for gamma ray counting.

The Electronics

The electronic circuitry illustrated schematically in Figure 15 served to linearly amplify the signals from the electron and gamma ray counters. The Nuclear Data ND2200 System Analyzer in Dual Singles experiment mode was used to collect and store the gamma ray and electron spectra simultaneously.

FIGURE 9
Apparatus for Electrodeposition
of Thin Electron Sources

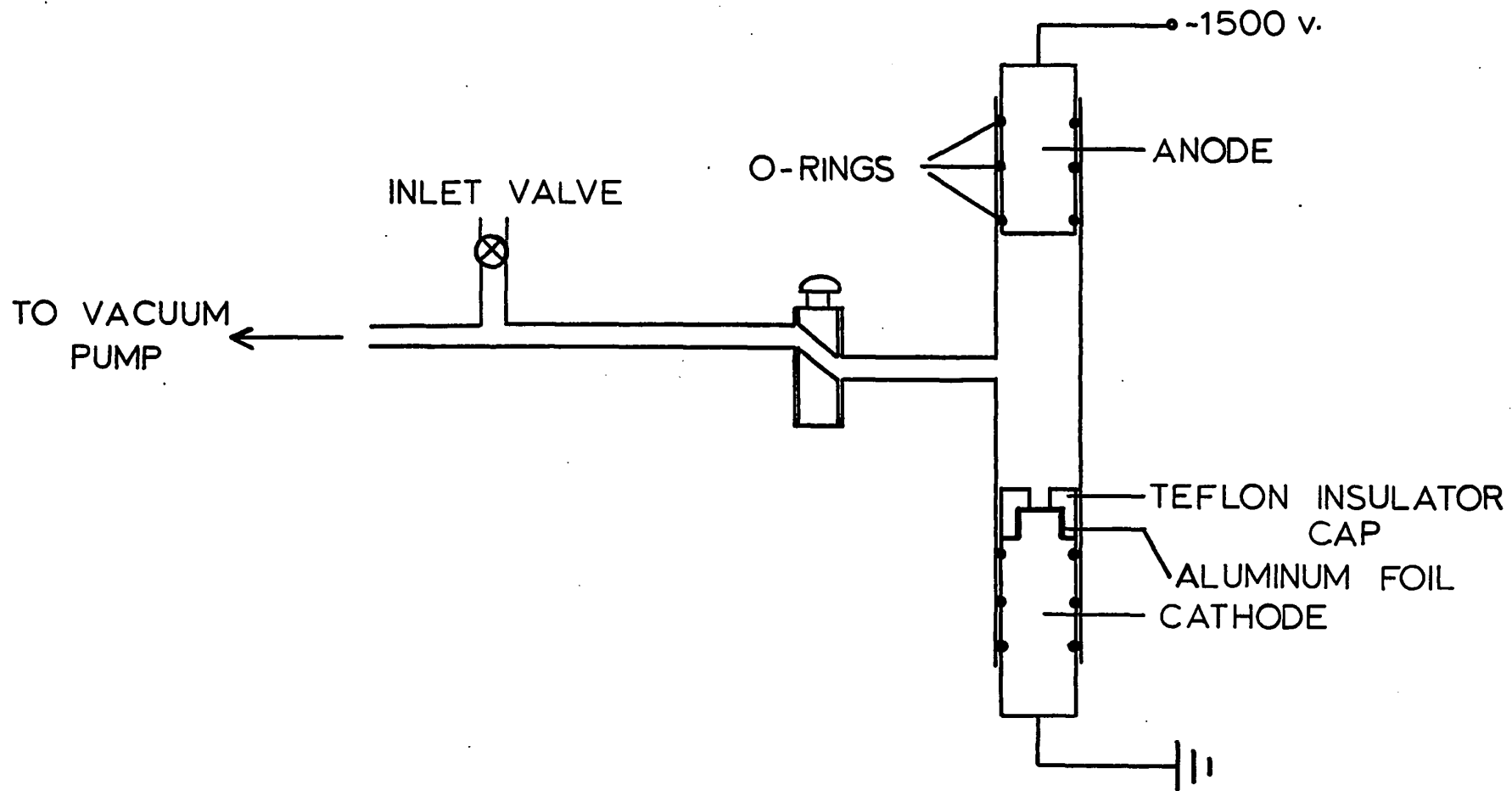


FIGURE 10
Counting System for Energy
and Half-life Measurements

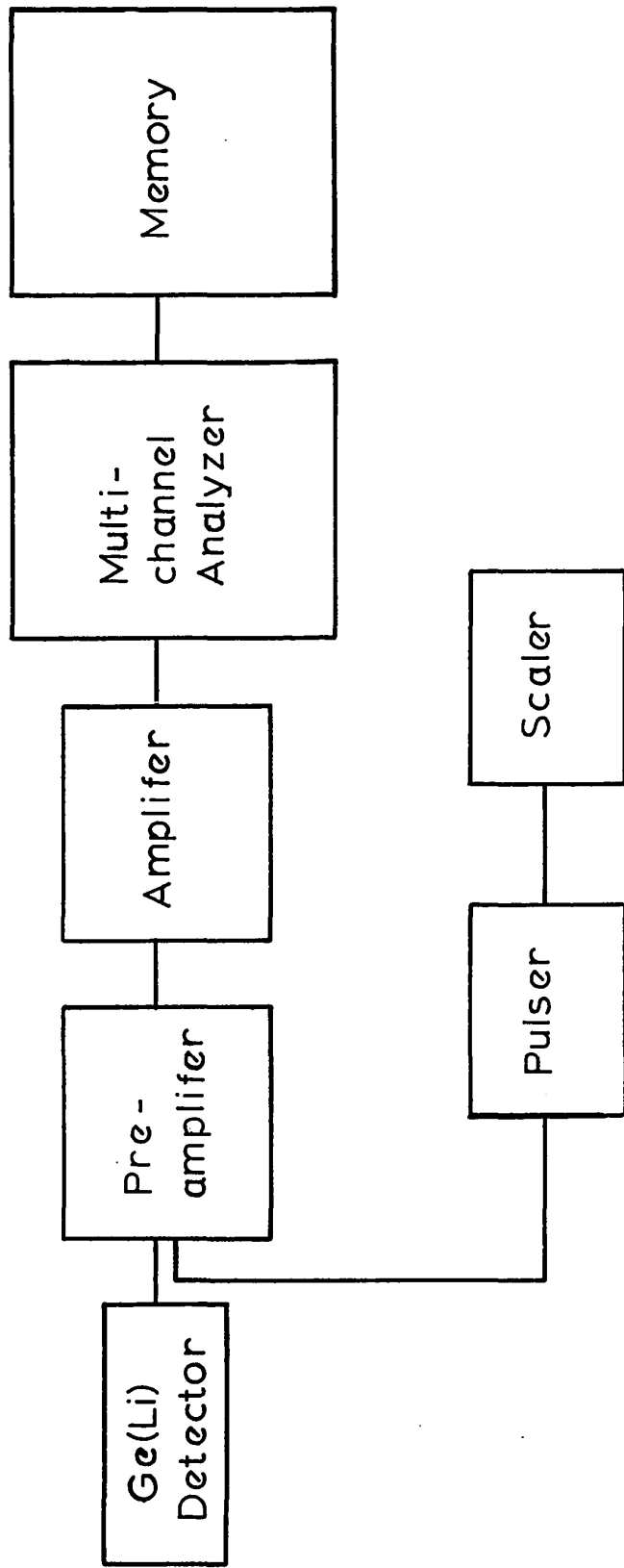


FIGURE 11
Fast-slow Coincidence Circuit

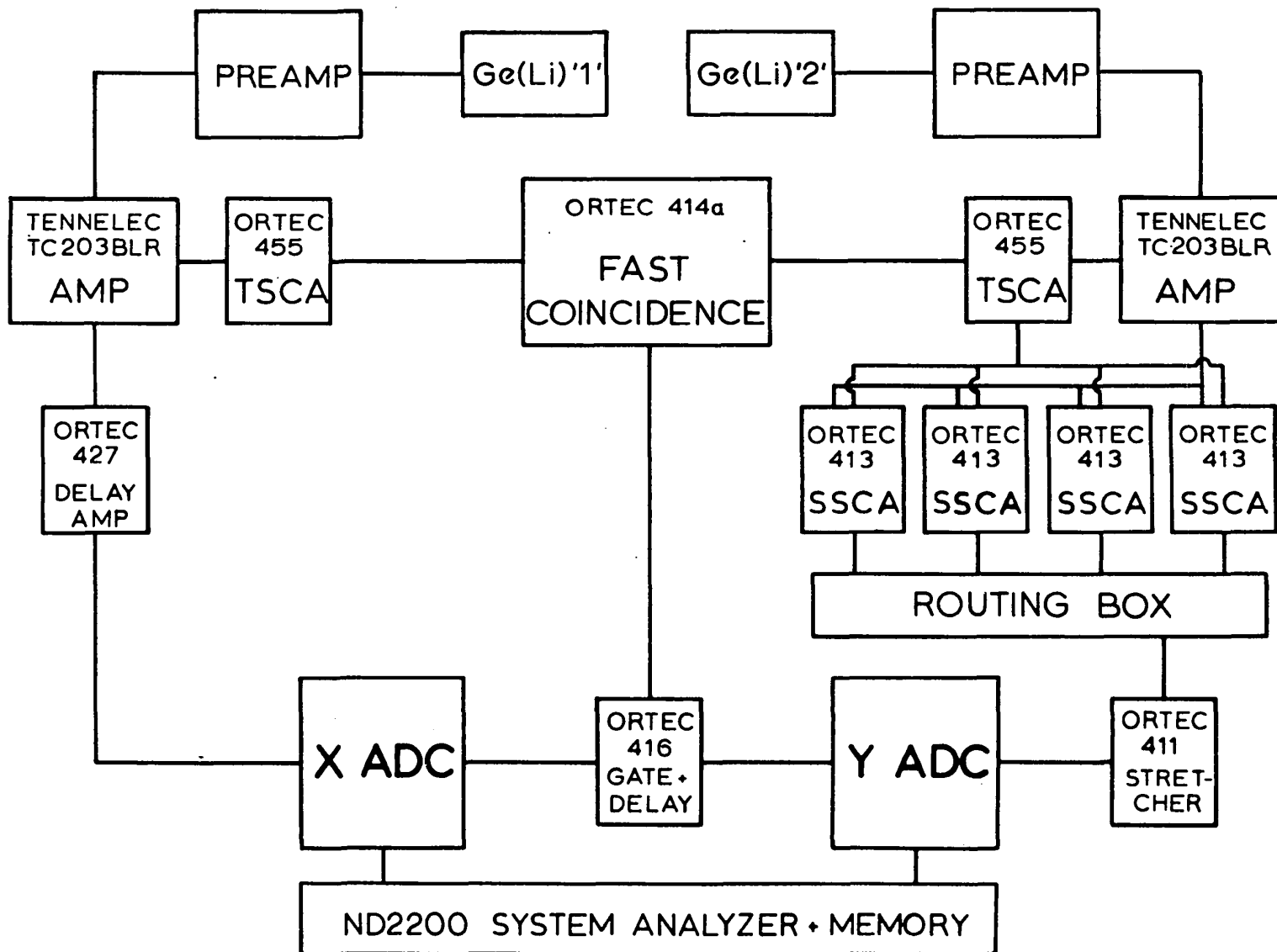


FIGURE 12

Detector Configuration for Coincidence Experiments

1. Source position
2. Lead shielding
3. Ge(Li) detector #1
4. Preamplifier for Ge(Li) detector #1
5. Ge(Li) detector #2
6. Preamplifier for Ge(Li) detector #2

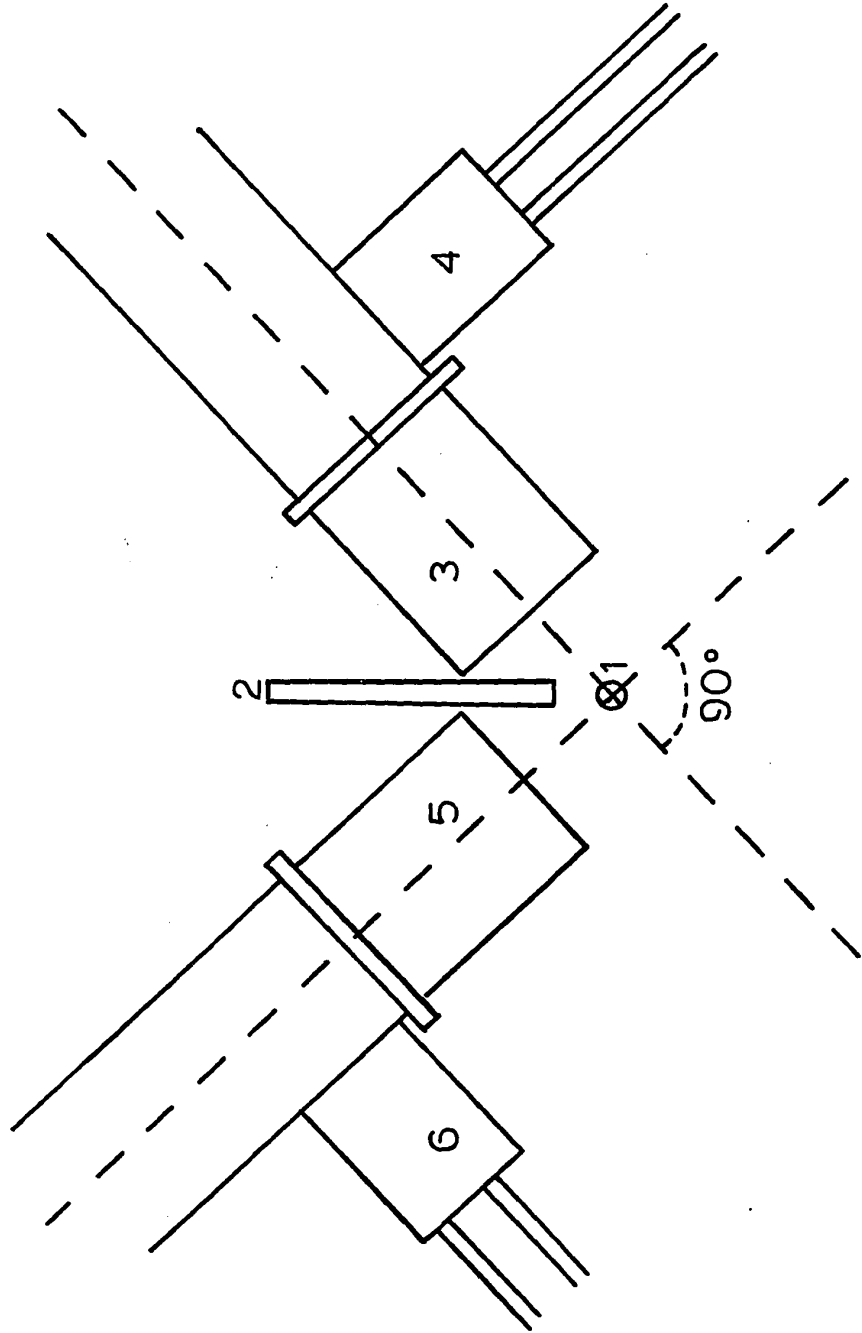


FIGURE 13

Circuit Diagram of Routing Box Used in
Coincidence Experiments.
(All inputs have 1K resistor to ground across them)

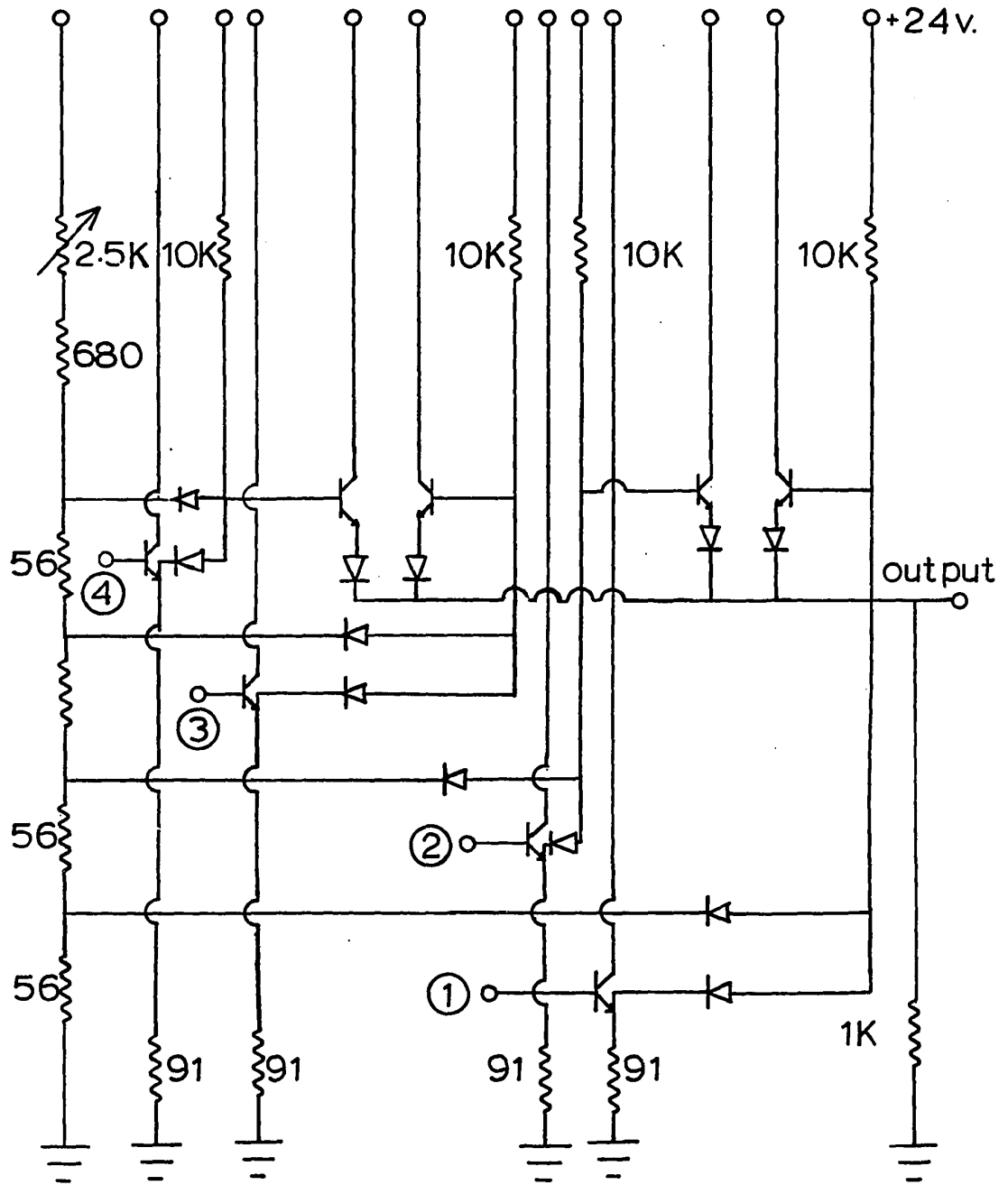


FIGURE 14

Vacuum Chamber for Internal Conversion Measurements

1. Ge(Li) detector
2. Sample
3. Electron detector
4. Liquid nitrogen reservoir
5. Preamplifier for electron detector
6. Vacuum gate
7. Cold trap
8. Vacuum gauge
9. Movable sleeve

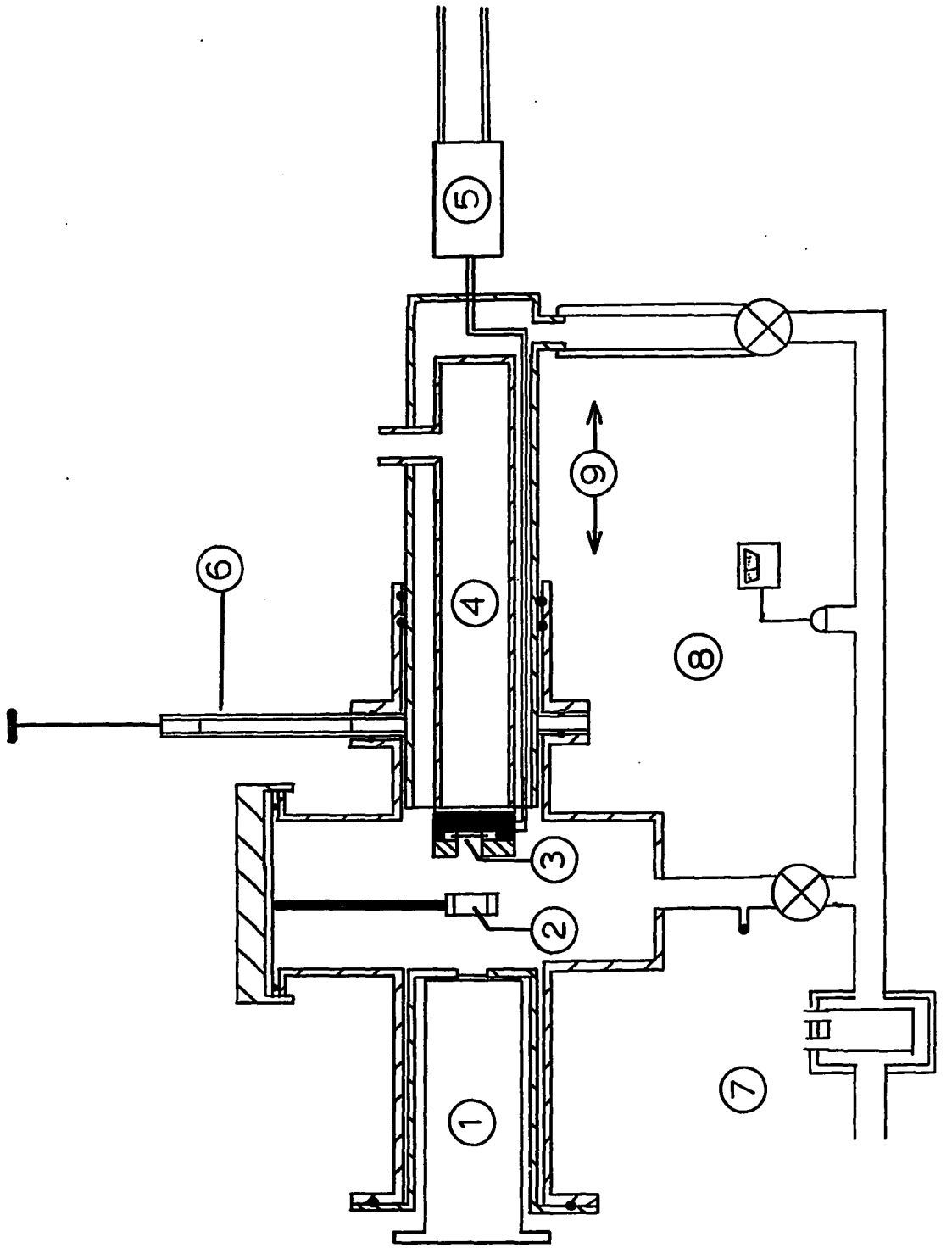
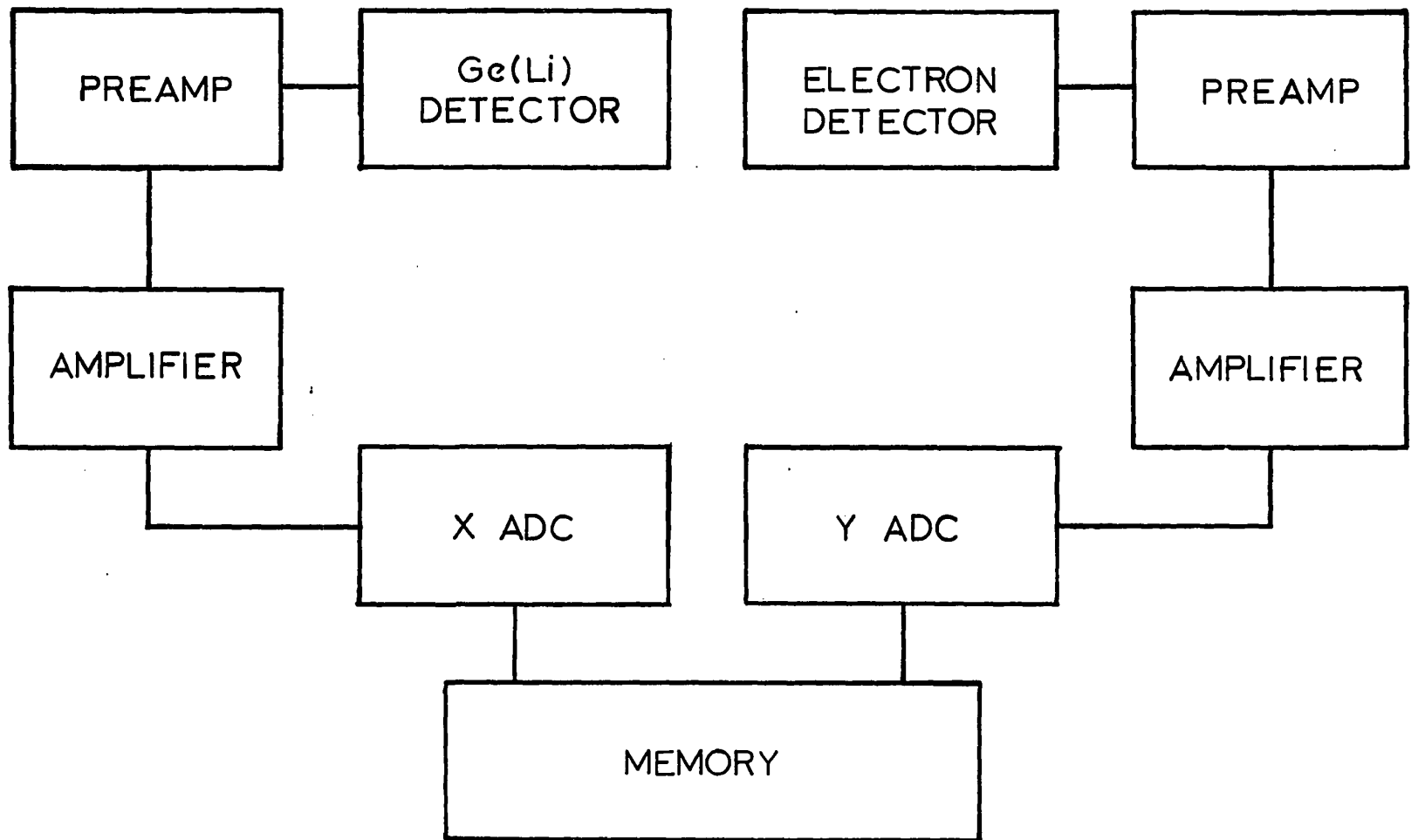


FIGURE 15
Counting System for Internal Conversion Measurements



CHAPTER IV
THE DECAY OF ^{86m}Y

The Background

Two activities associated with the decay of ^{86m}Y have previously been reported: a 14.6 hour ground state decay^{21,22} (Figure 1) and a 48 minute isomeric activity²³. For the latter activity Kim et al.²³ identified two electromagnetic transitions of 10.2 keV and 208.0 keV to other levels in ^{86}Y but no beta decay branch from ^{86m}Y to ^{86}Sr . The decay scheme they proposed is shown in Figure 2. In the course of conversion electron studies of ^{86m}Y the K and L conversion lines of a 98.5 keV transition with roughly the same half-life as the isomeric state, but converted in strontium, were observed. The relation of this transition to the level structure of ^{86}Sr was not established.

An $^{87}\text{Sr}(p,d)^{86}\text{Sr}$ reaction study¹⁰ resulted in the observation of a series of even spin, even parity levels at 2955 keV (8^+), 2855 keV (6^+), 2232 keV (4^+), 1077 keV (2^+) and 0 keV (0^+) and the tentative identification of these levels as members of the $(1g_{9/2})_{\nu}^{-2}$ multiplet of 'shell model' states. The existence of an 8^+ state of this character in ^{86}Sr strongly suggested the possibility of a direct beta decay branch feeding it from the 8^+ isomeric level of ^{86}Y , especially if this 8^+ isomeric level were due predominantly to the $(1g_{9/2})_{\pi} (1g_{9/2})_{\nu}^{-3}$ configuration as proposed by Kim et al.²³.

The present work was undertaken to clarify the situation. While this work was in progress the results of a study⁴²⁾ of the electromagnetic transition properties of the suggested $(1g_{9/2})_{\nu}^{-2}$ multiplet in ^{86}Sr revealed that the 8^+ state at 2955 keV decays with a half-life of $(0.46 \pm 0.03)\mu$ sec to the 6^+ level and then to 4^+ , 2^+ , and 0^+ levels in succession via pure E2 transitions.

Experimental Results

By means of a half-life analysis of the gamma rays in the recorded spectra the two previously reported activities from the decay of ^{86}Y and ^{86m}Y , and contaminants arising from reactions other than $^{87}\text{Sr}(p,2n)^{86}\text{Y}$ were identified. In addition to the gamma rays observed by Ramayya et al.²¹⁾ and Kim et al.²³⁾ a weak gamma ray at 98.6 ± 0.1 keV was observed which decayed with the same half-life as the 208.2 ± 0.2 keV gamma ray assigned to the decay of ^{86m}Y . The relative intensity of the 98.6 keV gamma ray to the 208.2 keV gamma ray was $(0.35 \pm 0.02)\%$. In Figure 16 the portion of the spectrum showing these two transitions and an insert comparing their half-life plots are displayed. Close scrutiny of the half-life curves of all the gamma rays in the spectrum revealed that three gamma rays of 627.7 ± 0.2 keV, 1153.1 ± 0.3 keV, and 1076.6 ± 0.2 keV energy associated with the 14.6 hour decay had weak shorter lived components, compatible with a 48 minute decay, in their half-lives (Figure 17).

Coincidence measurements were performed using the system (Figure 11) described earlier, with three windows set as indicated in Figure 16: one on the 98.6 keV peak, and one above and one below to monitor coincidences with 'background' events. Figure 18 presents for comparison relevant portions of a gamma ray singles spectrum of the 14.6 hour ^{86}Y decay, and coincidence spectra gated by the 98.6 keV gamma ray, by the window above this gamma ray, and by the 98.6 keV window after the 48 minute activity had been allowed to decay. Strong coincidences between the 98.6 keV transition and the 627.7 keV, 1153.1 keV, and 1076.6 keV transitions are evident. The 98.6 keV coincidence spectrum was approximately corrected for background and chance coincidence contributions by comparing the number of counts, in this spectrum and in the spectra gated by the background monitoring windows, in the 208.2 keV peak, a known metastable level which could not be in true coincidence with any gamma ray. After further corrections for detector efficiency the three coincident peaks were found to have equal intensities to within an experimental error of 10%.

In the ^{86}Y decay scheme proposed by Ramayya et al.²¹⁾ the 627.7 keV line is associated with a transition between a 3^- level at 2481.9 keV and a 2^+ level at 1854.2 keV, but the 1153.1 keV and 1076.6 keV gamma rays spring from the decay of the 4^+ level at 2229.7 keV to the 2^+ level at 1076.6 keV and subsequently to the 0^+ ground state. Since the 777.37 keV transition connecting the two 2^+ states does not appear in

coincidence with the 98.6 keV transition the results of the coincidence study suggest that the 627.7 keV line is a doublet, which was indeed found to be the case when high resolution examination of this gamma ray was undertaken. A small 627.2 keV shoulder, decaying with a half-life consistent with the ^{86m}Y activity was observed. It is, therefore, concluded that the 627.2 keV, 1153.1 keV and 1076.6 keV gamma rays are in coincidence with the 98.6 keV gamma ray.⁺

Discussion and Conclusions

A re-investigation of the decay of the 8^+ 218.4 keV isomeric level in ^{86}Y resulted in the observation of two new gamma rays of energies 98.6 keV and 627.2 keV in addition to the 10.2 keV and 208.2 keV transitions previously reported, all decaying with the same half-life. In coincidence spectra gated by the 98.6 keV transition the three gamma rays at 627.2 keV, 1153.1 keV, and 1076.6 keV all appeared with the same intensity. The 1076.6 keV and 1153.1 keV lines are known²¹⁾ to originate in ^{86}Sr .

On the basis of internal conversion measurements and the growth and decay character of the gamma rays from ^{86g}Y decay the 10.2 keV and 208.2 keV transition were assigned

⁺ The coincidence spectrum for the 1153.1 keV window as reported by Ramayya et al. clearly reveals a coincident 627 keV photon which was not explained by these workers.

to decays from ^{86m}Y to other levels in ^{86}Y ²³⁾. Such an assignment for the 98.6 keV and 627.2 keV transitions could not be made since these gamma rays occur in coincidence with the 1076.6 keV and 1153.1 keV gamma rays from transitions in ^{86}Sr . This argument is consistent with the observation by Kim et al.²³⁾ of a 98.5 keV transition converted in strontium.

Further evidence is provided by the results of the $^{87}\text{Sr}(p,d)$ reaction²⁴⁾ which imply that the 2955 keV 8^+ level of ^{86}Sr should decay via a cascade of predominantly E2 transitions through the 6^+ , 4^+ , 2^+ levels of the $(1g_{9/2})_{\nu}^{-2}$ multiplet to the 0^+ ground state, emitting in the process gamma rays of energies 100 keV, 626 keV, 1153 keV, and 1077 keV. Recent results⁴²⁾ have confirmed this supposition, and it seems reasonable to identify the gamma rays of energies 98.6 keV, 627.2 keV, 1153.1 keV, and 1076.6 keV observed in the present work with the E2 cascade transitions originating from the 8^+ level of ^{86}Sr at 2955 keV. Such an identification necessitates the postulation of a direct β^+ decay branch from the 8^+ 218.4 keV level of ^{86m}Y to this 8^+ level of ^{86}Sr . A summary of the proposed decay scheme of ^{86m}Y is presented in Figure 19.

The relative β^+ and gamma ray decay intensities shown in the figure are obtained from the relative gamma ray intensities of the 98.6 keV and 208.2 keV lines. Kim et al.²³⁾ have reported the value of the internal conversion coefficients for the 208.2 keV transition as $\alpha_K = 0.04$ and $\alpha_K:\alpha_L:\alpha_M$ as 100:83:1.7. Assuming the 98.6 keV transition to be pure

E2⁴²) the branching ratio for the β^+ decay of ^{86m}Y is $(0.69 \pm 0.04)\%$. The β^+ decay $\log_{10}ft$ value is deduced to be 6.51, a value somewhat high for allowed transitions but consistent with results for other such transitions in this region 20) as demonstrated in Table 7.

Such anomalously large $\log_{10}ft$ values are not compatible with a single particle shell model description of the states involved which predicts large β decay matrix elements (hence small $\log_{10}ft$ values) between initial and final states differing only in that a proton has beta decayed to a neutron in the same shell (or vice versa). This discrepancy suggests that the states involved are more complex than supposed in the simple shell model and that configuration mixing or weak coupling effects must be taken into account.

TABLE 7

Transition	J_{initial}^{π}	J_{final}^{π}	$\log_{10} f_t$
${}_{36}^{85}\text{Kr}_{49} \rightarrow {}_{37}^{85}\text{Rb}_{48}$	$9/2^{+}$	$9/2^{+}$	9.4
${}_{38}^{85}\text{Sr}_{47} \rightarrow {}_{37}^{85}\text{Rb}_{48}$	$9/2^{+}$	$9/2^{+}$	6.1
${}_{39}^{85}\text{Y}_{46} \rightarrow {}_{38}^{85}\text{Sr}_{47}$	$9/2^{+}$	$9/2^{+}$	6.3
	$9/2^{+}$	$7/2^{+}$	6.6
${}_{39}^{85\text{m}}\text{Y}_{46} \rightarrow {}_{38}^{85\text{m}}\text{Sr}_{47}$	$1/2^{-}$	$1/2^{-}$	6.3
${}_{39}^{87}\text{Y}_{48} \rightarrow {}_{38}^{87\text{m}}\text{Sr}_{49}$	$1/2^{-}$	$1/2^{-}$	6.7
${}_{39}^{87\text{m}}\text{Y}_{48} \rightarrow {}_{38}^{87}\text{Sr}_{49}$	$9/2^{+}$	$9/2^{+}$	7.5
${}_{38}^{86\text{m}}\text{Y} \rightarrow {}_{38}^{86}\text{Sr}$	8^{+}	8^{+}	6.51

FIGURE 16

A Partial Gamma Ray Spectrum of ^{86m}Y Obtained with the X-ray Detector. The vertical dashed bars indicate the energy window setting used for coincidence measurements. The insert shows the decay of the 98.6 and 208.2 keV gamma rays and their intensity ratio. The half-life obtained for these two gamma rays is 48 ± 2 minutes.

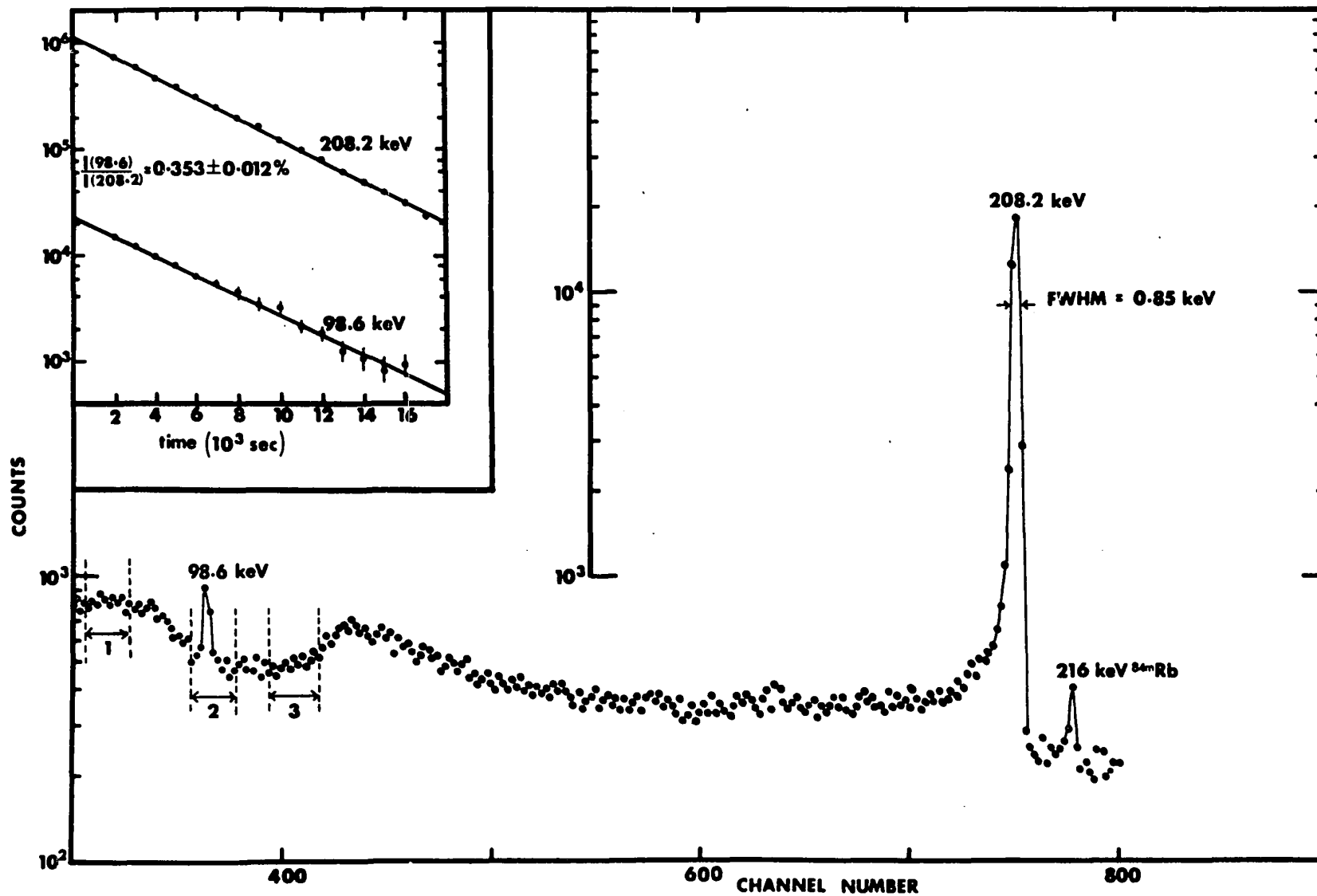


FIGURE 17
Half-life Curves of Gamma Rays
from the 14.6 hr ^{86}Y Decay
Showing Traces of a Shorter Half-life

1. 1076.6 keV
2. 627.7 keV
3. 1153.1 keV

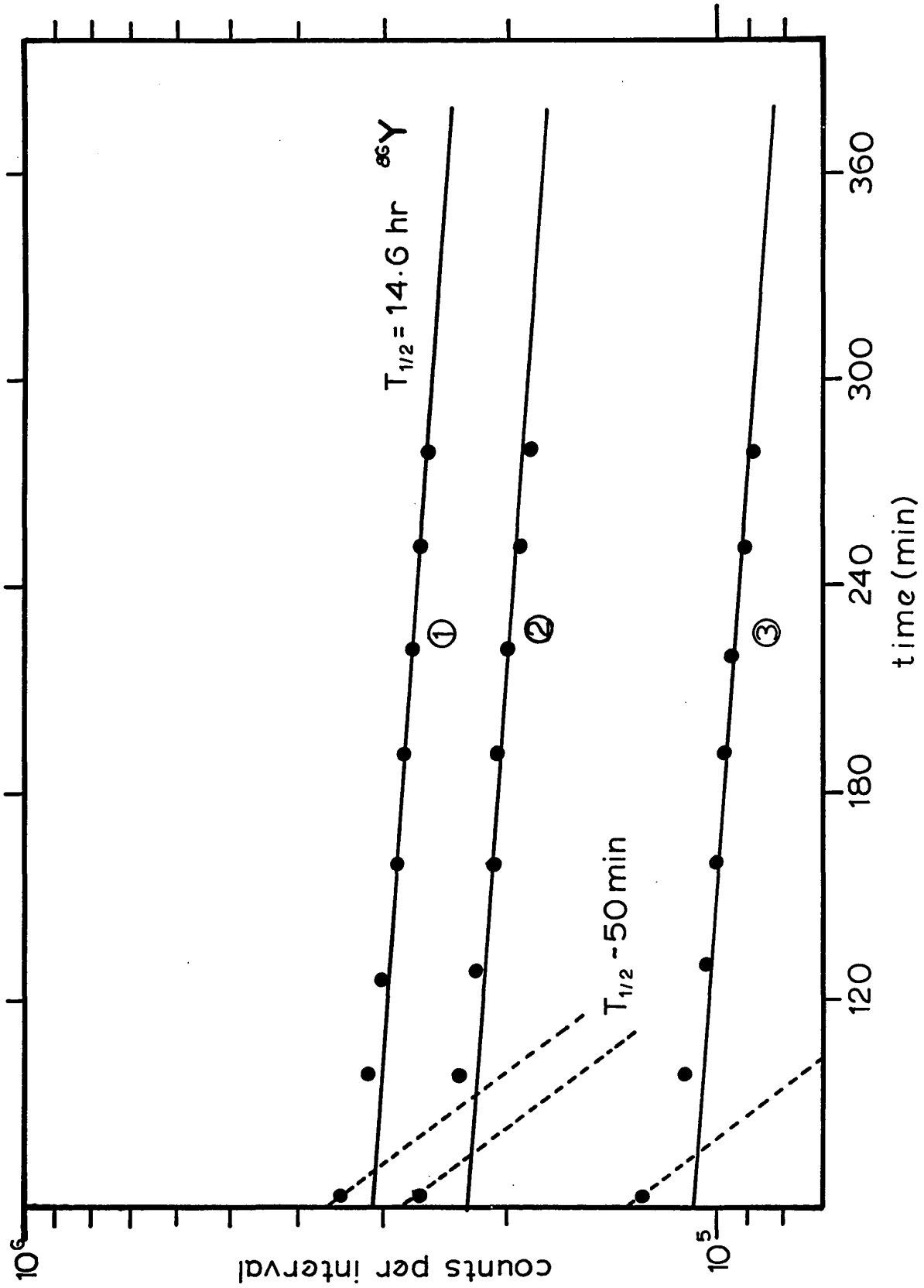


FIGURE 18

Comparison of the Relevant Portion of
the Gamma Ray Spectra From the Decay of
 ^{86m}Y and ^{86}Y (ground state). From Top to Bottom:

- (a) gamma rays from the decay of 14.6 hr. ^{86}Y ground state (spectrum accumulated four hours after bombardment).
- (b) coincidence spectrum gated by the window set on the 98.6 keV line.
- (c) coincidence spectrum gated by the window set just above the 98.6 keV line.
- (d) same as (b) except that the 48 minute activity had been allowed to decay for a period of four half-lives before counting.

The Energy Window Settings are Indicated in Figure 16.

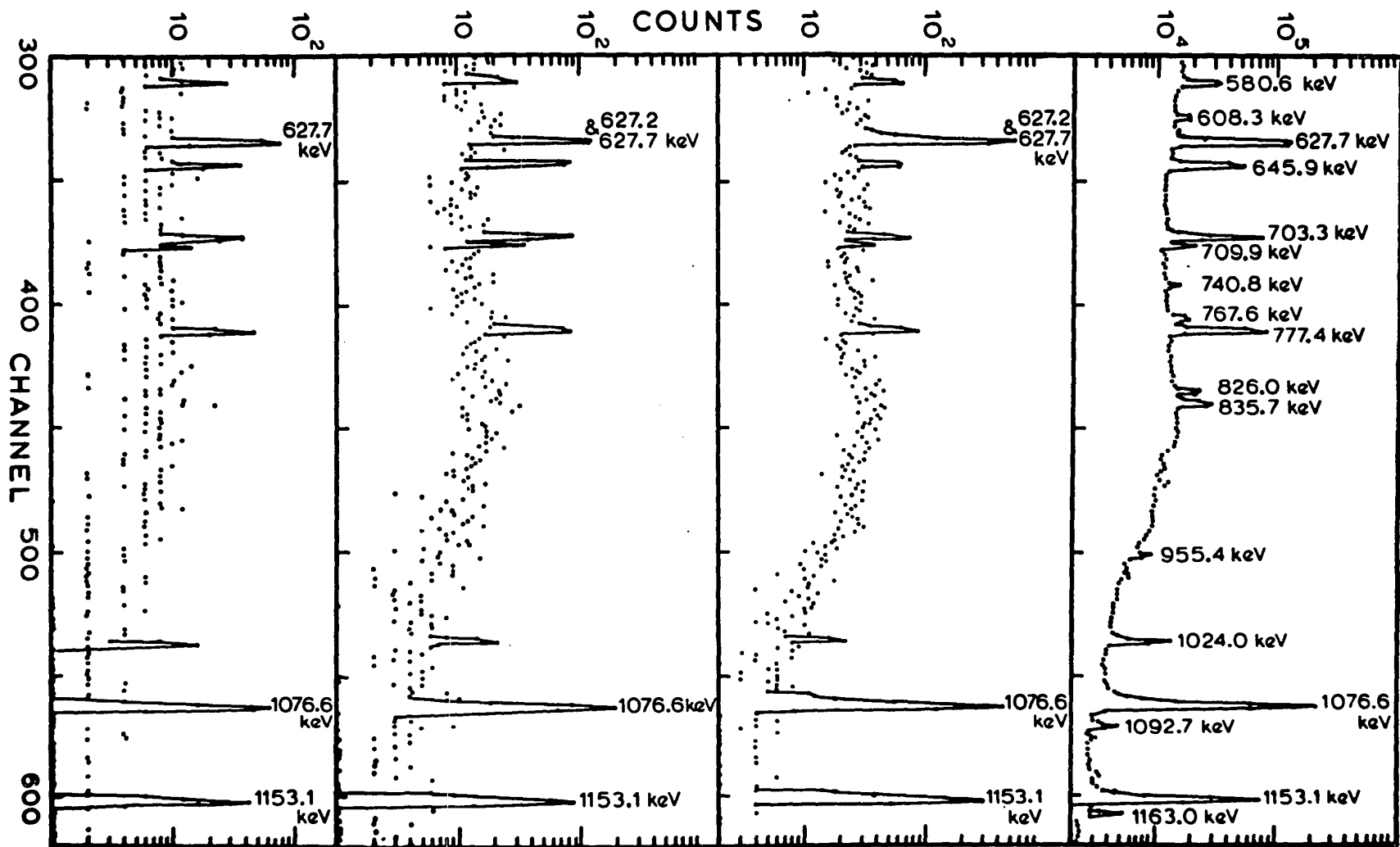
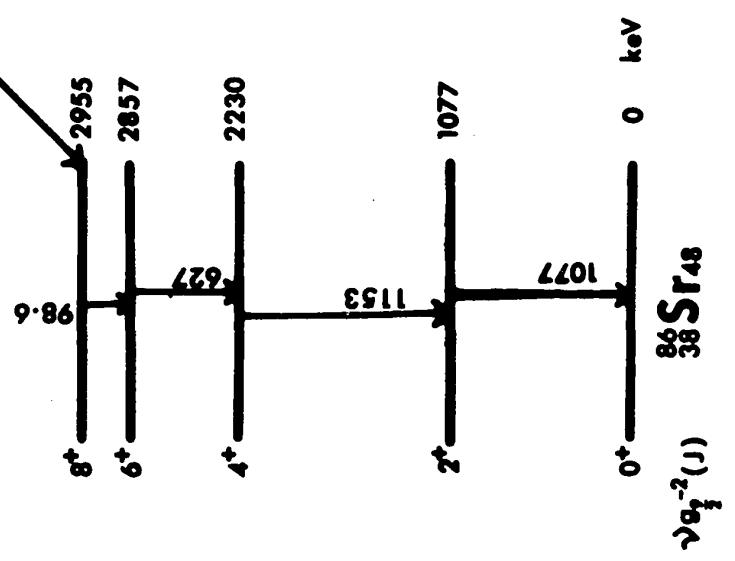
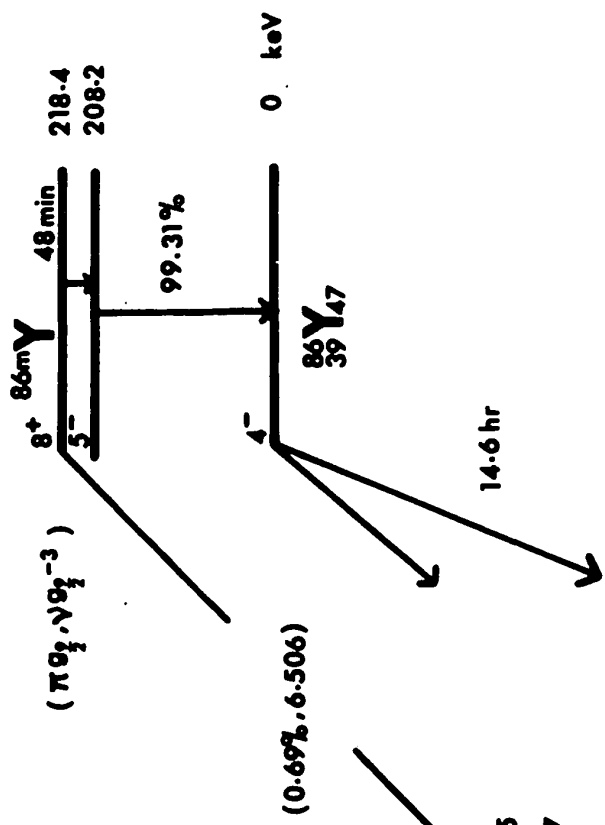


FIGURE 19
Proposed Decay Scheme for the 48 min. $^{86}\text{m}\gamma$



CHAPTER V
THE DECAY OF ^{83}Y AND $^{83\text{m}}\text{Y}$

Background

The A=odd N=45 nucleus ^{83}Sr is expected to possess a structure of some interest. Calculations of the excited levels of ^{83}Sr have been done in the shell model context¹⁰⁾ and in the weak coupling model context¹¹⁾. The former treatment included only the $2p_{1/2}$ and $1g_{9/2}$ neutron orbits in deriving the low-lying excited states of this nucleus; the latter calculation took into account the $2p_{1/2}$, $1g_{9/2}$, $2d_{5/2}$, $3s_{1/2}$, $2d_{3/2}$, $1f_{5/2}$, and $2p_{3/2}$ orbits and some collective effects as well. Seniority conservation appears to become less valid as N departs from the closed shell value 50, as shown in recent studies³⁵⁾ of $(1g_{9/2})^5, \nu=2, J^\pi = 0^+, 2^+, 4^+$ states in light strontium isotopes. However, a systematic feature of N = 45 isotones is a $7/2^+$ ground state spin attributed to a $(1g_{9/2})^5, \nu=3, J^\pi = 7/2^+$ neutron configuration (Appendix 2). Workers studying the beta decay of ^{83}Sr to ^{83}Rb ⁴³⁾ assigned the spin $7/2^+$ to the ^{83}Sr ground state. The level structure of ^{83}Sr has been explored experimentally via the $^{84}\text{Sr}(d,t)^{83}\text{Sr}$ reaction²⁹⁾. A comparison of this result with the calculated schemes referred to above appears in Figure 6.

Several conflicting values of the half-life of ^{83}Y have been reported: 3.5 hours³⁰⁾, 35 minutes³¹⁾, 8 minutes³²⁾, 7.5 minutes³³⁾, and 7.4 minutes³⁴⁾. Recent measurements per-

formed in this laboratory²⁶⁾ assigned a 7.06 ± 0.08 minute half-life to the ground state decay and a 2.85 ± 0.02 minute half-life to the isomeric decay of ^{83}Y . In addition the half-life of the 259.3 keV transition in ^{83}Sr was determined to be 4.96 ± 0.12 seconds.

Gamma rays from the decay of ^{83}Y , $^{83\text{m}}\text{Y}$ have been observed by various workers^{25,26,27,28)} and two decay schemes proposed^{25,28)} (Figures 4 and 5) based on gamma ray singles spectra and the results of the $^{84}\text{Sr}(d,t)^{83}\text{Sr}$ reaction work of Bercau and Warner²⁹⁾.

In the present work a search for additional gamma rays, coincidence studies, and internal conversion coefficient measurements were undertaken to establish a decay scheme for ^{83}Y , $^{83\text{m}}\text{Y}$.

Experimental Results

Energy and Half-life Measurements

By means of energy and half-life measurements performed with high resolution Ge(Li) detectors several gamma rays were identified as originating from the decay of ^{83}Y , $^{83\text{m}}\text{Y}$ and the decay of contaminants produced in reactions other than $^{84}\text{Sr}(p,2n)^{83}\text{Y}$ (Figure 20). Photons associated with the decay of yttrium isotopes were sorted from the rest by using fast, simple chemical techniques to separate the yttrium in the samples from the main contaminants, strontium and rubidium isotopes. Figures 21 and 22 show a spectrum of the separated

yttrium fraction counted for ten minutes immediately after separation and a spectrum of the contaminant fraction counted for sixty minutes beginning eighty minutes after separation. The energies and relative gamma ray intensities of transitions ascribed to the decay of ^{83}Y and their absolute intensities (corrected for internal conversion) in units of transitions per one hundred decays of the yttrium parent are listed in Table 8. A search for gamma rays in the energy range 1.5 MeV to 3.0 MeV revealed none that could be assigned to ^{83}Y .

Half-life plots of some of the prominent peaks in the decay are shown in Figure 23. The 259.3 keV photon was found to possess a weak 7 minute component. The 421.0 keV photon was not only found to contain a mixture of the two half-lives, but its energy also shifted towards a lower value as a function of time. Analysis of this photon suggested a doublet consisting of a large 421.0 keV radiation component (2.85 min.) and a weaker 420.4 keV photon (7.06 min.).

To obtain the intensity of the 511 keV annihilation radiation relative to other yttrium gamma rays (in order to determine beta branching ratios to various levels in the decay scheme) chemically separated sources of ^{83}Y activity were enclosed in an aluminum cylinder thick enough to stop the beta particles from the decay of any yttrium isotope produced in the experiment and spectra accumulated for three minute intervals over several decay periods.

TABLE 8
Gamma Ray Energies and Intensities
in the Decay of $^{83}\text{m}\text{Y}$

Energy (keV)	$^{86}\text{g}\text{Y}$ (7.06min) (a)		$^{83}\text{m}\text{Y}$ (2.85min) (a)	
	Relative Intensity	Transitions per 100 disintegrations	Relative Intensity	Transitions per 100 disintegrations
35.6 ± 0.1	100 ^(e) (275)	51.8	100 ^(e) (116)	100
259.3 ± 0.1 ^(b)				
391.2 ± 0.1	7.6	1.43		
420.4 ± 0.3 ^(c)	6.7	1.26		
421.0 ± 0.3 ^(c)			30	23.5
454.3 ± 0.1	12.7	2.39		
489.9 ± 0.1	38.8	7.30		
494.3 ± 0.1	8.8	1.66		
545.6 ± 0.2 ^(d, f)	3.4	0.64		
618.3 ± 0.2	3.3	0.62		
717.7 ± 0.2	6.0	1.13		
721.2 ± 0.2	5.5	1.04		
743.4 ± 0.1 ^(f)	6.3	1.19		
858.8 ± 0.1	16.3	3.07		
882.1 ± 0.1	33.7	6.35		
927.2 ± 0.1 ^(f)	4.7	0.88		
951.7 ± 0.2	9.8	1.85		
1336.5 ± 0.2	17.2	3.24		
1372.0 ± 0.2	4.6	0.87		

- (a) Intensities are believed accurate to $\pm 5\%$ except for the 420.4 and 421.0 keV photons for which a 20% figure is appropriate.
- (b) Possesses a weak 7.06 min. component whose intensity depends on the isomer ratio.
- (c) Unresolved doublet with 2.85 min and 7.06 min components.
- (d) Reported as having $3.5 \pm 0.$ min half-life in ref. 27.
- (e) Corrected for internal conversion.
- (f) Not placed in the decay scheme.

Gamma-Gamma Coincidence Measurements

Coincidence measurements were performed with the standard fast-slow coincidence system illustrated in Figure 11 with a resolving time of about 100 nsec. Since many samples were required for each run to accumulate reasonable statistics and enriched ^{84}Sr is expensive, no chemical techniques were applied and 'cooled' targets were recycled.

A large window placed just above the 511 keV annihilation radiation and extending to about 1.5 MeV revealed strong coincidences with gamma rays at 489.9, 454.3, and 421 keV and a weaker coincidence with a photon at 391.2 keV. No coincidences with the 259.3 keV transition from the metastable level of ^{83}Sr were seen (Figure 24). Coincidence experiments with narrow windows on the 489.9 and 454.3 keV gamma rays revealed coincidences with the 882.1 keV transition (Figures 25 and 26) and the result was confirmed by the reverse experiment (Figure 27). A coincidence spectrum accumulated with a window set on the 420.4 - 421.0 keV doublet showed a coincidence peak at 951.7 keV (Figure 28). This finding was corroborated by the reverse experiment. Gates set on weaker gamma rays - the 717.7 - 721.2 keV doublet, the 743.4, and 1336.5 keV lines - produced inconclusive results. No coincidences were observed involving the 35.6, 259.3 or 858.8 keV transitions. The experiment was repeated for the 35.6 keV photon window with a null result.

Internal Conversion Coefficient Measurements

The chamber and counting system for internal conversion experiments (Figures 14 and 15) were used to measure the low energy conversion electron spectrum of ^{83}Y , $^{83\text{m}}\text{Y}$. Because the electron detector is sensitive to low energy gamma radiation as well as charged particles, the 35.6 keV K-electron conversion line was masked by strong yttrium and strontium X-rays, and the L and higher shell conversion lines were masked by the 35.6 keV gamma ray itself even at the best resolution (4 keV FWHM) attained with the apparatus. A weak K-electron conversion line was observed belonging to the 259.3 keV transition (Figure 29). The α_K for this transition was determined to be 0.16 ± 0.02 by the method outlined under the discussion of experimental technique using the 388 keV transition of $^{87\text{m}}\text{Y}$ as the standard of comparison³⁹⁾.

Discussion

Two photons of energies 259.3 keV and 421.0 keV were assigned to the decay of the 2.85 minute isomeric state of ^{83}Y . Seventeen others were attributed to the 7.06 minute ground state decay.

No data was obtained in this experiment pertaining to the energy difference between the isomeric and ground states of ^{83}Y . On the basis of the systematics of odd A yttrium isotopes (Appendix 2) the most probable ground state of ^{83}Y is $9/2^+$ with a $1/2^-$ isomeric state. Since the $9/2^+$, 35.6 keV state is fed by the 7 minute activity and the $1/2^-$, 259.3 keV

state by the shorter lived 2.85 minute activity it is reasonable to assume that the 7 minute decay of ^{83}Y proceeds from a high spin ($9/2^+$) level and the 2.85 minute decay from a low spin ($1/2^-$) level. In this region generally (but certainly not always) the metastable state is the shorter lived of the isomeric pair of states; therefore it seems logical to refer to the 7 minute and 2.85 minute activities as the ground state and isomeric decays respectively. The absence of any observed transition between $^{83\text{m}}\text{Y}$ and ^{83}Y suggests that the energy separation between these levels is small since transition probability is proportional to $E_{\gamma}^{2\lambda+1}$ where λ in this instance is 3²⁰⁾.

The Decay of $^{83\text{m}}\text{Y}$

Of the two photons associated with the decay of $^{83\text{m}}\text{Y}$ the more intense is the 259.3 keV transition. This transition is characterized by a half-life of 4.96 ± 0.12 seconds²⁶⁾ and an $\alpha_K = 0.16 \pm 0.02$, properties consistent with a gamma ray transition of multipolarity E3.

Bercaw and Warner²⁹⁾ observed states of spin and parity $1/2^-$ or $3/2^-$ at 250 keV and 680 keV above a $9/2^+$ state, which on the basis of Q value considerations they placed about 24 keV above a $7/2^+$ ground state in ^{83}Sr . The assignment of spin and parity $7/2^+$ to the ground state of ^{83}Sr is in keeping with the systematics of N=45 odd A nuclides (Appendix 2) and has been confirmed experimentally by the beta decay work of

Etherton et al.⁴³⁾. In the present work an intense 35.6 keV transition, observed in the 7 minute ground state decay, is assumed to connect the low-lying $9/2^+$ state and the $7/2^+$ ground state. The lack of coincidences with this gamma ray suggests that it is of a retarded M1 nature.

The systematics of neutron deficient odd A strontium isotopes (Appendix 2) indicate that in these nuclei the $2p_{1/2}$ excitation lies below the $2p_{3/2}$ excitation. The character of the 259.3 keV transition leads to the conclusion that it connects a $1/2^-$ state at 259.3 keV to the $7/2^+$ ground state. The 421.0 keV radiation, then, is associated with a transition from a $3/2^-$ level at 680.3 keV to the 259.3 keV state. This decay scheme is included in Figure 30.

The log ft values of the beta transitions leading to these levels (calculated assuming a beta decay Q value of 4.5 MeV⁴⁴⁾) are classified in the allowed category and are consistent with the spins and parities deduced for these levels.

The Decay of ^{83}gY

Energy Levels

The decay of ^{83}gY appears to proceed by beta decay to four levels primarily of ^{83}Sr : the 1372.0 keV, 858.8 keV, 35.6 keV and ground states. The intermediate levels are populated for the most part by electromagnetic transitions from the 1372.0 keV level.

The existence of a level at 35.6 keV is postulated

on the presence of a very intense gamma ray of this energy in the spectrum of ^{83}gY and is in agreement with the findings of $^{84}\text{Sr}(d,t)^{83}\text{Sr}$ reaction studies²⁹⁾.

Evidence for the existence of an excited state at 1372.0 keV is strong. Coincidences between the 882.1 keV gamma ray and gamma rays of 489.9 and 454.3 keV, and coincidence between the 420.4 keV gamma ray and the 951.7 keV gamma ray firmly establish such a level. The presence in the decay of photons with energies 1372.0 and 1336.5 keV reinforce this assignment. Together these results establish excited levels of ^{83}Sr at 35.6, 489.9, 951.7 and 1372.0 keV with reasonable security. Reaction data²⁹⁾ indicates levels at 490 keV and 960 keV which correspond quite well to levels at 489.9 and 951.7 keV proposed in the present work.

The fact that the intense 858.8 keV gamma ray did not appear in coincidence with any gamma ray and could not be positioned in the decay scheme by energy sum relations with other gamma rays led to the postulation of an 858.8 keV excited state decaying directly to the ground state.

Other levels are suggested by energy sums in stop-over transitions from the 1372.0 keV level. A level at 753.5 keV is proposed, fed by a 618.3 keV transition from the 1372.0 keV level and decaying via a 717.7 keV transition to the 35.6 keV level and via a 494.3 keV transition to the metastable 259.3 keV level. Similarly it is hypothesized that a 651.0 keV state is fed by a 721.2 keV transition from the 1372.0 keV level and de-excited by a 391.2 keV transition to the 259.3

keV state. The latter supposition is consistent with the appearance of the 391.2 keV photon in the coincidence spectrum gated by all gamma rays of energy greater than 511 keV. Both assignments are consistent with the weak seven minute component observed in the 259.3 keV transition. (Energy sum relations are shown in Table 9)

Beta decay branching ratios for all levels were derived from the relative intensity of the 511 keV annihilation radiation (measured with sample encased in a 1.2 cm. thick aluminum beta stopper) to the other gamma rays in the decay. A 32% branch to the ground state was found. The corresponding log ft values were calculated assuming a Q value of 4.5 MeV for the beta decay of ^{83}Y to $^{83}\text{Sr}^{44}$.

Spin and Parity Assignments

The ground state of ^{83}Sr and states at 35.6 keV and 259.3 keV have securely established spins and parities $7/2^+$, $9/2^+$ and $1/2^-$ respectively. An $l_n = 1$ transition to the 680.3 keV level²⁹⁾, an allowed log ft value (5.1), and its gamma decay character indicate an assignment of $(3/2, 1/2)^-$ with the choice of $3/2^-$ favoured by systematics (Appendix 2). The $l_n = 3$ transition to the 489.9 keV state²⁹⁾ and the gamma decay properties of the state (it feeds the $7/2^+$ ground state and $9/2^+$ first excited state) are consistent with $5/2^-$ and $7/2^-$ spin and parity assignments. Since the $1f_{5/2}$ excitation is known to lie close in energy to the $2p_{1/2}$ and $2p_{3/2}$ excitations a spin assignment of $5/2^-$ is chosen for 489.9 keV level.

TABLE 9
Summing Relations of Gamma Ray Energies

Gamma Ray Energy Sum (keV)	Single Gamma Ray Energy or Associated Sum (KeV)
$1336.5 + 35.6 = 1372.1$	1372.0
$882.1 + 489.9 = 1372.0$	1372.0
$882.1 + 454.3 + 35.6 = 1372.0$	1372.0
$951.7 + 420.4 = 1372.1$	1372.0
$618.3 + 717.7 + 35.6 = 1371.6$	1372.0
$721.2 + 391.2 + 259.3 = 1371.7$	1372.0
$618.3 + 494.3 + 259.3 = 1371.9$	
$454.3 + 35.6 = 489.9$	489.9

The log ft value for beta transitions from the $9/2^+$ ground state of ^{83}Y to the 1372.0 keV level is in the range of allowed transition values, implying a spin and parity of ($7/2^+$, $9/2^+$, $11/2^+$) for this level. The intense 882.1 keV photon connecting this level to the 489.9 keV $5/2^-$ state rules out the choice of $11/2^+$ and favours a $7/2^+$ spin for this level. The level at 951.7 keV is populated mainly by gamma ray decays from the 1372.0 keV state and depopulated by a direct decay to the ground state which suggests a spin assignment of ($5/2$, $7/2$, $9/2$) for this level. The 651.0 keV level is fed chiefly by electromagnetic decays from the 1372.0 keV level and decays to the 259.3 keV level. A low spin value, possibly ($3/2$, $5/2$), is likely. Similar arguments may be produced for the spin assignment of the 753.5 keV level. However, it decays to the $9/2^+$ first excited state as well. A choice of $5/2$ seems appropriate in this instance.

No useful conclusions may be ascertained concerning a spin and parity assignment for the 858.8 keV state.

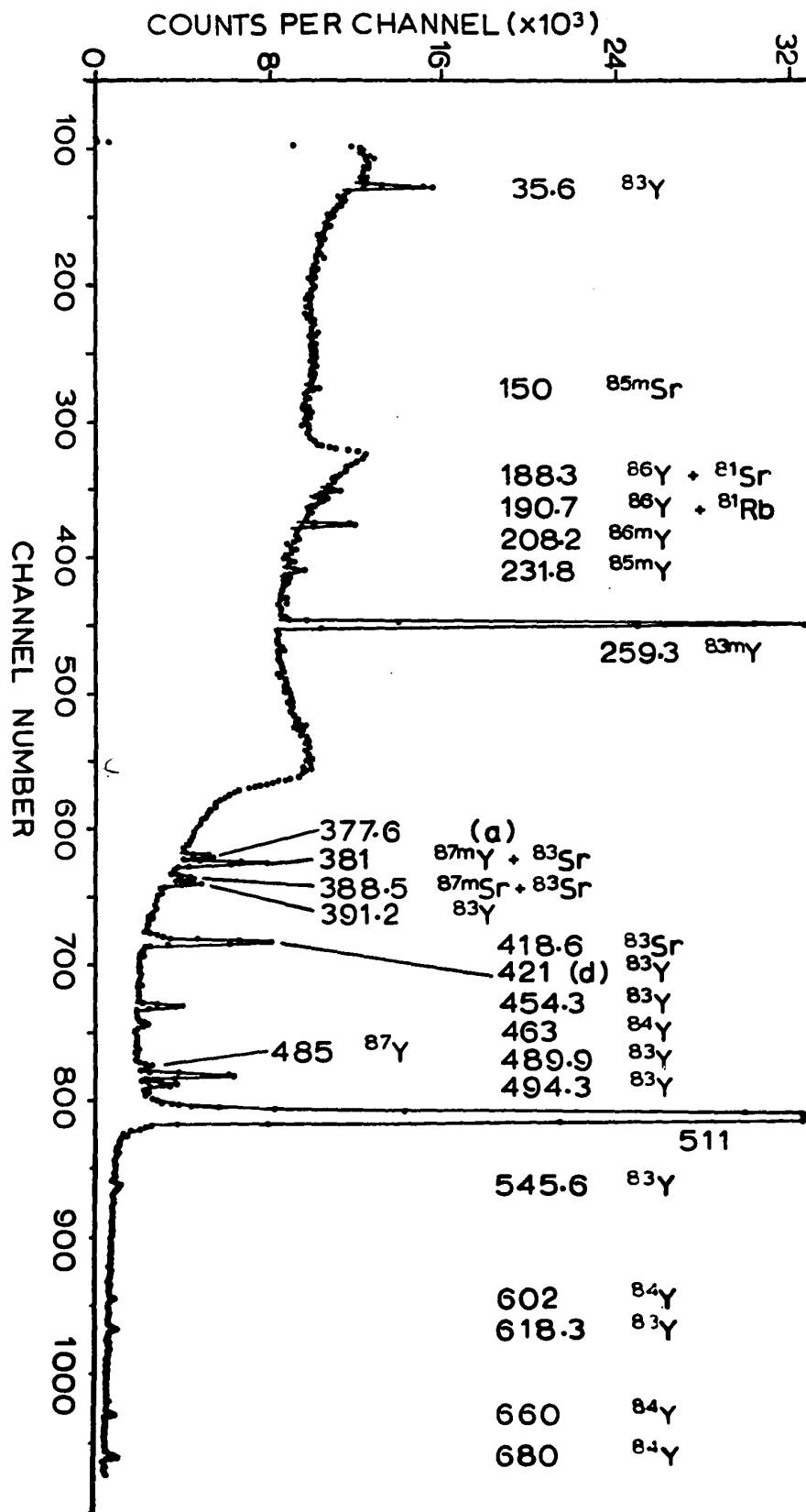
Conclusions

The decay scheme of Figure 30 is proposed for the decay of ^{83m}Y and ^{83g}Y on the basis of energy and half-life measurements, coincidence studies, internal conversion measurements, and reaction data²⁹⁾. The locations of the $1g_{9/2}$ (35.6 keV), $2p_{1/2}$ (259.3 keV), $1f_{5/2}$ (489.9 keV) and $2p_{3/2}$ (680.3 keV) excitations above the $7/2^+$ ground state are observed.

The metastable character of the 259.3 keV level is corroborated by its absence from all coincidence spectra. It is hypothesized that the 35.6 keV level is of retarded MI nature because of its failure to be coincident with any gamma ray.

FIGURE 20

A Gamma Ray Spectrum of $^{83,83m}\text{Y}$
Activity From a Target of Enriched ^{84}Sr Bombarded
at 31 MeV. No chemical separation has been
performed. Other activities identified in the spectrum are
 $^{84}\text{Y}^{45}$, $^{86}\text{Y}^{21}$, ^{86m}Y , $^{87,87m}\text{Y}^{20}$, $^{81}\text{Sr}^{27}$, $^{83}\text{Sr}^{43}$,
 $^{85m}\text{Sr}^{20}$ and $^{81}\text{Rb}^{46}$.
Peaks marked (a) are unidentified peaks from activities other
than ^{83}Y .
(The peak labelled 421(d) is a doublet
consisting of lines at 420.4 keV and 421.0 keV).



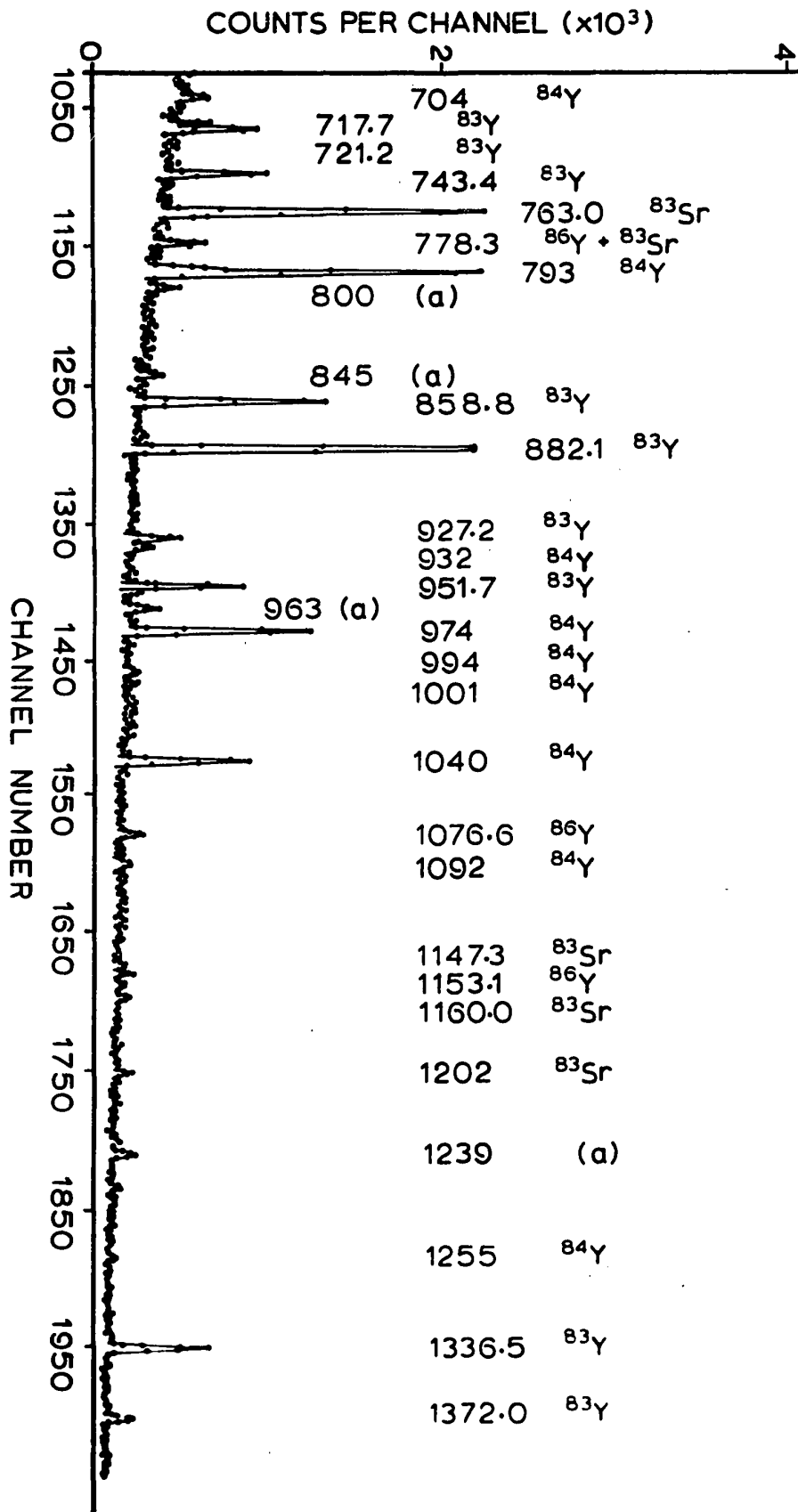
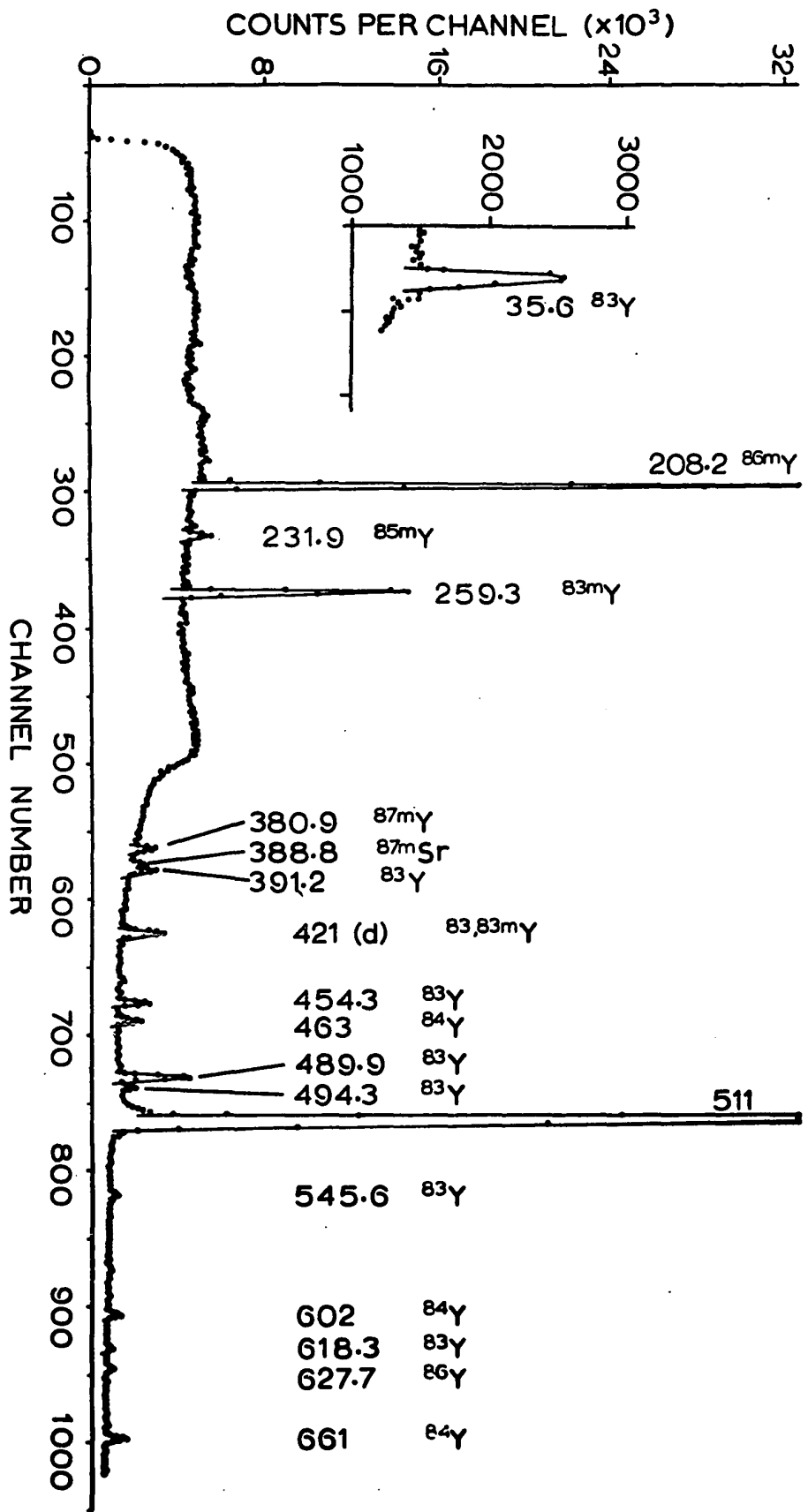


FIGURE 21

A Gamma Ray Spectrum of $^{83,83m}\text{Y}$ From the Yttrium
Fraction Separated From an Enriched
 ^{84}Sr Target Bombarded at 40 MeV.

All the activities present were identified in Figure 20.
Peaks marked (a) are unidentified peaks from activities other
than ^{83}Y .
(The peak labelled 421(d) is a doublet consisting of lines at
420.4 keV and 421.0 keV.)



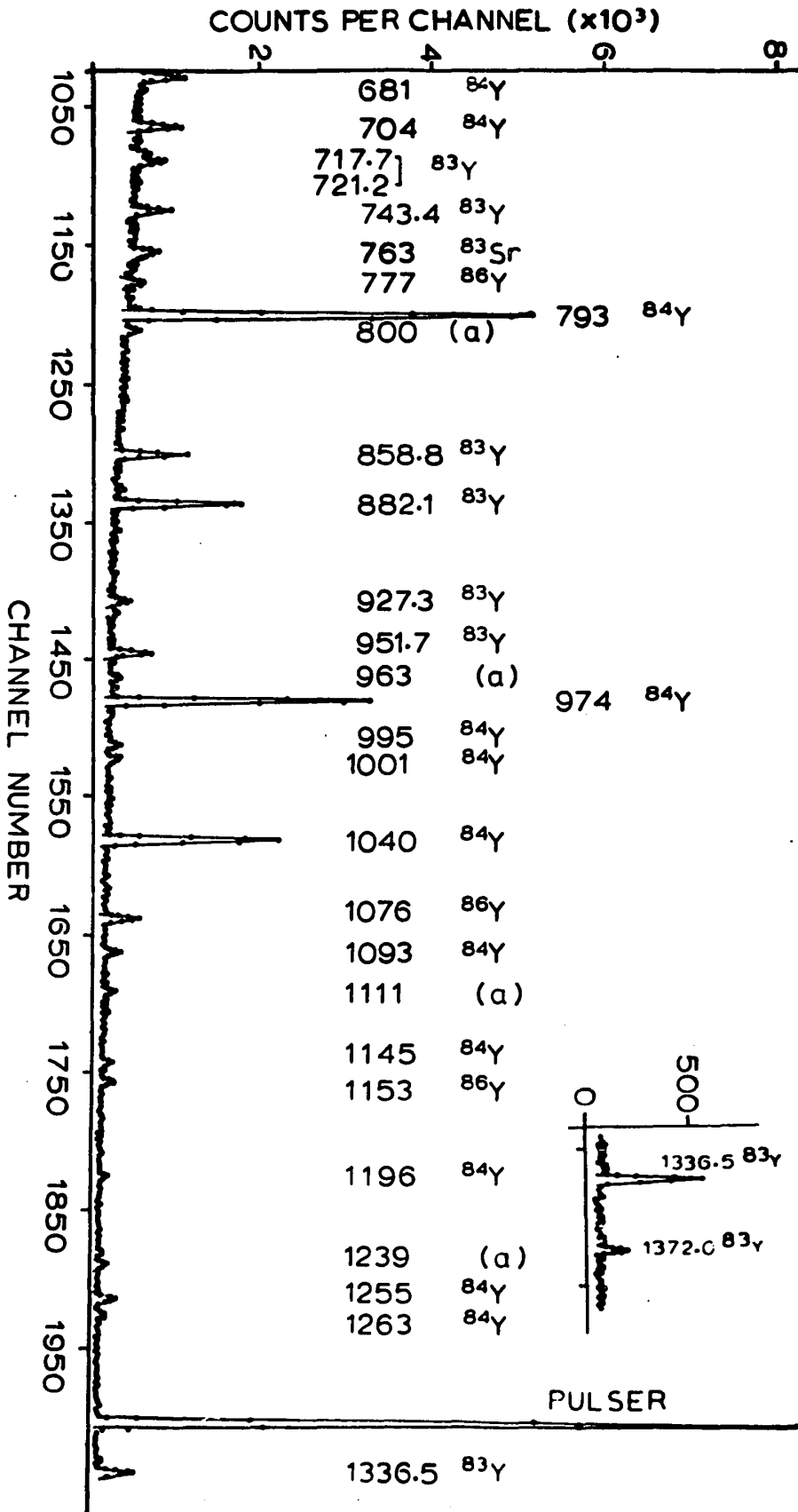
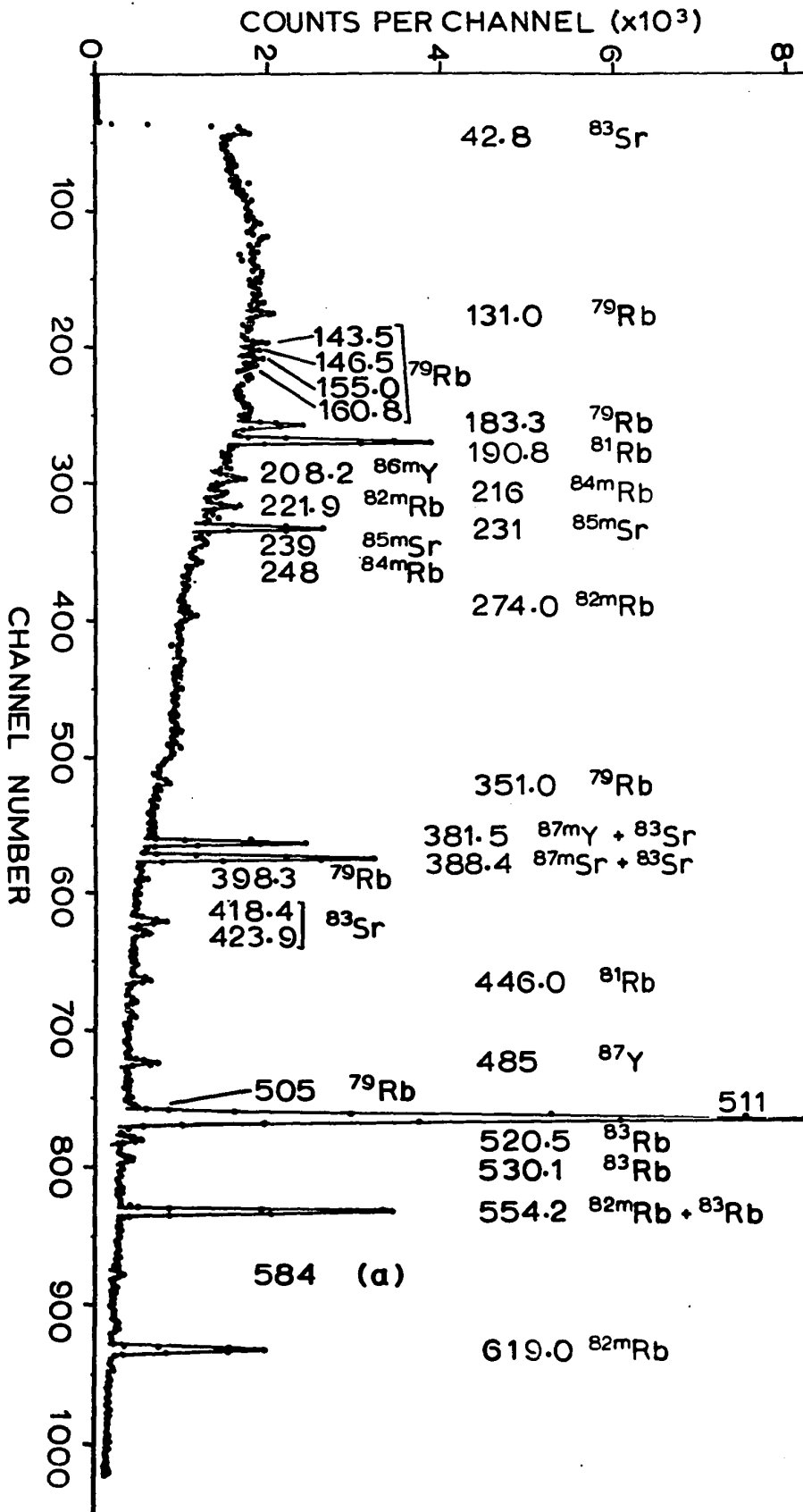
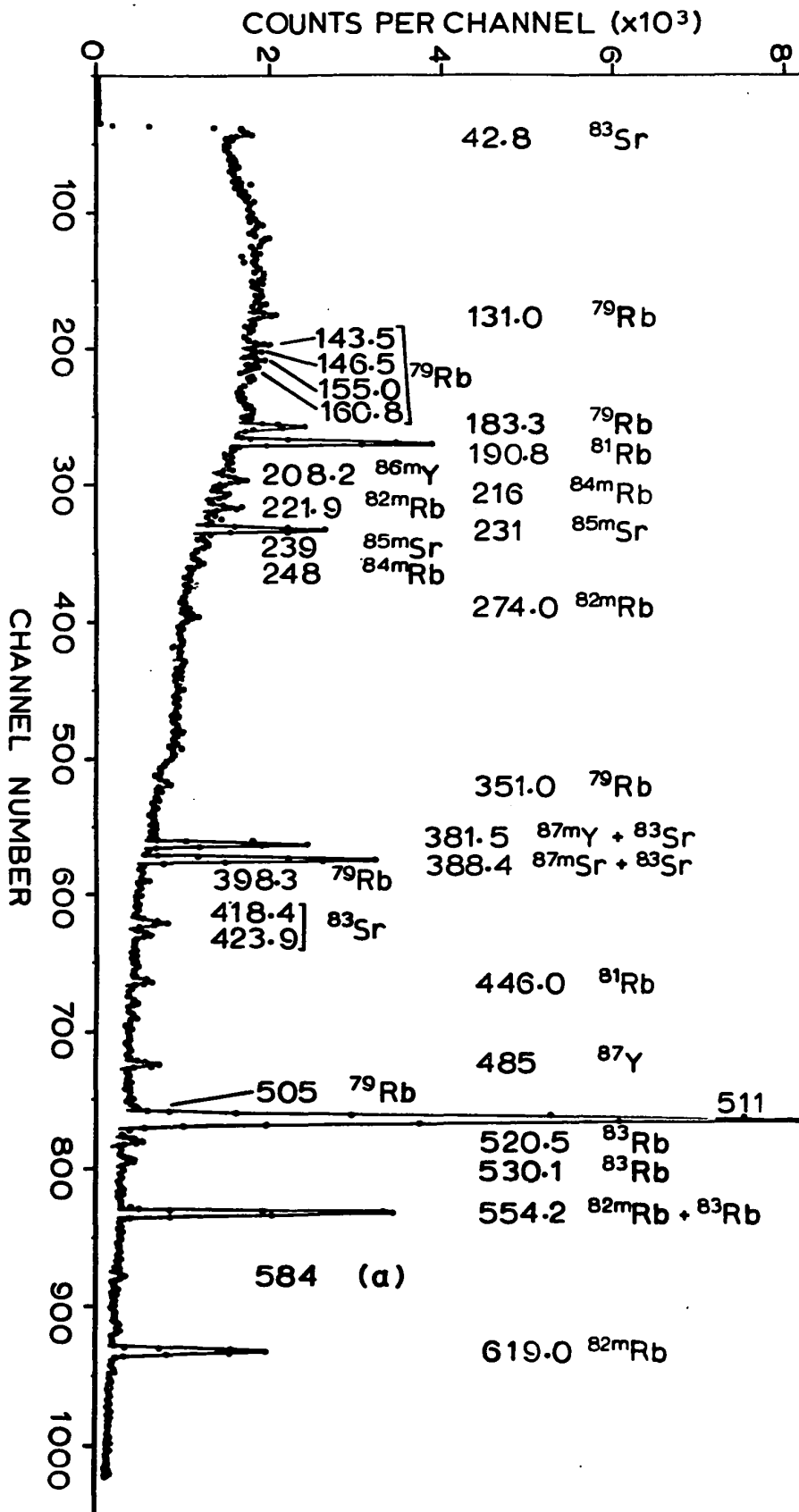


FIGURE 22

A Gamma Ray Spectrum From the Contaminant Fraction of
an Enriched ^{84}Sr Target Bombarded at 40 MeV, Recorded
Eighty Minutes After Separation.
Activities Which Appear in this Spectrum
but not in Figure 20 or 21 are
 ^{79}Rb ⁴⁷⁾, $^{82\text{m}}\text{Rb}$ ⁴⁸⁾ and ^{83}Rb ⁴⁹⁾.





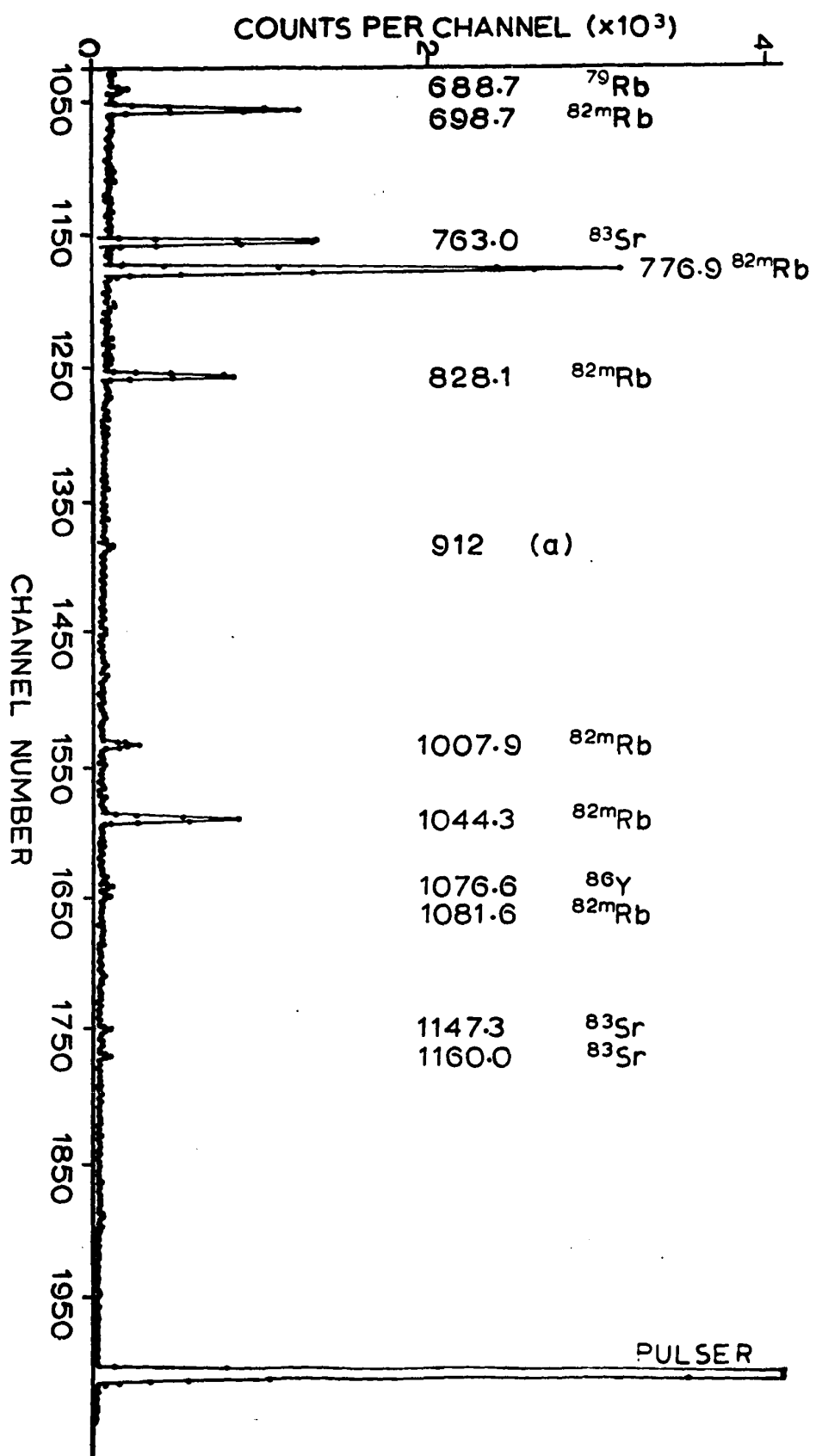


FIGURE 23
Half-life Plots of Some Prominent Gamma Rays
in the Decay of $^{83}\text{m}\text{Y}$

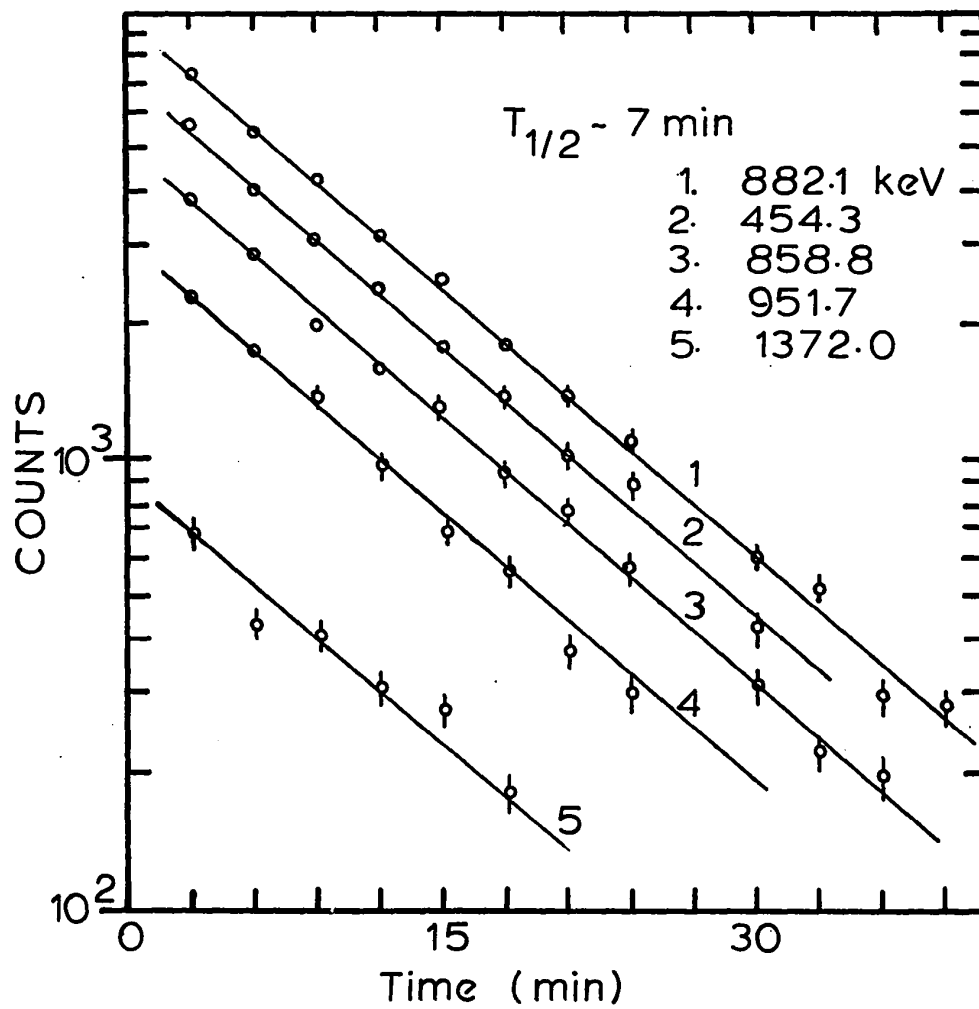
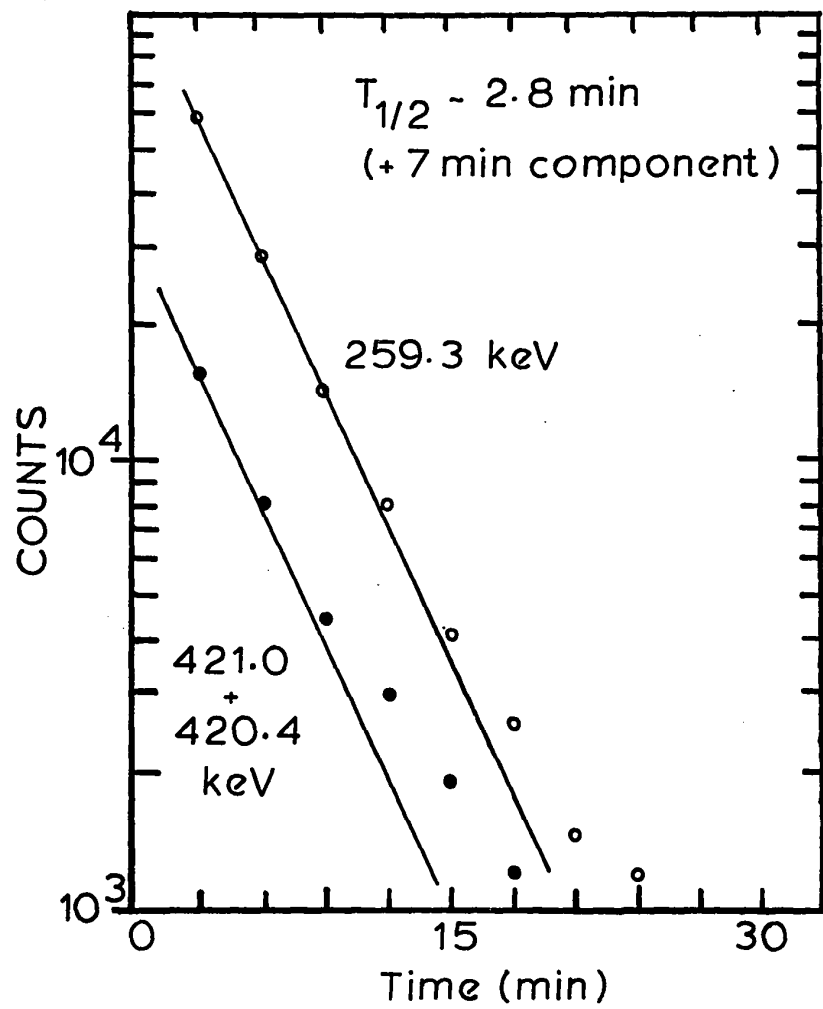


FIGURE 24

Coincidence Spectrum Gated by all Gamma Rays Above
511 keV and Below 1.5 MeV.
(The Peak Labelled 421(d) is a Doublet Consisting of
Lines at 420.4 keV and 421.0 keV.)

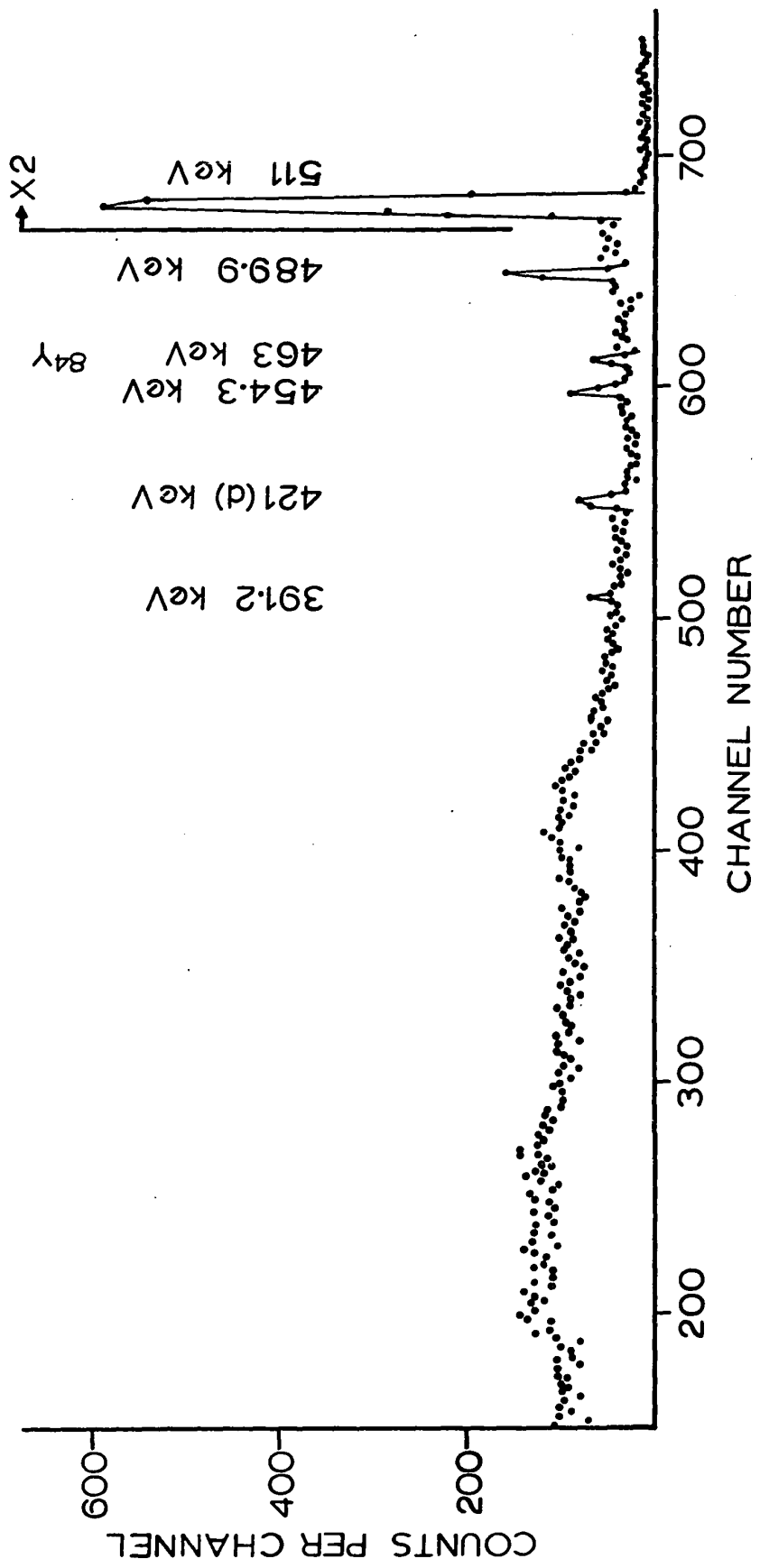


FIGURE 25
Coincidence Spectrum Gated by the 489.9 keV Transition

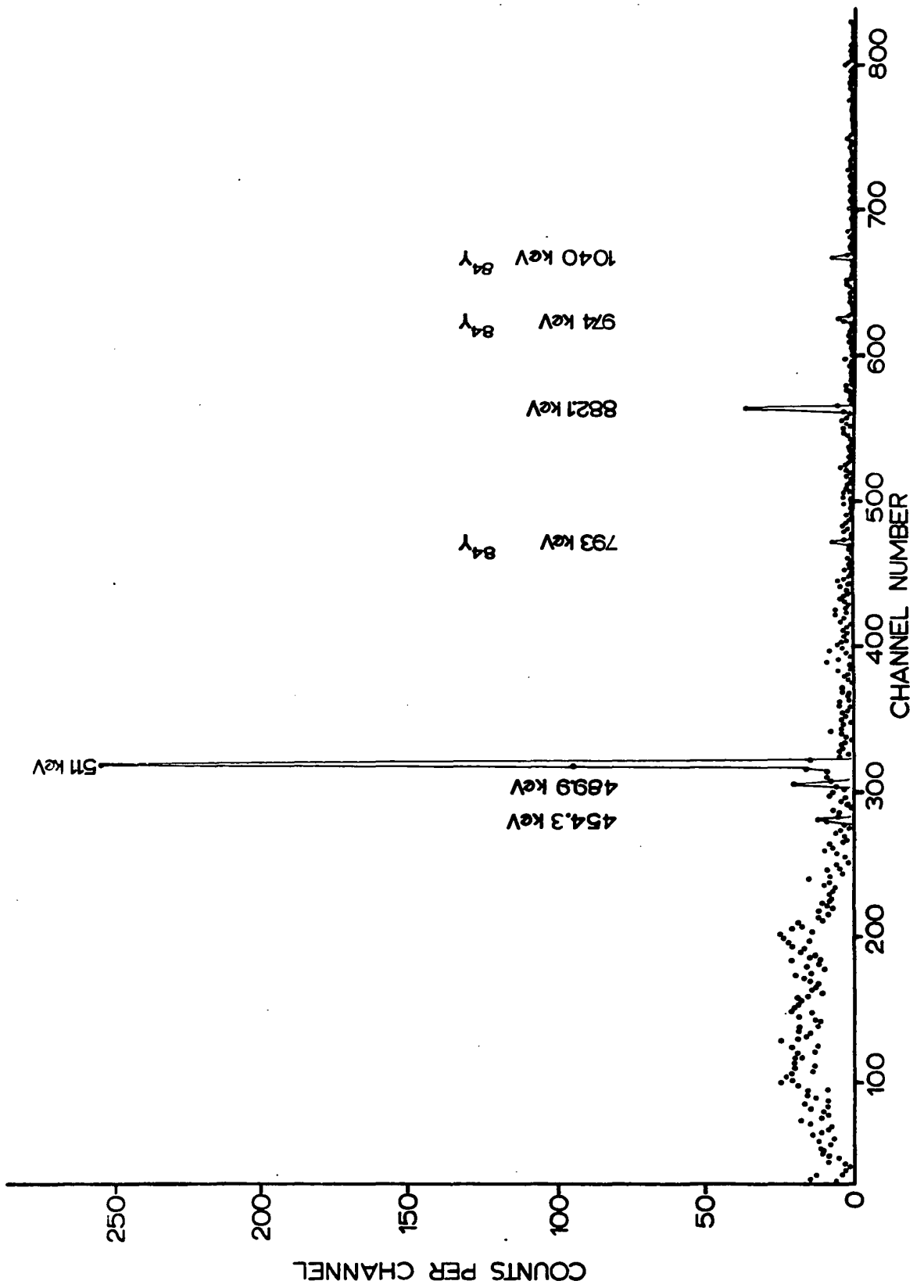


FIGURE 26

Coincidence Spectrum Gated by the 454.3 keV Transition.
(The Peak Labelled 421(d) is a Doublet Consisting of
Lines at 420.4 and 421.0 keV)

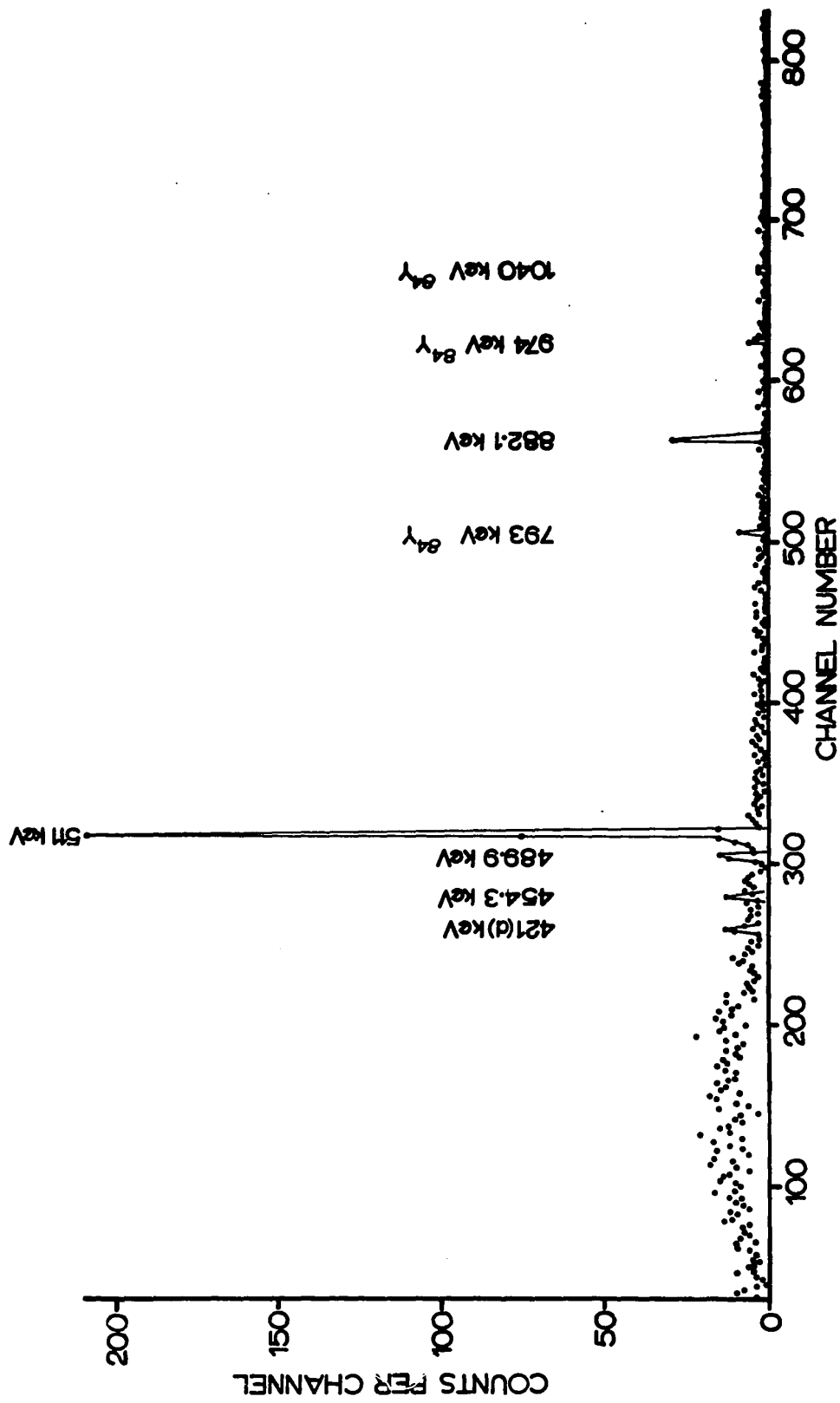


FIGURE 27

Coincidence Spectrum Gated by the 882.1 keV Transition.
(The Peak Labelled 421(d) is a Doublet Consisting of
Lines at 420.4 and 421.0 keV)

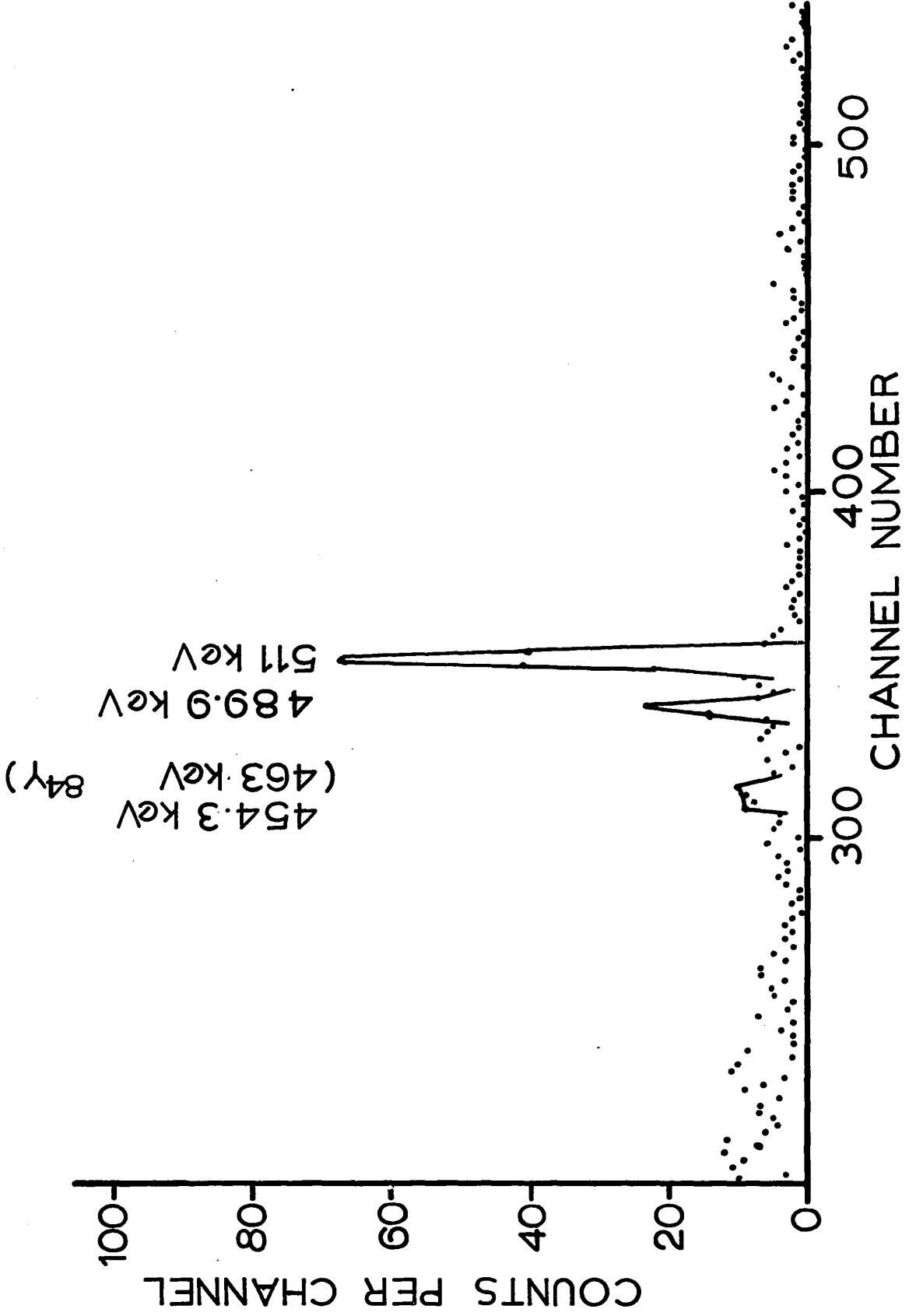


FIGURE 28

Coincidence Spectrum Gated by the 421(d) Transitions.
(A Doublet Consisting of Lines at 420.4 keV and 421.0 keV)

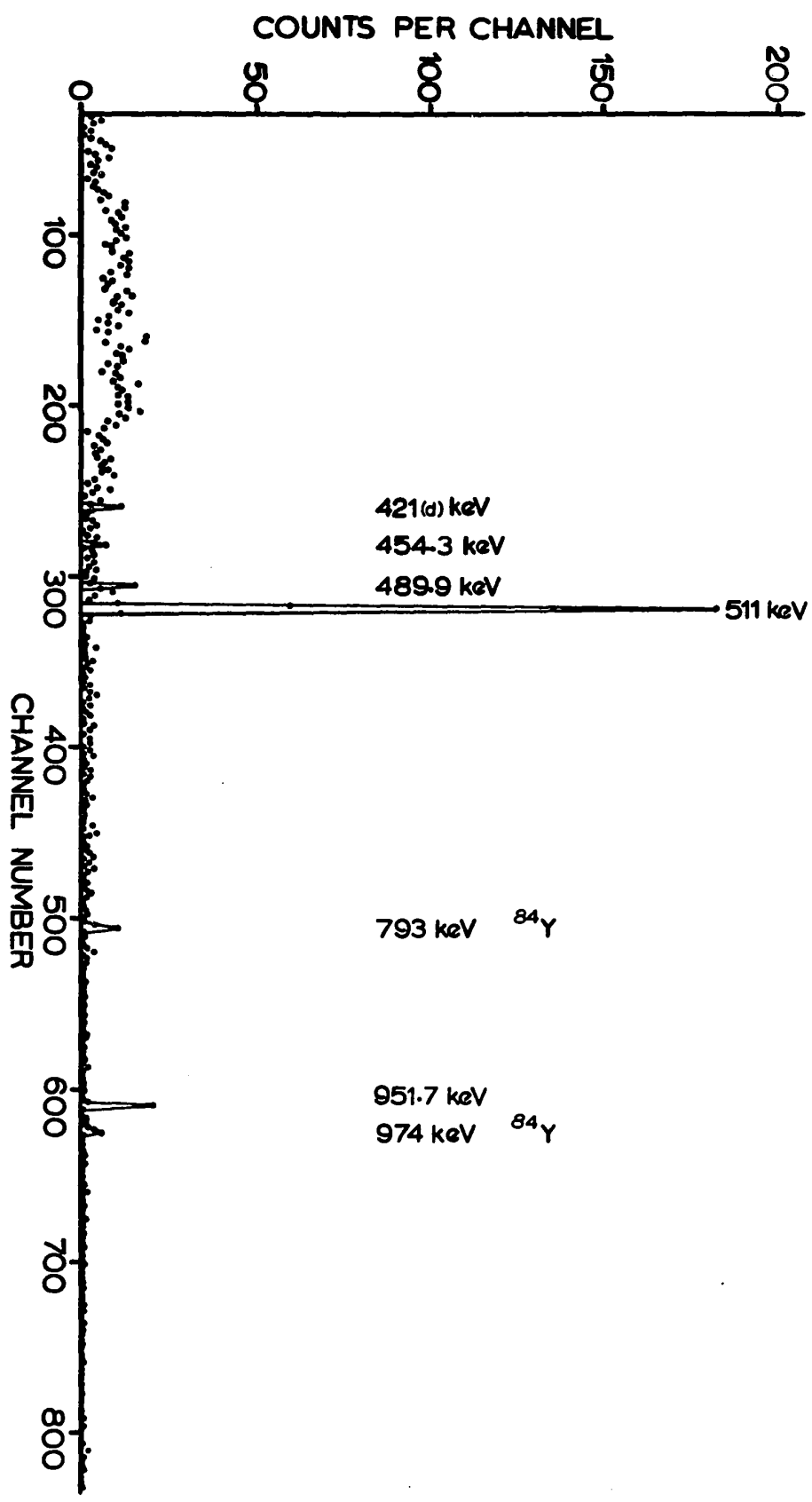


FIGURE 29

The K-electron Internal Conversion Line From the
259.3 keV Transition

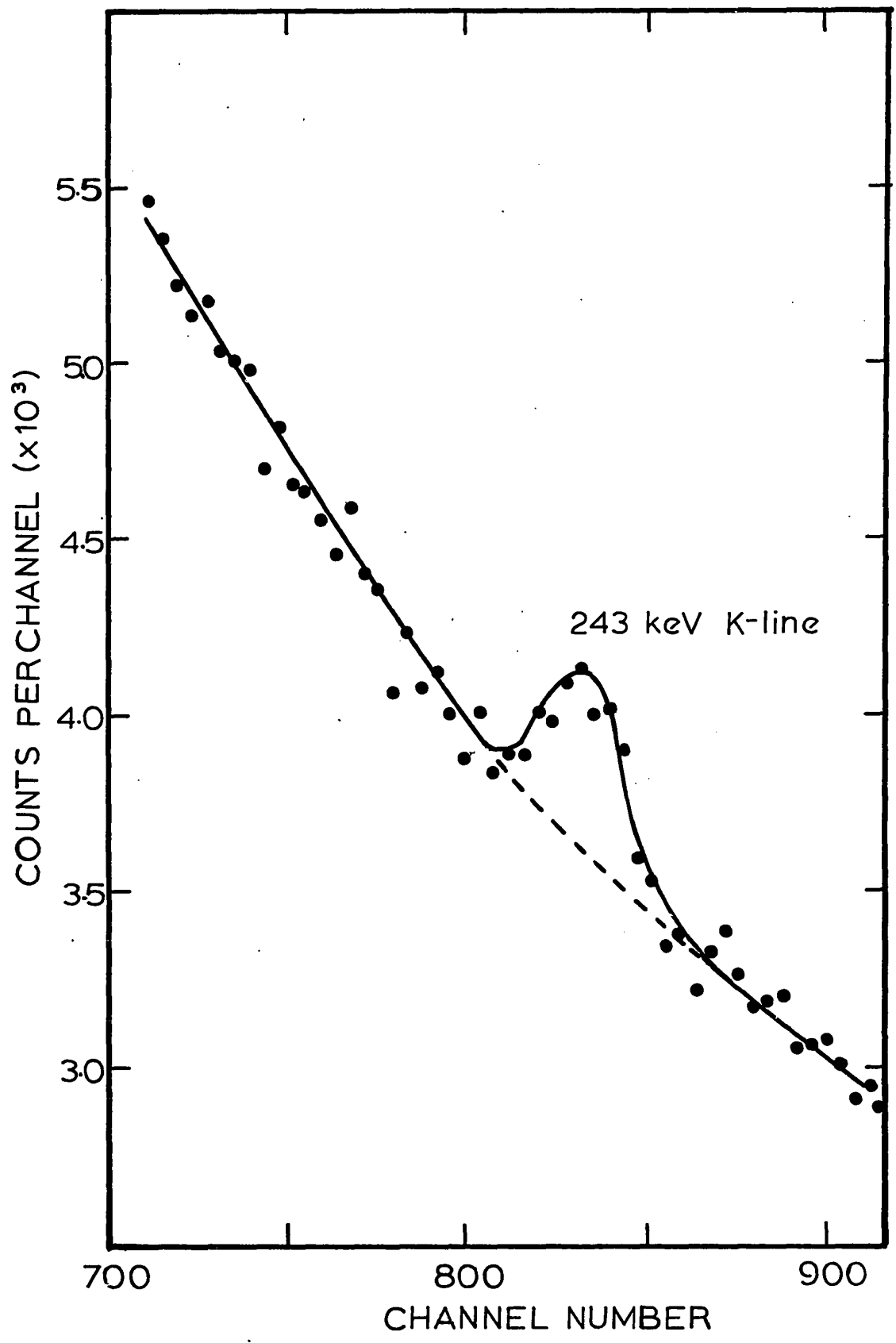
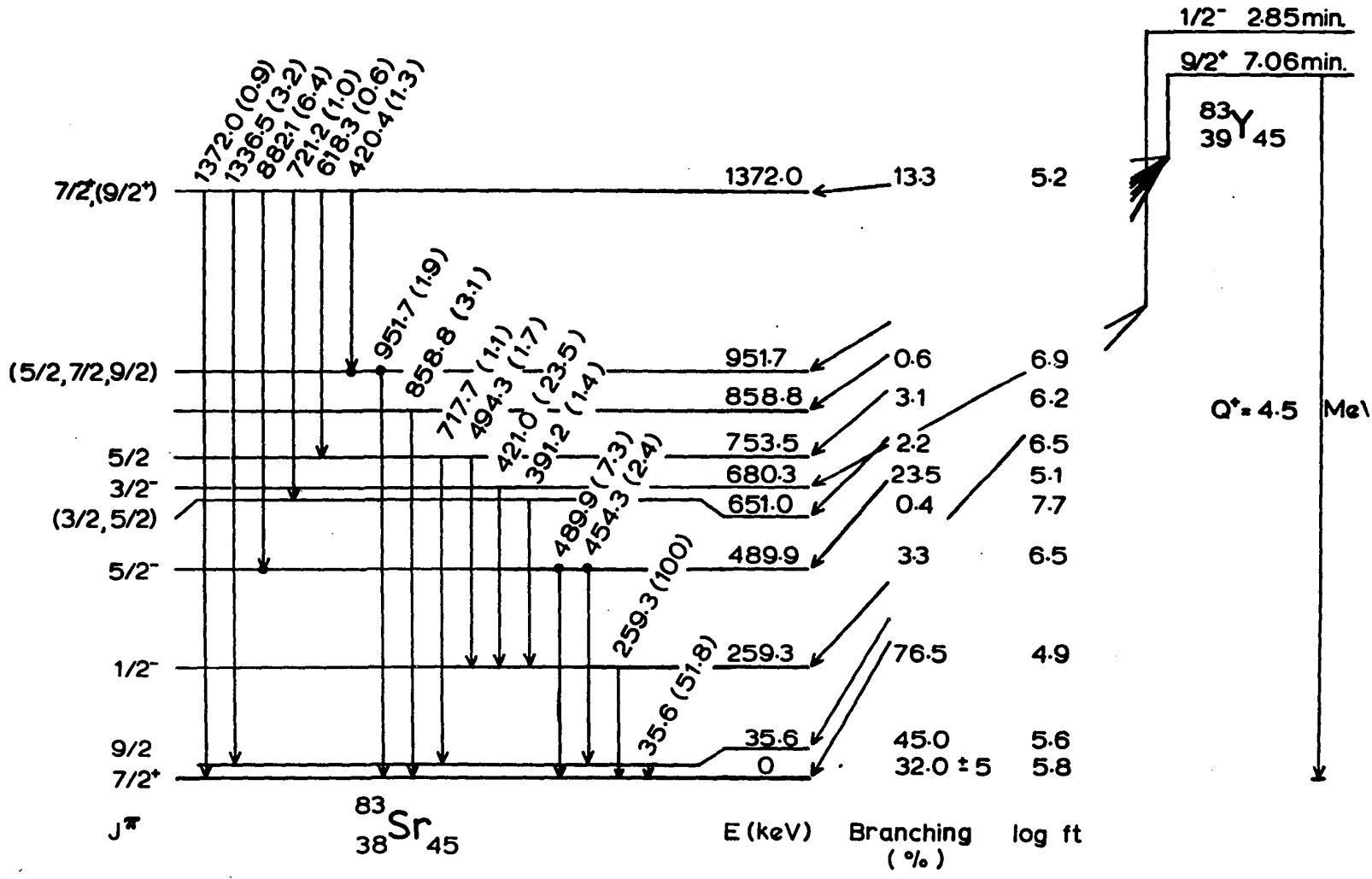


FIGURE 30
Proposed Decay Scheme of ^{83}mY



61

CHAPTER VI
THE SEARCH FOR ^{82}Y DECAY

Background

The history of the decay of ^{82}Y is a confused one. Half-lives of ^{82}Y measured using radiochemical 'milking' techniques have varied from 70 minutes to less than 1.5 minutes (30,31,32,33). Turcotte²⁶⁾ reported four gamma rays at energies of 143.4 keV, 147.2 keV, 155.0 keV, and 160.8 keV decaying with a half-life of $22.80 \pm .34$ minutes and attributed them to the decay of ^{82}Y . A spectrum made up entirely of such low energy gamma rays in a decay to an even-even nucleus in this mass region is highly suspect, in sharp disagreement with the predictions of shell model calculations of ^{82}Sr levels¹⁰⁾ (Figure 8) and with decay schemes for similar nuclei, for instance ^{84}Y decay⁴⁵⁾. Recent results from a $^{74}\text{Ge}(\text{C}^{12}, 4n)^{82}\text{Sr}$ reaction study³⁵⁾ indicate the level structure for ^{82}Sr shown in Figure 7. It is not in agreement with the effective interaction shell model calculation results¹⁰⁾ and this non-agreement is thought to be due to deterioration of the stability of the $Z = 38$ proton shell when N is several units less than 50³⁵⁾.

Experimental Results

Targets of enriched ^{84}Sr were bombarded at energies from 40 to 45 MeV (similar to the bombarding energies of Ref. 26) well above the $(p,3n)$ reaction Q value. The gamma rays assigned to the decay of ^{82}Y by Turcotte²⁶⁾ were observed, along with several others of the same half-life. When the

yttrium activities were chemically separated from the strontium and rubidium activities, these gamma rays were found to emanate not from the yttrium fraction but from the contaminant fraction. (See Figures 21 and 22). The photons of 22.8 minutes half-life observed by Turcotte²⁶⁾ and in the present work have recently been identified as originating from the decay of ^{79}Rb ⁴⁷⁾.

These workers induced the observed activity by ^3He bombardments on ^{79}Br targets. The production of yttrium activity by this process is impossible. Table 10 shows the energies and relative intensities of strong lines from the decay of ^{79}Rb seen in this work.

None of the gamma rays reported in the $^{74}\text{Ge}(\text{C}^{12}, 4n)^{82}\text{Sr}$ reaction work³⁵⁾ were observed in samples counted within five minutes of bombardment. Subsequently, an experiment was carried out using the rapid extractor system which enabled counting to begin one minute and fifteen seconds after bombardment. No trace of the expected gamma rays was recorded.

Speculations on Reasons for the Failure to Observe ^{82}Y Activity

Failure to produce ^{82}Y activity: There are two possible reasons for not producing ^{82}Y in observable amounts - wrong bombarding energy or very low reaction cross-section. The bombarding energies used were 10 - 15 MeV above the calculated (p,3n) reaction threshold and even at the highest bombarding energy the (p,n) and (p,2n) reaction yields were significant. It seems unlikely that the bombarding energies used could have been entirely inappropriate. A very low cross-section is a possibility that cannot be ruled out.

TABLE 10
Gamma Rays From ^{79}Rb Observed in This Work

Energy (keV)	Relative Intensity
130.01 \pm 0.02	41.5 \pm 2.1
* 143.49 \pm 0.03	46.6 \pm 2.2
* 147.23 \pm 0.03	32.2 \pm 1.7
* 154.84 \pm 0.02	24.6 \pm 1.2
* 160.68 \pm 0.02	28.9 \pm 1.1
182.82 \pm 0.10	67.2 \pm 3.3
350.66 \pm 0.06	28.1 \pm 1.4
397.65 \pm 0.01	22.3 \pm 1.5
505.30 \pm 0.04	53.6 \pm 2.7
688.12 \pm 0.04	100

* Gamma ray energies preceded by * match those misassigned by Turcotte²⁶⁾ to the decay of ^{82}Y .

A very short half-life for the ^{82}Y decay: the ^{82}Y activity was counted within 1.25 minutes of bombardment and no trace of the gamma rays reported by Inamura et al.³⁵⁾ from reaction studies was seen. This suggests an appropriate upper limit of 30 seconds on the half-life of ^{82}Y if it decays to excited states of ^{82}Sr which subsequently emit gamma radiation. A rough estimate of the half-life of an allowed beta transition from ^{82}Y to ^{82}Sr is of the order of ten to twenty seconds⁵⁴⁾.

^{82}Y may decay entirely by β^+ decay to the 0^+ ground state of ^{82}Sr : Several different ground state spins are possible for ^{82}Y . If the odd (39^{th}) proton is in the $2p_{1/2}$ orbit and the odd neutron (43^{rd}) in the $1g_{9/2}$ orbit Nordheim's strong coupling rule indicates a ground state spin of 4^- . This is consistent with the systematics of low mass even A yttrium isotopes (Appendix 2). On the other hand if the odd proton is in the $2p_{1/2}$ shell and the odd neutron is in the $2p_{1/2}$ shell the ground state spin of ^{82}Y is predicted to be most probably 1^+ . Systematics of $N=43$ isotones (Appendix 2) indicate that the 43^{rd} neutron tends to be in the $2p_{1/2}$ orbit. The two other possibilities 5^- and 0^+ are not entirely excluded by these rules. Of these four possible spins only the 0^+ is compatible with the hypothesis of an allowed or superallowed beta decay from the ground state of ^{82}Y directly to the 0^+ ground state of ^{82}Sr , with no other branches. Of the four possible ground state spins for ^{82}Y 0^+ is not the most probable.

If such a $0^+ \rightarrow 0^+$ allowed or superallowed transition does occur in ^{82}Y the half-life of this activity would be expected to be of the order of a few seconds, undetectable in the present experiment.

^{82}Y decay may proceed by delayed proton emission: the Q value for beta decay from ^{82}Y to ^{82}Sr is -8.4 MeV based on mass table predictions³⁷⁾. The binding energy of a proton in ^{82}Sr is only 6.8 MeV. If in ^{82}Sr there is an analogue state above 6.8 MeV then ^{82}Y may decay via delayed proton emission. This is an unlikely decay mode.

Conclusions

To date attempts to observe beta decay from ^{82}Y to ^{82}Sr have been entirely unsuccessful. An upper limit of 30 seconds is determined for its half-life. Further experiments are required to clarify the situation.

REFERENCES

1. M.G. Mayer, Phys. Rev. 75 (1949) 1969.
2. M.G. Mayer, Phys. Rev. 78 (1950) 16.
3. O. Haxel, J.H.D. Jensen and H.E. Suess, Phys. Rev. 75 (1949) 1766.
4. O. Haxel, J.H.D. Jensen and H.E. Suess, Z. Physik 128 (1950) 295.
5. A.M. Lane, 'Nuclear Theory, Pairing Force Correlations and Collective Motion', W.A. Benjamin Inc., New York (1964).
6. L.S. Kisslinger and R.A. Sorenson, Dan. Mat. Fys. Selkb. 32 (1960) 1.
7. S.G. Nilsson, K. Danske Vidensk. Selskab. mat.-fys. Medd. 29 No.16 (1955).
8. I. Talmi and I. Unna, Nucl. Phys. 19 (1960) 225.
9. N. Auerbach and I. Talmi, Nucl. Phys. 64 (1965) 458.
10. J.E. Kitching, W.G. Davies, W.J. Darcey, W. McLatchie and J. Morton, Nucl. Phys. A177 (1971) 443.
11. J.E. Kitching, to be published.
12. M.A. Preston, 'The Physics of the Nucleus', Addison-Wesley, Reading, Mass. (1962).
13. A.H. Wapstra, G.J. Nijgh, and R. van Lieshout, 'Nuclear Spectroscopy Tables', North Holland Publ. Co., Amsterdam (1959).
14. M.E. Rose in 'Alpha-, Beta- and Gamma-Ray Spectroscopy' (ed. K. Siegbahn, North Holland Publ. Co., Amsterdam, 1968) Ch. 16, p.887.
15. R.S. Hager and E.C. Seltzer, Nucl. Data A4 (1968) 1.
16. E. Fermi, Z. Phys. 88 (1934) 161.
17. E.J. Konopinski and M.E. Rose in 'Alpha-, Beta- and Gamma-Ray Spectroscopy' (ed. K. Siegbahn, North Holland Publ. Co., Amsterdam, 1968) Ch. 23, p. 1327.

18. E. Feenberg and G. Trigg, Rev. Mod. Phys. 22 (1950) 399.
19. C.F. von Weiszäcker, Naturwiss. 24 (1936) 813.
20. C.M. Lederer, J.M. Hollander, and I. Perlman, 'Table of Isotopes, Sixth Edition' John Wiley and Sons, Inc., New York (1967).
21. A.V. Ramayya, B. van Nooijen, J.W. Ford, D. Krmpotic, J.H. Hamilton, J.J. Pinajian and N.R. Johnson, Phys. Rev. C2 (1970) 2248.
22. R. Arl't, N.G. Zaitseva, B. Kratsik, M.G. Loshchilov, G. Muziol' and Chan Tkhan' Min', Bulletin of the Academy of Sciences of the USSR - Physical Series 33 (1969) 1463.
23. Y.E. Kim, D.J. Horen and J.M. Hollander, Nucl. Phys. 31 (1962) 447.
24. J.E. Kitching, W. Darcey, W.J. Davies, W. McLatchie and J.M. Morton, Phys. Lett. 32B (1970) 343.
25. J.E. Kitching, private communication.
26. R.E. Turcotte, Ph.D. thesis, McGill University (1971), unpublished.
27. T.A. Doron and M. Blann, Nucl. Phys. A161 (1971) 12.
28. A.A. Abdyrzakov, A. Balanda, B. Kratsik, M. Toshev, T. Khamsayev, to be published.
29. R.W. Bercaw and R.E. Warner, Phys. Rev. C2 (1970) 297.
30. A.A. Caretto and E.O. Wigg, J. Am. Chem. Soc. 74 (1952) 5235.
31. F.D.S. Butement and G.B. Briscoe, J. Inorg. Nucl. Chem. 25 (1963) 151.
32. V. Maxia, W.H. Kelly and D.J. Horen, J. Inorg. Nucl. Chem. 24 (1962) 1175.
33. W.J. Nieckarz Jr. and A.A. Caretto Jr., J. Inorg. Nucl. Chem. 27 (1965) 919.
34. I. Dostrovsky, S. Katcoff and R.W. Stoenner, J. Inorg. Nucl. Chem. 26 (1964) 209.
35. T. Inamura, S. Nagamiya, A. Hashizume and Y. Tendow, IPCR Cyclotron Progress Report, Vol.5 (1971) 46.

36. C. Maples, G.W. Goth and J. Cerny, Nucl. Data A2 (1966) 429.
37. W.D. Myers and W.J. Swiatecki, UCRL-11980 (1965).
38. D.R. Sachev and L. Yaffe, Can. J. Chem. 45 (1967) 2711.
39. W.H. Zoller, W.B. Walters and C.D. Coryell, Phys. Rev. 185 (1969) 1537.
40. A.L. Carter, Ph. D. thesis, McGill University (1958).
41. Ortec Instruction Manual, Surface Barrier Detectors, published by Ortec, Oakridge, Tenn..
42. M. Ishihara, H. Kawakami, N. Yoshikawa, M. Sakai and K. Ishii, Phys. Lett. 35B (1971) 393.
43. R.C. Etherton, L.M. Beyer, W.H. Kelly and D.J. Horen, Phys. Rev. 168 (1968) 1249.
44. A.H. Wapstra and N.B. Gove, Nuclear Data Tables 9 (1971) 265.
45. R.L. Auble, Nucl. Data B5 (1971) 109.
46. S.L. Waters, D.J. Sylvester and I.W. Goodier, Phys. Rev. C2 (1970) 2441.
47. E.W.A. Lingeman, F.W.N. de Boer, P. Koldewijn and P.R. Maurenzig, Nucl. Phys. A160 (1971) 630.
48. G. Graeffe, S. Väisälä and J. Heinonen, Nucl. Phys. A140 (1970) 161.
49. A. Artna, Nucl. Data B1 (1966) 125.
50. H.E. Bosch, A.J. Haverfield, E. Szichman and S.M. Abecasis, Nucl. Phys. A108 (1968) 209.
51. Y. Gurfinkel and A. Notea, Nucl. Inst. 57 (1967) 173.
52. G. Aubin, J. Barrette, M. Barrette and S. Monaro, Nucl. Inst. 76 (1969) 93.
53. D.M. White, R.E. Biskett and T. Thompson, Nucl. Inst. 77 (1970) 261.
54. R.I. Verrall, J.C. Hardy and R.E. Bell, Nucl. Inst. 42 (1966) 258.

APPENDIX I
GAMMA RAY ENERGY STANDARDS

Source	Energy (keV)		Relative Intensity	
^{133}Ba (49, 50)	53.40	.06	2.17	.10
	79.70	5	2.0	2
	80.94	5	30.1	1
	160.64	7	0.55	02
	223.14	7	0.44	03
	276.54	5	6.10	15
	302.84	5	15.4	4
	356.24	5	51.7	
	383.78	5	7.39	16
^{60}Co (20)	1173.226	40	100	
	1332.483	46	100	
^{154}Eu (51)	123.10	3	113.10	3.31
	247.92	3	18.75	52
	444.34	7	1.44	10
	591.71	4	14.03	33
	692.42	6	4.85	17
	723.27	4	57.13	141
	756.82	5	12.54	30
	873.21	5	33.35	90
	996.30	5	29.42	80
	1004.78	5	50.33	130

Source	Energy (keV)		Relative Intensity	
^{154}Eu (continued)	1274.42	5	100	
	1494.08	7	1.84	10
	1596.45	7	4.77	15
$^{182}\text{Ta}^{52)}$	31.375	.001		
	42.714	2	0.70	.04
	65.720	2	8.13	40
	67.748	2	119.	6.
	84.679	2	7.64	37
	100.102	2	407	1.5
	113.672	2	5.53	30
	116.414	2	1.28	08
	152.428	2	21.0	8
	156.386	2	8.10	40
	179.392	2	9.44	40
	198.351	3	4.37	25
	222.106	2	22.7	9
	229.317	8	11.1	5
	264.071	3	10.7	4
	891.982	15	0.15	02
	927.995	15	1.79	09
	957.730	15	1.02	06
1001.694	15	5.98	30	
1044.409	15	0.69	08	
1113.398	52	1.13	10	

Source	Energy (keV)	Relative Intensity
^{182}Ta (continued)		
	1121.298 .013	100
	1157.311 13	1.84 .35
	1158.080 15	0.99 28
	1189.046 13	47.4 7
	1221.399 13	79.3 1.2
	1231.010 13	33.4 5
	1257.412 13	4.33 07
	1273.725 13	1.90 04
	1289.147 13	4.05 07
	1342.714 51	0.75 02
	1373.825 13	0.66 02
	1387.396 13	0.217 010
	1410.100 100	0.117 008
	1453.115 13	0.123 010

APPENDIX 2
SYSTEMATICS

- A. $N=45$, $A=\text{odd}$ isotones
- B. Odd A yttrium isotopes
- C. Odd A strontium isotopes
- D. Even A yttrium isotopes
- E. $N=43$, $A=\text{even}$ isotones

A. N=45 A=ODD ISOTONES (20)

<u>1/2⁻ 0.159</u>	<u>1/2⁻ 0.096</u>	<u>1/2⁻ 0.190</u>
<u>7/2⁺ 0</u>	<u>7/2⁺ 0</u>	<u>7/2⁺ 0</u>
$\begin{matrix} 77 \\ 32 \text{Ge} \\ 45 \end{matrix}$	$\begin{matrix} 79 \\ 34 \text{Se} \\ 45 \end{matrix}$	$\begin{matrix} 81 \\ 36 \text{Kr} \\ 45 \end{matrix}$

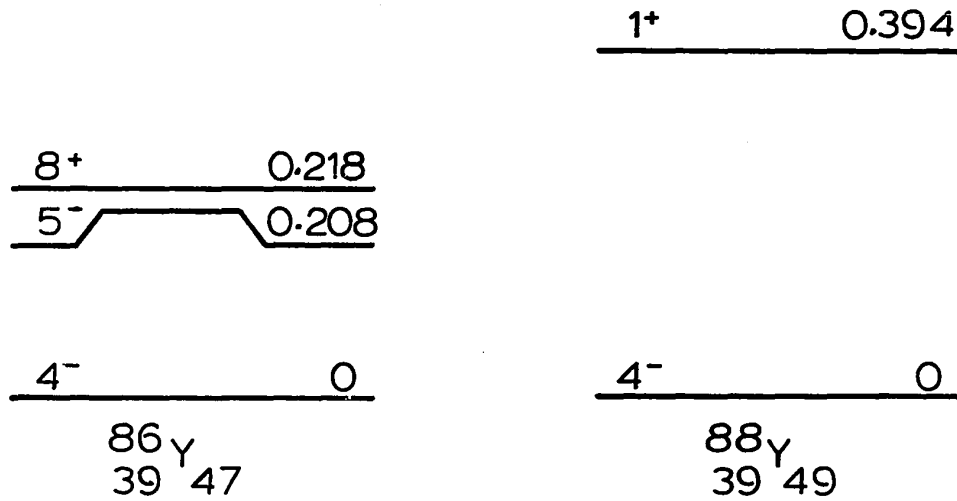
B. ODD A YTTRIUM ISOTOPES (20)

<u>9/2⁺ 0.91</u>		
<u>9/2⁺ 0.381</u>		
<u>1/2⁻ 0.04</u>	<u>9/2⁻ 0</u>	<u>1/2⁻ 0</u>
<u>9/2⁺ 0</u>	<u>9/2⁻ 0</u>	<u>1/2⁻ 0</u>
$\begin{matrix} 85 \\ 39 \text{Y} \\ 46 \end{matrix}$	$\begin{matrix} 87 \\ 39 \text{Y} \\ 48 \end{matrix}$	$\begin{matrix} 89 \\ 39 \text{Y} \\ 50 \end{matrix}$

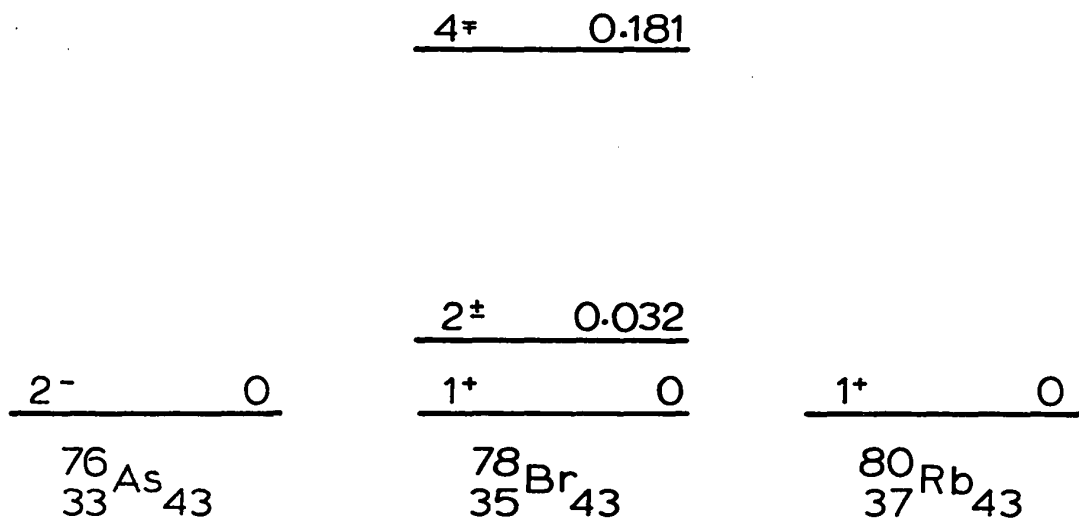
C. ODD A STRONTIUM ISOTOPES (10)

	<u>5/2⁻ 1.259</u>
	<u>5/2⁺ 1.231</u>
	<u>3/2⁻ 0.876</u>
	<u>1/2⁻ 0.387</u>
	<u>9/2⁺ 0</u>
<u>5/2⁻ 0.767</u>	
<u>5/2⁺ 0.740</u>	
<u>3/2⁻ 0.237</u>	
<u>7/2⁺ 0.231</u>	
<u>9/2⁺ 0</u>	
$\begin{matrix} 85 \\ 38 \text{Sr} \\ 47 \end{matrix}$	$\begin{matrix} 87 \\ 38 \text{Sr} \\ 49 \end{matrix}$

D. EVEN A YTTRIUM ISOTOPES (20)



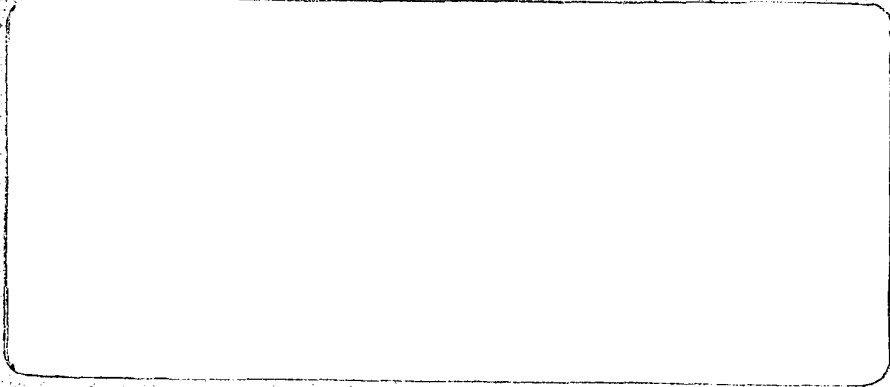
E. N = 43 A EVEN ISOTONES (20)



APPENDIX 3

Reprint of Publication:
The Decay of $^{86}\text{m}\gamma$

Reprinted from:



NORTH  HOLLAND
AMSTERDAM

1.E.4:
3.A

Nuclear Physics A186 (1972) 171—176; © North-Holland Publishing Co., Amsterdam

Not to be reproduced by photoprint or microfilm without written permission from the publisher

THE DECAY OF ^{86m}Y

M. L. SIMPSON, J. E. KITCHING and S. K. MARK

Foster Radiation Laboratory, McGill University, Montreal, Quebec, Canada

Received 10 December 1971

(Revised 8 February 1972)

Abstract: The decay of the 8^+ , 218.4 keV isomeric state of ^{86}Y has been re-investigated. It was observed that this state decays with a weak β^+ branch to a state at 2955.5 keV in ^{86}Sr as well as γ -decaying to states in ^{86}Y . The relative β^+ decay strength was measured to be $(0.69 \pm 0.04)\%$, corresponding to a $\log ft$ value of 6.51. Gamma-gamma coincidence measurements indicated that the 2955.5 keV state undergoes four successive cascade transitions to the ground state of ^{86}Sr with the emission of γ -rays at 98.6 ± 0.1 , 627.2 ± 0.2 , 1076.6 ± 0.3 and 1153.1 ± 0.3 keV. A new decay scheme is proposed.

E

RADIOACTIVITY ^{86m}Y [from $^{87}\text{Sr} (p, 2n)^{86m}\text{Y}$]; measured $T_{1/2}$, E_γ , I_γ , $\gamma\gamma$ -coinc.; deduced $\log ft$. ^{86}Sr deduced levels J, π . Enriched targets, X-ray and Ge(Li) detectors.

1. Introduction

Two activities are associated with the decay of ^{86}Y : a 14.6 h ground state decay and 48 min isomeric state decay¹⁾. The decay of the ^{86}Y ground state to levels in ^{86}Sr has been a subject of much study²⁾. The shorter-lived activity was investigated by Kim *et al.*³⁾ who attributed it to the decay of an isomeric state at 218.2 keV in ^{86}Y with a spin and parity of 8^+ . They observed that this state decays to the 5^- , 208.0 keV state, thence to the 4^- ground state of ^{86}Y , but found no evidence of a direct β^+ decay branch to levels in ^{86}Sr . However, in the course of their studies of internal conversion electrons, they observed a 98.5 keV transition which they assigned to ^{86}Sr on the basis of its K and L conversion lines energy separation, but its relationship in the level structure of ^{86}Sr was not established.

In a $^{87}\text{Sr} (p, d)^{86}\text{Sr}$ reaction study, Kitching *et al.*⁴⁾ observed a series of levels in ^{86}Sr with even spin and positive parity. They suggested that the levels at 2995 keV (8^+), 2855 keV (6^+), 2232 keV (4^+), 1077 keV (2^+) and 0 keV (0^+) are members of the $(g_{7/2}^-)^2$ multiplet. The identification of an 8^+ state at 2955 keV in ^{86}Sr suggested the possibility that a direct β^+ decay branch connecting this state to the 8^+ , 218.2 keV isomeric state in ^{86}Y may exist, particularly if the dominant shell-model configuration of the latter is $(g_{7/2}^-)\pi (g_{7/2}^-)^3\nu$ (π and ν denote proton and neutrons, respectively). The present work was thus undertaken to clarify this situation. During the course of this work, the electromagnetic transition characteristics of the suggested multiplet

in ^{86}Sr were studied by Ishihara *et al.* ⁵⁾ and they concluded that the 8^+ state decays with a half-life of $0.46 \pm 0.03 \mu\text{s}$ to the 6^+ , 4^+ , 2^+ and 0^+ states successively via pure E2 transitions.

2. Experimental details

The 48 min $^{86\text{m}}\text{Y}$ sources were produced by means of the $^{87}\text{Sr}(p, 2n)^{86}\text{Y}$ reaction in the McGill synchrocyclotron at 24 MeV bombarding energy. The targets were enriched (93.3 %) $^{87}\text{Sr}(\text{NO}_3)_2$. The relatively high spin value ($\frac{9}{2}^+$) of the ground state of ^{87}Sr is conducive to the production of the 8^+ isomeric state in ^{86}Y , and the chosen bombarding energy corresponds to the maximum isomer to ground state yield ratio.

Two detectors were used in this work: an X-ray spectrometer with energy resolution of 0.85 keV at 200 keV and a 35 cm^3 Ge(Li) detector with an energy resolution of 2.4 keV at 1.33 MeV. Singles γ -ray spectra were collected in a 4096-channel Nuclear Data analyser, which was interfaced to a PDP-8 computer for data analysis. Gamma-gamma coincidence measurements were recorded by operating the analyser in a 4×1024 -channel two-dimensional mode. Four coincidence spectra each of 1024 channels were collected simultaneously. The lifetime of the activities was measured by means of an on-line computer program control with a selectable counting interval.

3. Results

A half-life analysis of the γ -rays appearing in the recorded spectra was used to identify the two activities from the decay of ^{86}Y ground state and $^{86\text{m}}\text{Y}$, together with contaminants arising from reactions other than $^{87}\text{Sr}(p, 2n)^{86}\text{Y}$. Apart from all the γ -rays observed by Ramayya *et al.* ²⁾ and Kim *et al.* ³⁾, a weak γ -ray at 98.6 ± 0.1 keV was observed. This γ -ray decays with the same half-life as those at 10.2 ± 0.1 keV and 208.2 ± 0.2 keV as observed by Kim *et al.* (10.15 ± 0.1 and 208.0 ± 0.3 keV) in their study of the decay of $^{86\text{m}}\text{Y}$. The intensity of the 98.6 keV line relative to that of the 208.2 keV line has been measured to be $(0.35 \pm 0.02 \%)$. Fig. 1 presents that part of the spectrum which includes both the 98.6 and 208.2 keV γ -rays with their half-lives being shown in the insert. A careful half-life analysis of the other γ -rays in the spectra revealed that photons of energy 627.7 ± 0.2 , 1076.6 ± 0.3 and 1153.1 ± 0.3 keV, which are known to be associated with the decay of the 14.6 h ^{86}Y ground state ²⁾, contained a small shorter-lived component whose half-life is similar to that of the $^{86\text{m}}\text{Y}$ decay.

A γ - γ coincidence measurement with the X-ray and 35 cm^3 Ge(Li) detectors was performed to investigate the relationship of the 98.6 keV γ -ray and the 627.7, 1076.6 and 1153.1 keV γ -rays. The output of the Ge(Li) detector was routed into different quadrants of the analyser by the energy selection window set on the output of the X-ray detector. Three windows were used: one set on the 98.6 keV line and the other

two sets on the background just above and below this γ -ray, respectively, as indicated in fig. 1. This arrangement permitted simultaneous recording of the 98.6 keV line and background coincidence spectra. Fig. 2 presents for comparison the relevant portion of a γ -ray singles spectrum of the 14.6 h ^{86}Y decay, and coincidence spectra

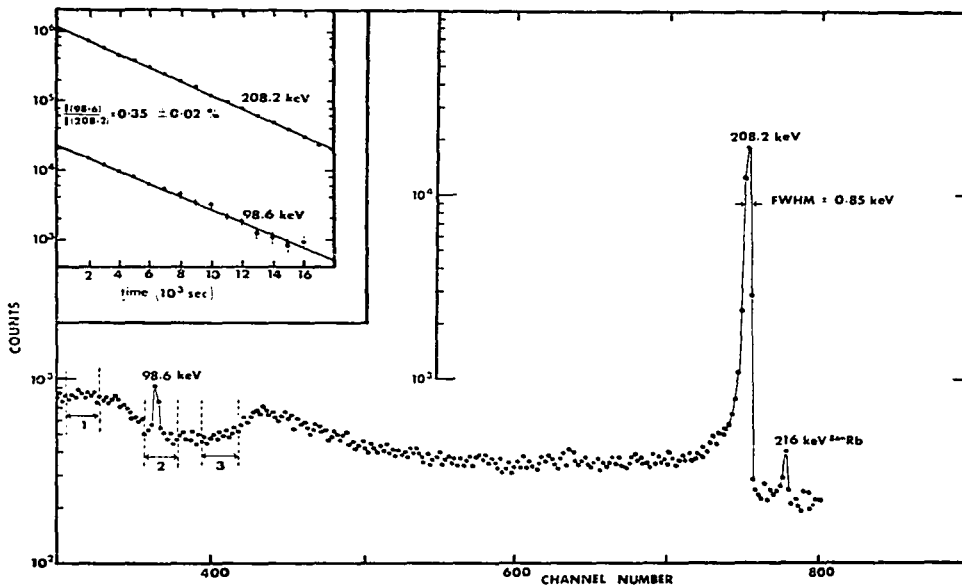


Fig. 1. A partial γ -ray spectrum obtained with the X-ray detector. The vertical dashed bars indicate the energy window setting used for coincidence measurements. The insert shows the decay of the 98.6 and 208.2 keV γ -rays and their intensity ratio. The half-life obtained for these two γ -rays is 48 ± 2 min.

gated by the 98.6 keV γ -ray, by the window above this γ -ray, and by the 98.6 keV window after the 48 min activity had been allowed to decay. An analysis of the data reveals that there are strong coincidences between the 98.6 KeV transition and the 627.7, 1076.6 and 1153.1 keV transitions and that these γ -rays have equal intensities in the coincidence spectrum (within an experimental error of $\pm 10\%$). No other γ -ray was observed in coincidence with the 98.6 keV line. This result indicates that the four γ -rays originate from transitions in ^{86}Sr .

The decay scheme of 14.6 h ^{86}Y as proposed by Ramayya *et al.*²⁾ associates the 627.7 keV γ -ray with a transition between the 2481.9 keV (3^-) and 1854.2 keV (2^+) levels while the 1153.1 keV and 1076.6 keV γ -rays arise from the decay of the 2229.7 keV (4^+) level to the 1076.6 keV (2^+) level which subsequently decays to the ground state. No transition between the two 2^+ levels was observed and, consequently, the present coincidence experiment in which the 98.6 keV transition is observed to be

in coincidence with the above three γ -rays suggests that the 627.7 keV γ -ray is in fact a doublet. A high-resolution study of the three γ -rays revealed a low-energy shoulder on the 627.7 keV photopeak which decays with a half-life consistent with the ^{86m}Y decay. A line shape analysis revealed a weak transition at 627.2 ± 0.2 keV. It is therefore concluded that the 627.2, 1076.6 and 1153.1 keV γ -rays are in coincidence with the 98.6 keV line.

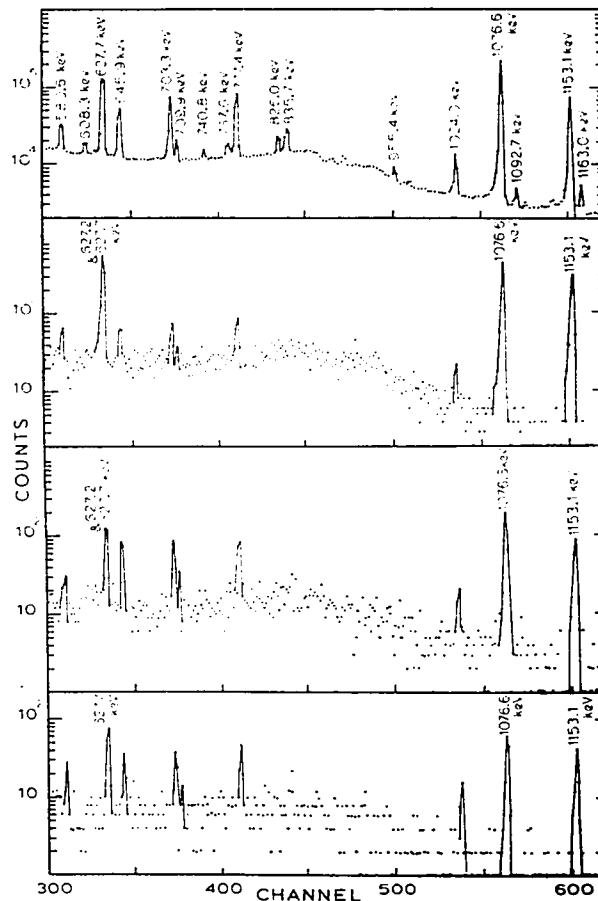


Fig. 2. Comparison of the relevant portion of the γ -ray spectra from the decay of ^{86m}Y and ^{86}Y (ground state). From top to bottom: (a) γ -rays from the decay of 14.6 h ^{86}Y ground state (spectrum accumulated four hours after bombardment), (b) coincidence spectrum gated by the window set on the 98.6 keV line, (c) coincidence spectrum gated by the window just above the 98.6 keV line, (d) same as (b) except that the 48 min activity had been allowed to decay for a period of four half-lives before counting. The energy window settings are indicated in fig. 1.

4. Discussion and conclusions

The decay of the 8⁺, 218.4 keV isomeric state of ⁸⁶Y has been re-investigated. Besides the transitions at 10.2 and 208.2 keV attributed to the decay of this isomer by Kim *et al.*³⁾ γ-rays at 98.6 and 627.2 keV were observed to decay with the same half-life. The 627.2, 1076.6 and 1153.1 keV γ-rays appeared in the coincidence spectrum gated by the 98.6 keV line with equal intensity. The 1153.1 and 1076.6 keV γ-rays are known²⁾ to originate in ⁸⁶Sr.

Based on the internal conversion measurements and the growth-decay character of the γ-rays from the decay of 14.6 hr. ⁸⁶Y, Kim *et al.* assigned the 10.2 and 208.2 keV transitions to the decay of ^{86m}Y to levels in ⁸⁶Y. The 98.6 and 627.2 keV γ-rays observed here cannot be assigned to transitions in ⁸⁶Y because these γ-rays are in coincidence with the 1076.6 and 1153.1 keV γ-rays, which are known to come from transitions in ⁸⁶Sr. It appears that both the 98.6 and 627.2 keV transitions are also in ⁸⁶Sr. This observation is consistent with the results of Kim *et al.*, who noted a 98.5 keV transition in their conversion electron spectrum and tentatively assigned it to ⁸⁶Sr.

The results of Kitching *et al.*⁴⁾ imply that the 8⁺ state at 2955 keV should decay predominantly by E2 transitions through 6⁺, 4⁺, 2⁺ and 0⁺ states in succession with the emission of γ-rays of energy 100, 626, 1153 and 1077 keV, respectively. This sup-

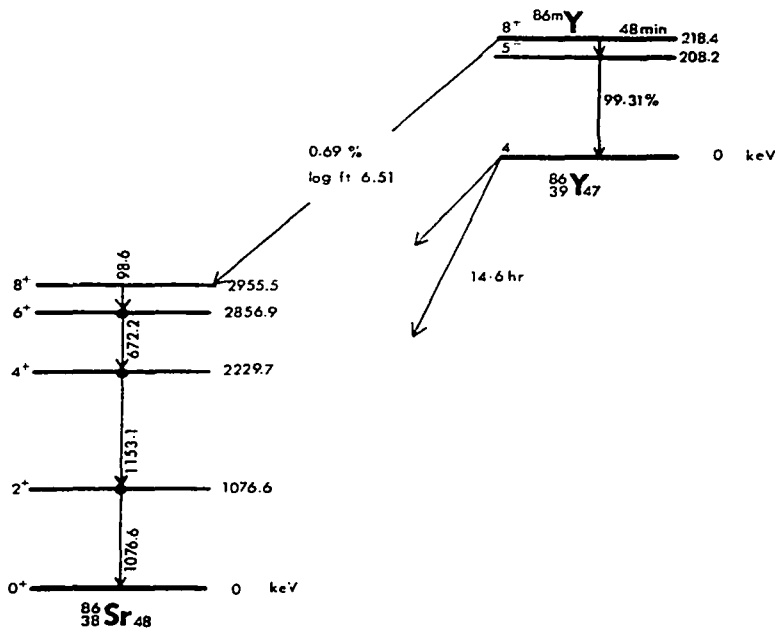


Fig. 3. Proposed decay scheme for the 48 min ^{86m}Y.

position has recently been confirmed by Ishihara *et al.* ⁵⁾ in an on-line γ -ray study experiment. It is reasonable therefore, to propose that the γ -rays with energies 98.6, 627.2, 1153.1 and 1076.6 keV observed in the present work are the results of cascade E2 transitions originating from the 8^+ state in ^{86}Sr . This proposition necessitates a direct β^+ decay from ^{86}Y to the 2955.5 keV level in ^{86}Sr . A summary of the proposed decay scheme of $^{86\text{m}}\text{Y}$ is presented in fig. 3.

The relative β^+ and γ -decay intensities shown in the figure are obtained from the relative γ -ray intensities of the 98.6 and 208.2 keV lines. Kim *et al.* have reported the value of the internal conversion coefficient for the 208.2 keV transition as $\alpha_K = 0.04$ and $\alpha_K : \alpha_L : \alpha_M = 100 : 83 : 1.7$. Assuming the 98.6 keV transition is pure E2 [ref. ⁵⁾] the branching ratio for the β -decay of $^{86\text{m}}\text{Y}$ is $(0.69 \pm 0.04)\%$. The β^+ decay $\log ft$ value is therefore deduced to be 6.51; a value somewhat high for an allowed transition but nevertheless consistent with such transitions in this mass region ¹⁾.

This work is supported by a grant from the Atomic Energy Control Board of Canada. The authors wish to thank Mr. R. E. Turcotte for assistance in some of the half life measurements. Thanks are also due to Messrs. C. Flaum and M. Ballantyne for their help in the γ -ray measurements.

References

- 1) R. L. Auble, Nucl. Data Sheets **5B** (1971) 151
- 2) A. V. Ramayya, B. van Nooijen, J. W. Ford, D. Kimpotic, J. H. Hamilton, J. J. Pinajian and N. R. Johnson, Phys. Rev. **C2** (1970) 2248
- 3) Y. E. Kim, D. J. Horen and J. M. Hollander, Nucl. Phys. **34** (1962) 447
- 4) J. E. Kitching, W. Darcy, W. A. Davies, W. McLatchie and J. M. Morton, Phys. Lett. **32B** (1970) 343
- 5) M. Ishihara, H. Kawakami, N. Yoshikawa, M. Sakai and K. Ishii, Phys. Lett. **35B** (1971) 393

